Universitätsklinikum Ulm

Zentrum für Chirurgie

Klinik für Allgemein- und Viszeralchirurgie
der Universität Ulm

Ärztliche Direktorin: Prof. Dr. med. Doris Henne-Bruns

Effects of CK1 specific inhibitors on wild type and mutant CK1δ *in vitro* and their ability to inhibit growth of tumor cell lines

Dissertation

zur Erlangung des Doktorgrades der Medizin
der Medizinischen Fakultät der Universität Ulm

vorgelegt von

Congxing Liu
geboren in Huai'an, Jiangsu, China
2019

Amtierender Dekan: Prof. Dr. Thomas Wirth

1. Berichterstatter: Prof. Dr. Uwe Knippschild

2. Berichterstatter: PD Dr. Karl Föhr

Tag der Promotion: 31.07.2020

Parts of this dissertation have already been published in the following journal articles:

Liu C, Witt L, Ianes C, Bischof J, Bammert M, Henne-Bruns D, Xu P, Kornmann M, Peifer C, Knippschild U. Newly developed CK1-specific inhibitors show specifically stronger effects on CK1 mutants and colon cancer cell lines. Int. J. Mol. Sci. 2019, 20, 6184. https://doi.org/10.3390/ijms20246184.

Table of Contents

List of Abbreviations IV

1. Introduction 1

1.1 The eukaryotic protein kinase (ePK) superfamily 1

1.2 The casein kinase 1 (CK1) family 1

1.2.1 Classification and structure 2

1.2.2 Regulation of CK1 activity 4

1.2.3 Biological functions of CK1 isoforms 5

1.2.4 CK1 specific inhibitors 16

1.3 Aim of the study 19

2. Materials and Methods 22

2.1 Materials 22

2.1.1 Consumables 22

2.1.2 Chemicals and biochemicals 23

2.1.3 Kits 25

2.1.4 Primers 25

2.1.5 Devices 26

2.1.6 Software, online tools and databases 27

2.2 Methods 28

2.2.1 Purification of Glutathione S Transferase (GST) tagged proteins 28

2.2.2 Sodium dodecyl sulfate-polyacrylamide gel electrophoresis (SDS-PAGE) 30

2.2.3 Coomassie staining 31

2.2.4 Silver staining 31

2.2.5 Determination of kinase activity *in vitro* 32

2.2.6 Determination of inhibitory effects of CK1 specific inhibitors *in vitro* 32

2.2.7 Determination of IC_{50} values 34

2.2.8 Cell lines and cell culture 34

2.2.9 G418 selection 35

2.2.10 Transfection 35

2.2.11 Picking of stably transfected clones 36

2.2.12 Purification of total RNA....36
2.2.13 First-strand cDNA synthesis....37
2.2.14 Polymerase chain reaction (PCR)....38
2.2.15 Preparation of cell extracts....38
2.2.16 Determination of protein concentrations....39
2.2.17 Western Blot analysis....39
2.2.18 MTT viability assay....40

3. Results....42

3.1 Introduction of selected mutations into *hum*CK1δ on pcDNA™ 3.1/V5-His TOPO®42
3.2 Expression and purification of recombinant GST fusion proteins....43
3.3 Effects of small molecule inhibitors on the activity of (*hum*)CK1δ wild type and mutants....44
3.4 Determination of IC50 values against GST-(*hum*)CK1δ wt and GST-(*hum*)CK1δ mutants....46
3.5 Validation of newly designed CK1 small molecule inhibitors....48
3.5.1 *In vitro* effects of LKP_compounds on CK1 isoforms activity....48
3.5.2 Determination of IC_{50} values of LKP_compounds against GST-(*hum*)CK1δ....49
3.5.3 Effects of LKP_compounds on the activity of (*hum*)CK1δ wild type and mutants....50
3.5.4 *In vitro* effects of second generation set of LKP_compounds on CK1 isoforms activity....52
3.5.5 Determination of IC_{50} values of second generation set of LKP_compounds against GST-(*hum*)CK1δ....53
3.6 Establishment of new Hela$^{CK1\delta-/-}$ cell lines stably expressing either wt CK1δ wt or CK1δ mutants....54
3.6.1 Experimental proof of successful transfection of Hela$^{CK1\delta-/-}$ cells on RNA level by Polymerase chain reaction (PCR)....55
3.6.2 Experimental proof of successful transfection of Hela$^{CK1\delta-/-}$ cells on protein level by Western Blot analysis....55
3.7 Effects of newly designed LKP_compounds on the viability of Hela cell lines....56

4. Discussion.... 63

4.1 CK1-specific inhibitors have altered effects on CK1δ variants....63
4.2 Effects of newly optimized and synthesized CK1δ inhibitors on CK1δ wt and mutants in in vitro kinase assays and cell-based assays....65

5. Summary....68

6. References: 70

Acknowledgement 85

Curriculum Vitae 87

Statutory declaration 88

List of Abbreviations

#	number
%	percent
°C	Degree Celsius
µl	microliter
A, Ala	alanine
aa	amino acid
AD	Alzheimer´s disease
AKAP450	A-kinase anchor protein 450
Akt	protein kinase B
ALS	amyotrophic lateral sclerosis
AML	Acute Myeloid Leukemia
AMPK	5´-AMP-activated kinase
APC	adenomatous polyposis coli
aPKs	atypical protein kinases
ARNT	aryl hydrocarbon receptor nuclear translocator
ATM	ataxia telangiectasia mutated
ATP	adenosine triphosphate
ATR	ataxia telangiectasia and Rad3-related protein
Aβ	amyloid β
Bax	Bcl-2-associated X protein
Bid	BH3-interacting domain death agonist
BMAL1	brain and Muscle ARNT-Like 1
cAMP	cyclic adenosine monophosphate
Cdc25	cell division cycle 25
CDK	cyclin-dependent kinase
CDK2/E	cyclin-dependent kinases 2/cyclin E
CDK5/p35	cyclin-dependent kinases 5/p35
Chk1	checkpoint kinase 1
Ci	cubitus interruptus
CK1	casein kinase 1
CK1BP	CK1 binding protein
CLK2	CDC-like kinase 2
CLL	chronic lymphocytic leukemia
CMGC	group of cyclin-dependent kinases (CDKs, MAPKs, GSKs, CLKs)
CRY	cryptochrome
DD	dimerization domain
dH_2O	distilled water
ddH_2O	double distilled water
Dhh	desert hedgehog
DMSO	dimethyl sulfoxide

DNA	deoxyribonucleic acid
DR5	death receptor 5
DVL	Disheveled
EC_{50}	50% effective concentration
EGFR	epidermal growth factor receptor
ePKs	eukaryotic protein kinase
FADD	fas-associated death domain
Fas	tumor necrosis factor receptor superfamily member 6
FBS	fetal bovine serum
FCS	fetal calf serum
FZD	Frizzled
G, Gly	glycine
GRK2	G Protein-coupled receptor kinase 2
GSK3β	glycogen synthase kinase 3β
GST	glutathione-S tranferase
GTP	guanosine triphosphate
h	hours
H, His	histidine
HCl	hydrochloric acid
Hh	hedgehog
HIF	hypoxia inducible factor
HPI	hydrophobic pocket I
HRII	hydrophobic region II
Hpo	hippo
hum	human
I, Ile	isoleucine
IC_{50}	50% inhibitory concentration
IGFBP-3	insulin-like growth factor binding protein 3
Ihh	indian hedgehog
IPTG	isopropyl β-D-1-thiogalactopyranoside
JNK	c-Jun N-terminal kinase
KD	kinase domain
kDa	kilo Dalton
KHD	kinesin homology domain
L, Leu	leucine
LATS1/2	large Tumor Suppressor 1/2
LB	lysogeny broth
LRP5/6	lipoprotein receptor-related protein 5/6
M	molar
M, Met	methionine
MAPK	mitogen-activated protein kinase
MDM2	mouse double minute 2 homolog
min	minutes

ml	milliliter
MM	master mix
MOB1A/B	MOB kinase activator 1A/B
MST1/2	mammal sterile-20 like kinase 1/2
MW	molecular weight
N-	N-terminal
NaCl	sodium chloride
NGF1B	nerve growth factor 1B
NLS	nuclear localization signal
nm	nanometer
NP40	Nonidet® P 40
NSCLC	non-small cell lung cancer
p75NTR	p75 neurotrophin receptor
P, Pro	proline
PBS	phosphate-buffered saline
PCR	polymerase-chain reaction
PD	Parkinson´s disease
PER	period
PHB2	prohibitin 2
PIP2	phosphatidylinositol-4,5-bisphosphate
PKA	cAMP-dependent protein kinase
PKB	protein kinase B
PKCα	protein kinase C isoform α
PP5	protein phosphatase 5
Ptch	Patched
PTEN	phosphatase and tensin homolog
Q, Gln	glutamine
R, Arg	arginine
Rap1	Ras-related protein 1
Rho	Ras homolog
RNA	ribonucleic acid
ROS	reactive oxygen species
rpm	revolutions per minute
RT	room temperature
RXR	retinoid X receptors
s	second
S, Ser	serine
SCF	skp, cullin, F-box containing complex
SD	standard deviation
SDM	side-directed mutagenesis
SDS	sodium-dodecyl sulfate
Sgg	Shaggy

Shh	sonic hedgehog
Sipa1L1	signal-induced proliferation-associated 1-like protein
Slmb	Slimb
SMAD	SMA/mothers against decapentaplegic
SMI	small molecule inhibitor
Smo	smoothened
SUFU	suppressor of fused
T, Thr	threonine
TAZ	Tafazzin
TCF/LEF	T-cell factor/lymphoid enhancer factor
TEAD	TEA domain
TOPO-IIα	phosphorylate topoisomerase IIα
TP53	tumor protein 53
TTBK1/2	tau tubulin kinases1/2
TV	transcription variant
UV	ultraviolet
VRK1-3	vaccinia-related kinases 1-3
V, Val	valine
v/v	volume/volume
W, Trp	tryptophan
w/v	weight/volume
Wnt	wingless
wt	wild type
Y, Tyr	tyrosine
YAP	yes-associated protein
YCK1	yeast casein kinase I homolog 1
YCK2	yeast casein kinase I homolog 2
α	alpha
β	beta
β-TRCP	beta-transducin repeat containing protein
γ	gamma
δ	delta
ε	epsilon

1. Introduction

1.1 The eukaryotic protein kinase (ePK) superfamily

Eukaryotic protein kinases (ePKs) are building one of the largest superfamilies of homologous proteins, which account for about 1.7% of protein coding genes of the human genome [88][92]. In eukaryotes, ePKs are phosphotransferases which can transfer the γ-phosphate of adenosine triphosphate (ATP) or guanosine triphosphate (GTP) to the hydroxyl groups of their protein substrate [56]. Depending on their acceptor amino acid specificity, ePKs are classified into five categories: protein-serine (Ser)/ threonine (Thr) kinases, protein-tyrosine kinases, protein-histidine kinases, protein-cysteine kinases and protein-aspartyl or glutamyl kinases [66]. Among 518 identified kinases, 478 are classified as ePKs exhibiting a characteristical domain structure and 40 as atypical protein kinases (aPKs), not showing any similarity to the domain structure of ePKs [44].

ePKs have been subdivided into eight subgroups, which constitute in a phylogenetic tree [20]. ePKs are involved in many eukaryotic cellular processes like cell metabolism and differentiation, transcription, cell cycle progression, adhesion, apoptosis, motility, proliferation, chromosome segregation, DNA-processing and repair as well as inflammatory diseases. Therefore, abnormal phosphorylation often results in deregulation of proteins and as a consequence, it can cause numerous human diseases, like neurological diseases and cancer [27][44][56][66]. Thus, protein kinases represent interesting targets for drug development as they are often overexpressed in various diseases [164].

1.2 The casein kinase 1 (CK1) family

Casein kinases (CKs) can be subdivided into casein kinase 1 (CK1) and casein kinase 2 (CK2), both exhibiting acidtrophic character [135]. However, whereas CK1 builds an own kinase family [44][88], CK2 belongs to the group of cyclin-dependent kinases (CMGC) family.

Members of the CK1 family were one of the first kinases that had been described and characterized in literature [41]. The initial name casein kinase comes from the preference to phosphorylate serine or threonine residues of the milk protein casein which are N-terminally flanked by phosphorylated amino acid residues or acidic amino acids at position -3 [16][83].

CK1 kinases are evolutionarily highly conserved and ubiquitously expressed in all eukaryotes from yeast to plants, mammals, and human [58][70]. The CK1 superfamily includes the families of tau tubulin kinases1/2 (TTBK1/2), vaccinia-related kinases 1-3 (VRK1-3) and CK1 family (**Figure 1A**). In the following chapters, exhaustive knowledge about the classification and structure, regulation, function and specific inhibitors of the CK 1 family will be described.

1.2.1 Classification and structure

All members of the CK1 family belong to the serine/threonine specific protein kinases [44][51][88]. There are seven CK1 isoforms in mammals: α, β, γ1, γ2, γ3, δ, and ε as well as multiple post-transcriptionally processed splice variants (transcription variants; TV). Except CK1β they are all expressed in humans [49][83][135]. All CK1 isoforms contain a highly conserved kinase domain (51-98%), while CK1δ and ε display the highest homology level [41][51][86]. However, CK1 isoforms differ significantly in terms of length and amino acid sequence of their regulatory N- and especially C-terminal non-catalytic domains. While the short N-terminus comprises 9-76 amino acids, the length of the C-terminus ranges from 24 up to more than 200 amino acids. Therefore, molecular weights of various CK1 isoforms range from 32 kDa (CK1α) to 52.2 kDa (CK1γ3) (**Figure 1B**) [83].

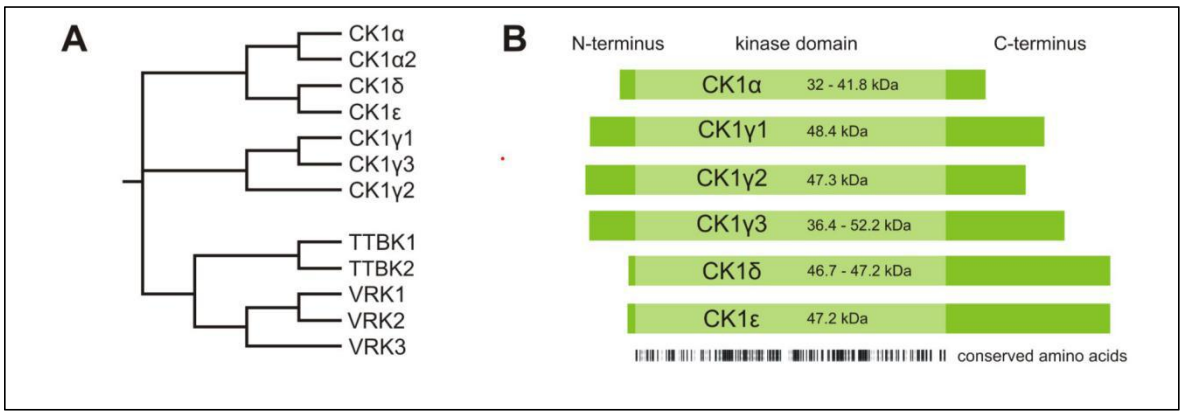

Figure 1: CK1 Family. A: Phylogenetic relation of human CK1 isoforms α, γ1-3, δ, ε and other CK1 family members: TTBK1–2 and VRK1–3. **B:** Schematic alignment of human CK1 isoforms α, γ1-3, δ and ε are shown with their molecule weights (MW). The light green boxes represent the highly conserved kinase domain, while the variable N- and C-terminus are displayed in the dark green [83]. This Figure is licensed under a Creative Commons Attribution 3.0 Generic License http://creativecommons.org/licenses/by/3.0/. **Abbreviations:** CK1: casein kinase 1; TTBK1–2: tau tubulin kinases1-2; VRK1–3: vaccinia-related kinases 1-3.

As a member of the superfamily of serine/threonine-specific kinases, CK1 family represents the typical bilobal structure which includes a smaller N-terminal lobe mainly

containing β- sheets, and a larger α-helical C-terminal lobe (**Figure 2**). The hinge region bridges the smaller N-terminal and the larger C-terminal lobe thereby forming a catalytic cleft which functions as ATP binding pocket and the substrate binding site [83][100]. Within the variable N-terminus, antiparallel 5-stranded β- sheets consist of various regions with different functions, while a salient α-helix within the N-terminal region is essential for conformational regulation of the kinase activity [83]. The P-loop, a conserved glycine-rich sequence, identified in the N-terminal lobe, seems to bridge strands β1 and β2, thereby forming the roof of the ATP active site. Furthermore, it devotes to the coordinated transfer of the γ-phosphate part of ATP [83]. Loop L-78 contributes to structure-based inhibitor design and triggers CK1 inhibitor selectivity because of the approaching of the hinge region [83]. The regulatory non-catalytic C-terminus participates in subcellular targeting and CK1 interaction, which is believed to be regulated by a specific phosphate moiety binding motif (W1). Additionally, CK1 protein kinases contain additional functional structures, like a kinesin homology domain (KHD), which has been shown to contribute to the interaction of kinesins with microtubules, as well as loop L-9D (activation-loop), which play a role in CK1 regulation and substrate recognition [8][100][165]. Furthermore, a nuclear localization signal (NLS) sequence, is located next to the ATP-binding site [82][83]. The dimerization domain (DD), being present in CK1δ, seems to be necessary for complex formation, which affects the kinase activity of CK1δ [8]. The catalytic cleft of CK1 was observed to be hydrophobic because of sharing one deep hydrophobic pocket (HPI) and a larger hydrophobic region (HRII) [53]. All CK1 isoforms use ATP as a phosphate donor and recognize N-terminally acidic amino acids for substrate recognition [8].

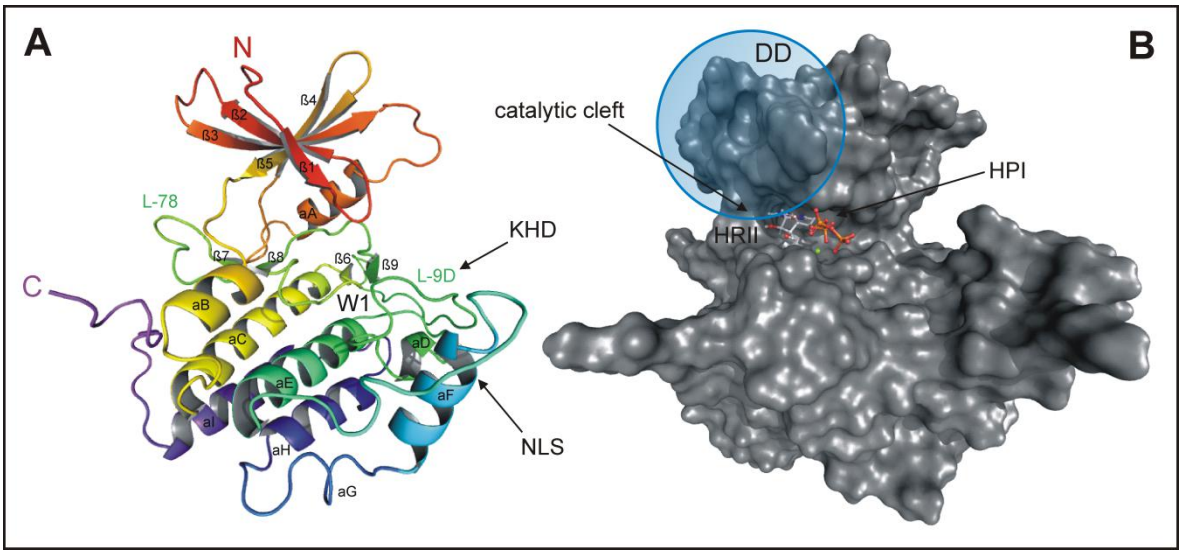

Figure 2: Schematic structure of human CK1δ. A: Ribbon structure of CK1δ: The variable N-terminal lobe is characterized by β-sheets, while α-helices characterized the non-catalytic C-terminal lobe.

The kinesin homology domain (KHD) and the L-9D loop, as well as the nuclear localization sequence (NLS) are displayed. **B**: Surface diagram of CK1δ: The catalytic cleft, a putative dimerization domain (DD), a deep hydrophobic pocket (HPI) and a spacious hydrophobic region (HRII) are displayed. The kinase has a bilobal structure, N- and C-terminus are connected by the hinge region, which then constitute the catalytic cleft as ATP binding pocket and the substrate binding site. Figure obtained from Knippschild et al. [83]. The Figure is licensed under a Creative Commons Attribution 3.0 Generic License http://creativecommons.org/licenses/by/3.0/. **Abbreviations:** CK1 **δ :** casein kinase 1 δ ; KHD: kinesin homology domain; NSL: nuclear localization sequence; DD: dimerization domain; HPI: hydrophobic pocket; HRII: hydrophobic region; ATP: Adenosine triphosphate.

1.2.2 Regulation of CK1 activity

It has been described that CK1 expression levels differ in different tissue and cell types [98] [135]. Numerous factors on different levels have been described to participate in modulating the expression and activity of CK1 isoforms through different mechanisms, such as stimulation with insulin or gastrin, viral transformation, treatment with topoisomerase inhibitors or other small molecules like calotropin, γ-irradiation, or altered membrane concentrations of phosphatidylinositol-4,5-bisphosphate (PIP2) [26][85][86] [134].

On protein level, other mechanisms like dimerization, protein-protein interactions, post-translational modifications, and subcellular localization have been identified as regulatory mechanisms. CK1δ is able to form dimers, which results in the occupation of the adenine binding domain and excluding ATP from the active center of the kinase by the contacts of the dimerization domain [101]. Downregulation of endogenous CK1δ activity by the expression of mutant CK1δ with impaired kinase activity is caused by formation of dimers, thereby further supporting the obvious hypothesis [164].

Subcellular localization as well as cellular compartmentalization were also considered to be regulatory strategies of kinase-substrate interactions and result in variation of the availability or access of CK1 isoforms to their subset of substrates, which is ensured by the binding of CK1 to intracellular structures, small molecules and other proteins [139][157][161][168]. For example, in *Saccharomyces cerevisiae* the CK1 homologs Yeast Casein Kinase I homolog 1 (YCK1) and Yeast Casein Kinase I homolog 2 (YCK2) are recruited to the plasma membrane only when the CK1 homolog Hrr25 is already located in the nucleus. In a further study, it was demonstrated that both, the existence of the kinase domain and the catalytic activity of CK1 are needed for its subcellular localization, since the inactive mutants CK1δ^{K38M} and CK1δ^{T176I} accumulate in the nucleus, which was confirmed by analysis of CK1 kinase-dead mutants [110].

Furthermore, the activity of CK1 isoforms can be regulated by post-translational modifications, which have mostly been identified as reversible phosphorylation events, especially site-specific phosphorylation by autophosphorylation or other cellular kinases [12][48]. Within the regulatory C-terminal domains of CK1δ and ε, autophosphorylation events can consecutively act as pseudo substrates by blocking the catalytic center of the kinase, and some putative intramolecular phosphorylation sites have been identified for both isoforms [18][48][50]. Additionally, in the case of CK1δ, protein kinase A (PKA) (cAMP-dependent protein kinase) phosphorylates CK1δ at Ser-370, protein kinase C, isoform α (PKCα) phosphorylates CK1δ at Ser-328, Thr-329 and Ser-370, and checkpoint kinase 1 (Chk1) phosphorylates CK1 δ at Ser-328, Ser-331, Ser-370 and Thr-397. Furthermore, site-specific phosphorylation of CK1δ has also been shown for Akt (protein kinase B, PKB) and CDC-like kinase 2 (CLK2) [12][47][67][109]. Moreover, cyclin-dependent kinase 5/p35 (CDK5/p35) as well as cyclin-dependent kinase 2/cyclin E (CDK2/E) are also able to phosphorylate CK1 in the regulatory C-terminus. COLO357 cells treated with inhibitors of CDK5/p35 and CDK2/E led to higher CK1δ kinase activity [67]. Regarding forward investigations, Ser-370 was considered as the main target of other cellular kinases-mediated phosphorylation of CK1δ *in vitro* and *in vivo*. Additionally and interestingly, in the development of *Xenopus laevis* embryos expressing the CK1δ^{S370A} mutant, abnormalities have been observed, which insinuate the phosphorylation status of Ser-370 has an important physiological significance [47]. In addition, dephosphorylation mediated by phosphatases can increase CK1 kinase activity [18][48][117].

1.2.3 Biological functions of CK1 isoforms

In recent years, an increasing number of substrates have been identified which are phosphorylated by CK1 isoforms *in vitro* or *in vivo*. The wide range of substrates shows that CK1 family members are involved in multiple cellular processes including circadian rhythm, membrane trafficking, cytokinesis, vesicular transport, ribosome bio-genesis, DNA repair, Wingless (Wnt)-, Hippo (Hpo)- and Hedgehog (Hh)- signaling. In the following chapters, biological functions of the CK1 family in these cellular processes will be discussed in detail.

1.2.3.1 CK1 in circadian rhythm

An autonomous timer, which is known and referred to as the circadian clock, consists of a signal transduction pathway to integrate external signals for time adjustment, as well as

circadian signal inducing oscillator and a signal transduction pathway [80]. The positive regulator clock proteins brain and muscle ARNT- like protein1 (BMAL1) and negative regulator cryptochrome (CRY) as well as the period length modulator prohibitin 2 (PHB2) can be regulated by CK1 isoforms [79]. In general, CK1δ and ε are crucial regulators in circadian rhythm and able to influence the length of the circadian period and the level of Period (PER) degradation. Protein phosphatase 5 (PP5) was observed to dephosphorylate CK1ε, which leads to higher kinase activity [117].

1.2.3.2 CK1 in cellular stress and DNA repair

Under cellular stress, CK1 family members are involved in the regulation of several cellular functions, like DNA repair, cell cycle arrest, and checkpoint signaling through phosphorylating different proteins, for instance, the tumor suppressor protein tumor protein 53 (TP53), mouse double minute 2 homolog (MDM2), ataxia telangiectasia mutated/ ataxia telangiectasia and Rad3-related protein (ATM/ATR), cell division cycle 25 (Cdc25), Chk1, phosphatase and tensin homolog (PTEN), and topoisomerase IIα (TOPO-IIα) [52][54][85][114][121]

Upon DNA damage, CK1α/δ/ε can phosphorylate the tumor suppressor p53, which is mutated or inactivated in about 50% of all tumors and plays a key role in sustaining genomic stability [36][85][103][154]. As a response to stress, phosphorylation of p53 at Ser-15 and Thr-18 by CK1δ and ε leads to disruption of binding affinity between MDM2 and p53, thereby leading to subsequent accumulation of active p53 [55][158][164]. Activated p53 initializes the transcriptional activation of CK1δ, meanwhile, p53 can be activated by CK1δ-mediated phosphorylation. These connections between CK1δ and p53 lead to the conclusion that CK1δ and p53 are regulated via an autoregulatory feedback loop [85] (**Figure 3**). Additionally, as CK1δ/ε and p53 co-localize at the centrosome, the centrosomal functions of p53 seem to be regulated by CK1δ/ε [83][144] .

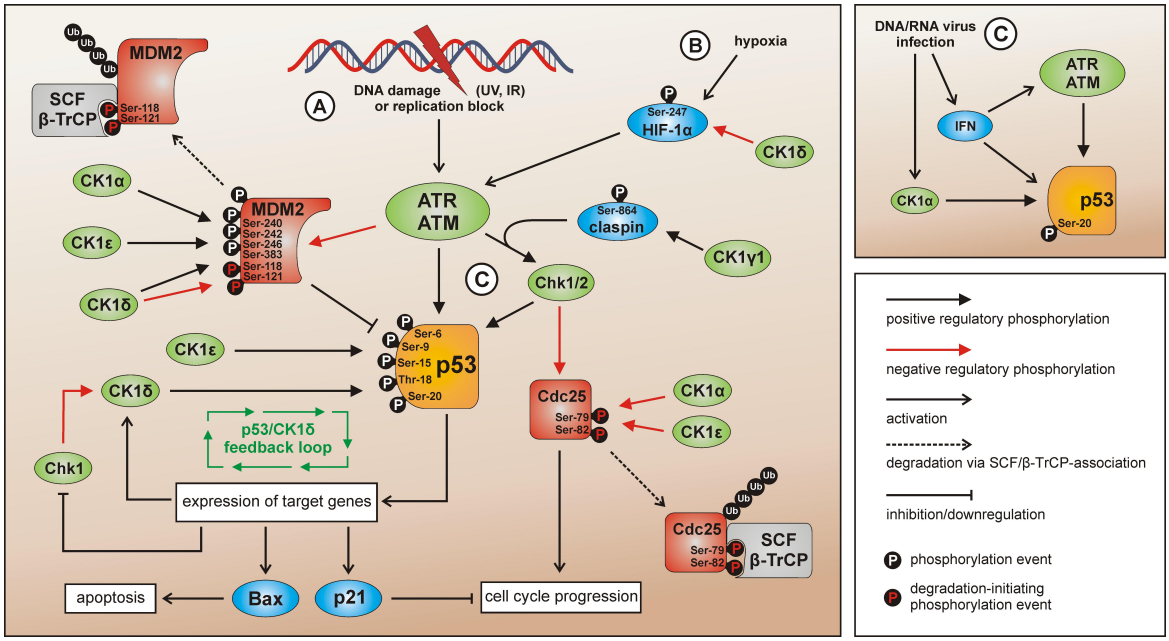

Figure 3: Interaction between CK1 isoforms and DNA damage-induced signal transduction. After DNA damage, the p53-regulatory component MDM2 will be phosphorylated by CK1 α, δ, and ε [36][84][85][154]. While MDM2 is phosphorylated, p53 and Chk1/2 will be activated by ATR/ATM-mediated phosphorylation. CK1δ and CK1ε can activate p53 by site-specific phosphorylation. Activated p53 can initiate the expression of genes, such as Bax, p21. p53 can also trigger the expression of CK1δ, which forms the autoregulatory feedback loop [85]. The binding of Chk1 and claspin, promoted by phosphorylation of claspin by CK1γ1, finally results in activation of Chk1[106]. CK1δ can also regulated HIF-1α, which will initiate the signaling mediated by p53 [78]. After DNA damage, CK1γ1 phosphorylate claspin, which will activate Chk1/2, and phosphorylates Cdc25 at Ser-79 and Ser-82 [62][121], as well as initiates cell cycle progression. Figure obtained from Knippschild et al. [83]. The Figure is licensed under a Creative Commons Attribution 3.0 Generic License http://creativecommons.org/licenses/by/3.0/. **Abbreviations**: CK1: casein kinase 1; p53: protein 53; MDM2: mouse double minute 2 homolog; ATR/ATM: ataxia telangiectasia and Rad3-related protein/ ataxia telangiectasia mutated; Chk1/2: checkpoint kinase 1/2; Bax: Bcl-2-associated X protein; p21: cyclin-dependent kinase inhibitor 1A; HIF-1α: hypoxia-inducible factor 1α; Cdc25:cell division cycle 25; SCF: skp, cullin, F-box containing complex; βTrCP: beta-transducin repeat containing protein; UV: ultraviolet.

Under stress conditions and consequent DNA damage, ATM is activated and then phosphorylates p53 and MDM2. ATM mediated phosphorylation of MDM2 at multiple sites and leads to ubiquitin-mediated degradation of MDM2 [22][111][155]. Therefore, p53 is not further degraded but indicated by its ability to transcriptionally activate various genes like Bcl-2-associated X protein (Bax) and cyclin-dependent kinase inhibitor 1A (p21) in order to intervene for the DNA repair [69][158]. The disruption of the binding affinity between MDM2 and p53 is mediated by both, phosphorylation of p53 at Thr-18 and hyperphosphorylation of MDM2 [36][132][160]. Conversely, higher levels of CK1δ-mediated MDM2 phosphorylation in its p53-central-binding domain resulted in enhanced p53 binding to MDM2 [90]. CK1δ also participates in cellular responses to hypoxia by regulating hypoxia-inducible factors 1α and 2α (HIF-1α, HIF-2 α) [78][116].

Interestingly, CK1α can promote p53 degradation by MDM2-binding and inhibition under normal conditions [65]. Moreover, inhibition or depletion of CK1α as well as inhibition of CK1α-MDM2 interaction was also associated with p53 stabilization and a consequent p53-dependent protective hyperpigmentation in response to sunburn via ultraviolet (UV)-independent pathways [19].

Under consequent DNA damage, CK1γ1 regulates the phosphorylation of claspin, which acts as an adaptor protein critically involved in ATR-mediated activation of Chk1, and finally enhances the binding of claspin and Chk1 [106].

1.2.3.3 CK1 in Hedgehog and Wnt pathways

Hedgehog and Wnt signal transduction pathways have been implicated in embryonic development and tissue homeostasis [75][102]. Deregulation of these signaling pathways can trigger various human diseases including embryonic development like differentiation, organogenesis, proliferation, and morphogenesis [68][76][86]. As some of the pathway components are the same, like GSK3, CK1, and E3 ubiquitin ligase skp, cullin, F-box containing complex (SCF)-Slimb (Slmb)/beta-transducin repeat containing protein (βTrCP), the canonical Hh and Wnt pathways are often considered as “sister” pathways [76].

Hedgehog is an evolutionary and developmental pathway, which regulates a variety of processes like differentiation, proliferation, and organogenesis during embryonic development. It plays a crucial role in regulating epithelial maintenance and organs regeneration in the adult organisms as well [7][68][76][152]. Consequently, mutations or deregulation of Hh pathway can trigger tumorigenesis and is associated with cancer development, including medulloblastoma, gliomas, basal cell carcinomas, gastrointestinal tumors, small-cell lung cancer, and prostate cancer [86][95][159].

The Hh family consists of three homologous ligands including Sonic Hedgehog (Shh), Desert Hedgehog (Dhh), and Indian Hedgehog (Ihh) [17][83]. In absence of Hh ligands, the negative regulatory 12-pass membrane receptor Patched (PTCH) represses the localization of Smoothened (SMO), a downstream protein in the pathway, to the cilia cell surface, consequently resulting in signaling transduction via the glioma-associated oncogene (GLI) transcription factors into the nucleus, which results in the inhibition of the activity of SMO and the induction of transcription of Hh target genes. CK1-, GSK3-, and PKA-mediated phosphorylation of the GLI transcription factors leads to their proteolytic processing into the repressor forms GLI2/3R, which triggers the inactivation of target gene

transcription [33][143]. On the contrary, in the presence of Hh ligands, binding of Hh to PTCH alleviates inhibition of SMO and initiates Hh signaling. Phosphorylation of SMO by G-protein coupled receptor kinase 2 (GRK2) and CK1 leads to accumulation of SMO on the surface of cilia cells and consequently to activation and release of GLI transcription factors from the multi-protein complex, consisting of intraflagellar transport proteins, PKA, GSK3, CK1, and suppressor of fused (SUFU). Activated GLI accumulates in the nucleus and controls the transcription of hedgehog target genes [33][60][76][83][143][162].

CK1 isoforms play both, negative and positive roles in the Hh pathway by regulating the transcription factors Cubitus interruptus (Ci) and SMO [73][74][123]. In the absence of Hh signal, PKA and the F-box protein Slmb are required for Ci processing. Meanwhile, additional phosphorylation of CK1 and Shaggy (Sgg) plays a role in conjunction with PKA to promote Ci processing by SCF^{Slim} E3 ubiquitin ligase [73][74][123]. Interestingly, CK1δ can additionally phosphorylate Ci thereby protecting it from degradation [137]. On the other hand, PKA and CK1α sequentially phosphorylate and activate Smo, with PKA acting as the priming kinase, which will positively influence Hh-signaling [3][74][77] (**Figure 4**).

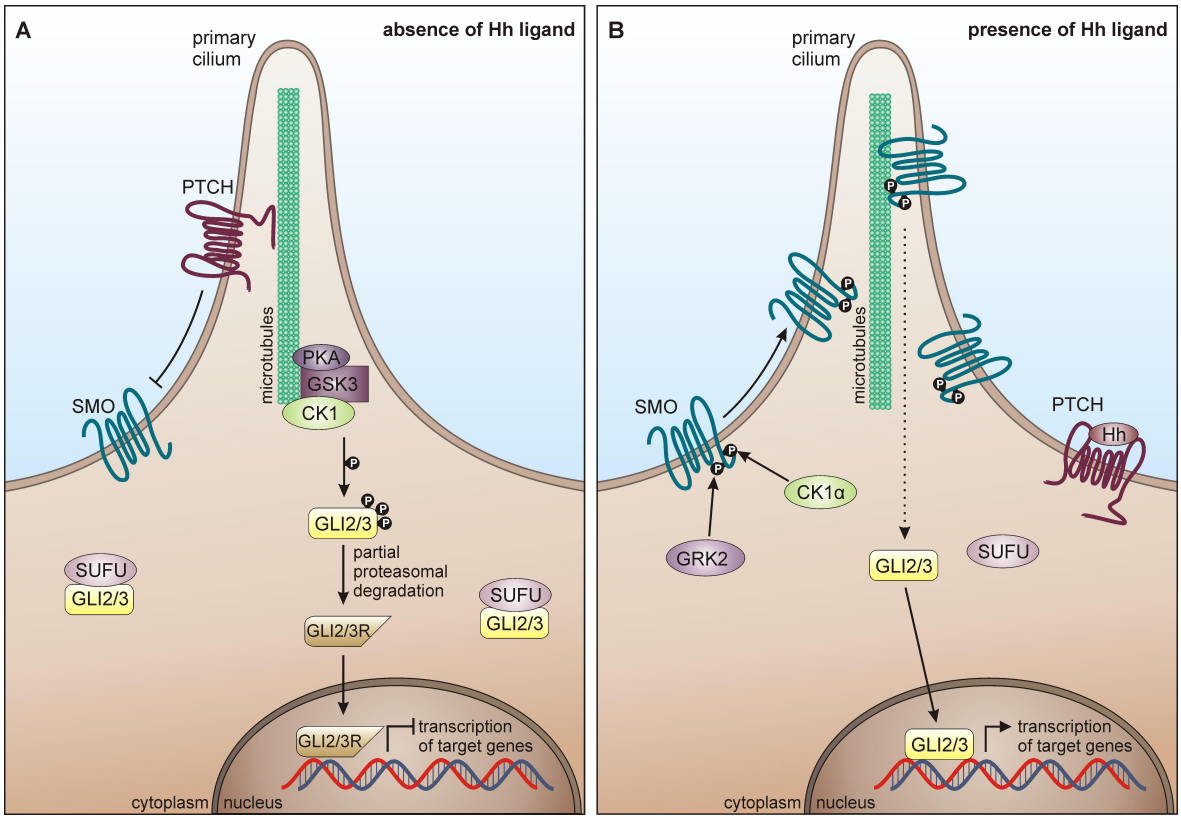

Figure 4: CK1 isoforms in Hh-signaling A: In the absence of Hh ligand, PTCH suppresses the localization of SMO, which results in the inhibition of SMO's activity. GLI transcription factors can be phosphorylated by PKA, GSK3 and CK1, which will generate the repressor forms GLI2/3R and stop transferring the transcription of target genes to the nucleus. B: In presence of the Hh ligand, GRK2

and CK1α phosphorylate and activate SMO, which can elicit a signaling cascade to stimulate the expression of the Hh target genes. Figure obtained from Knippschild et al. [83] The Figure is licensed under a Creative Commons Attribution 3.0 Generic License http://creativecommons.org/licenses/by/3.0/. **Abbreviations:** CK1: casein kinase 1; Hh: Hedgehog; PTCH: Patched; SMO: Smoothened; PKA: protein kinase A; GSK3: Glycogen synthase kinase 3; GLI: glioma-associated oncogene; GRK2: G-protein coupled receptor kinase 2; SUFU: suppressor of fused

It is well known that the Wnt signaling pathway is a conserved pathway which contributes to many processes like tissue patterning, cell proliferation, cell migration, cellular gene expression and stem cell regeneration [76][97]. Wnt signaling is subdivided in a canonical or Wnt/β-catenin dependent pathway and non-canonical or β-catenin-independent pathways [83].

In the canonical Wnt/β-catenin signaling pathway all CK1 isoforms are differently involved. Glycogen synthase kinase 3β (GSK3β), CK1, adenomatous polyposis coli (APC), Axin as well as β-catenin compose the β-catenin destruction complex. In absence of the Wnt ligand, CK1α phosphorylates Axin, APC and β-catenin. Phosphorylated β-catenin can be further phosphorylated by GSK3β. Thereafter, β-catenin will be subsequently degraded [24][148]. In the presence of the Wnt ligand, similar to its role in the Hh pathway, by phosphorylating different pathway components, CK1 also plays both, positive and negative roles in the Wnt pathway [29][77]. Once Wnt ligand binds to Frizzled (FZD), Wnt co-receptor low-density lipoprotein receptor-related protein 5/6 (LRP5/6) can be phosphorylated by CK1γ, which can permit the recruitment of Axin [31]. CK1ε-mediated phosphorylation on Ser-1420 and Ser-1430 of LRP6 negatively regulates the binding of Axin to LRP6 [142] Interestingly, Wnt stimulus will result in higher CK1ε activity because of its lower C-terminal phosphorylation, which represents a feedback loop between CK1ε and Wnt signaling. Moreover, CK1δ and ε can phosphorylate Axin and the scaffold protein Disheveled (DVL), which leads to conformational changes to the β-catenin destruction complex. Then the scaffold protein Axin and the β-catenin destruction complex can be recruited to the cell membrane by phosphorylated LRP5/6, which will introduce a conformational change to β-catenin, thereby preventing β-catenin from being phosphorylated and degraded. Accumulated β-catenin can then be translocated into the nucleus to bind to and to activate T cell factor/lymphoid enhancing factor (TCF/LEF), thereby triggering the transcription of Wnt-related genes (**Figure 5**) [13][113][148].

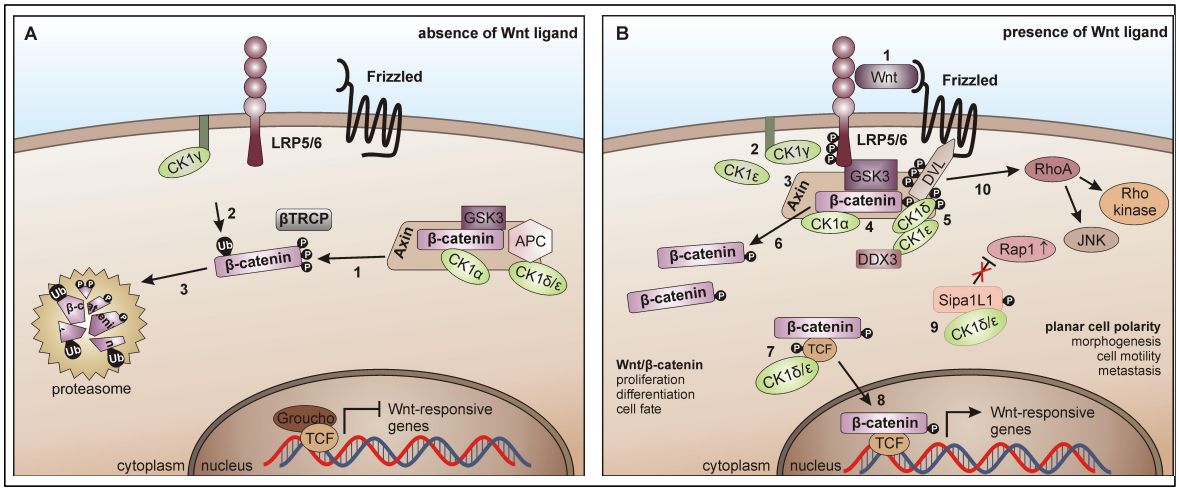

Figure 5: CK1 isoforms in Wnt-signaling. A: In the absence of Wnt ligand, β-catenin, Axin and APC are phosphorylated by CK1 isoforms (1). Then, GSK3β phosphorylated β-catenin, which is recruited to β-TrCP for ubiquitination (2) and subsequently is degraded in the proteasome (3). B: In the presence of a Wnt ligand, upon Wnt ligand binds to FZD (1), CK1γ or CK1ε will phosphorylate LRP5/6 (2). GSK3β gets inactivated as the recruitment of the β-catenin degradation complex (3,4). CK1δ and CK1ε phosphorylate Axin and DVL, which can cause a conformational change of the β-catenin degradation complex (5), and finally resulting in an accumulation of β-catenin (6). CK1δ or CK1ε can also phosphorylate TCF, which will increase the binding to β-catenin and format TCF/β-catenin-complex (7,8). Supplementary, in the non-canonical Wnt pathway, CK1δ and ε can phosphorylate the signal-induced proliferation-associated 1-like protein (Sipa1L1), which can release Ras-related protein 1 (Rap1) from its inhibition and finally result in positive regulation (9). The Ras homolog gene family/ c-Jun N-terminal kinase (Rho/JNK) signal cascade gets activated when DVL is phosphorylated (10). Figure obtained from Knippschild et al. [83]. This Figure is licensed under a Creative Commons Attribution 3.0 Generic License http://creativecommons.org/licenses/by/3.0/. **Abbreviations**: CK1: casein kinase 1; APC: adenomatous polyposis coli; GSK3β: Glycogen synthase kinase 3β; β-TrCP: beta-transducin repeat containing protein; FZD: Fizzled; LRP5/6: lipoprotein receptor-related protein 5/6; DVL: Disheveled; TCF: T cell factor; Sipa1L1: signal-induced proliferation-associated 1-like protein; Rap1: Ras-related protein 1; Rho: Ras homolog; JNK: c-Jun N-terminal kinase.

1.2.3.4 CK1 in the Hippo pathway

The evolutionarily conserved Hippo (Hpo) signaling pathway plays a pivotal role in limiting organ size and restricting tissue growth by controlling cell proliferation and apoptosis. Hence, deregulation of the pathway leads to tissue overgrowth and tumorigenesis [57][107][135].

Under low cell density, Yes-associated protein (YAP) and its co-activator Tafazzin (TAZ) can bind to the transcriptional factors TEA domain (TEAD) and SMA/mothers against decapentaplegic (SMAD), resulting in the activation of Hippo-related genes, which promotes cell growth and differentiation.

Once the Hippo pathway activity is elevated by factors like cell contact inhibition, mammalian STE20-like protein kinase 1/2 (MST1/2), as well as the scaffold proteins vertebrate homolog of *Drosophila* Salvador (WW45) and MOB kinase activator 1A/B

(MOB1A/B) will phosphorylate the large tumor suppressor 1 and 2 (LATS1/2). YAP/TAZ is then phosphorylated by LATS1/2 on Ser-381. Therefore, YAP/TAZ can be spatial separated from its nuclear target transcription factors, such as TEA-domain-containing proteins (TEADs)/Scalloped and Sma- and Mad-related proteins (SMADs), consequently leading to YAP/TAZ ubiquitination and degradation[57][83][174].

Recently, CK1δ and ε were identified as new temporal regulators of Hippo signaling. LATS1/2 primly phosphorylates YAP/TAZ on Ser-381 and provides a signal for CK1δ or ε to phosphorylate YAP on Ser-127, allowing the recruitment of β-TrCP, which finally results in YAP ubiquitination and degradation (**Figure 6**) [83]. Further investigations revealed an interaction of Wnt and Hpo pathways via CK1 and YAP/TAZ [151]. The Hippo upstream kinase MST1 can directly bind to CK1ε and inhibit CK1δ/ε-mediated phosphorylation of Disheveled (DVL), leading to the inhibition of the Wnt/β-catenin pathway [166]. Meanwhile, Wnt-signaling can also be inhibited by the Hpo-pathway effector YAP/TAZ binding to β-catenin, thereby reducing the Wnt-signaling dependent gene transcription [59].

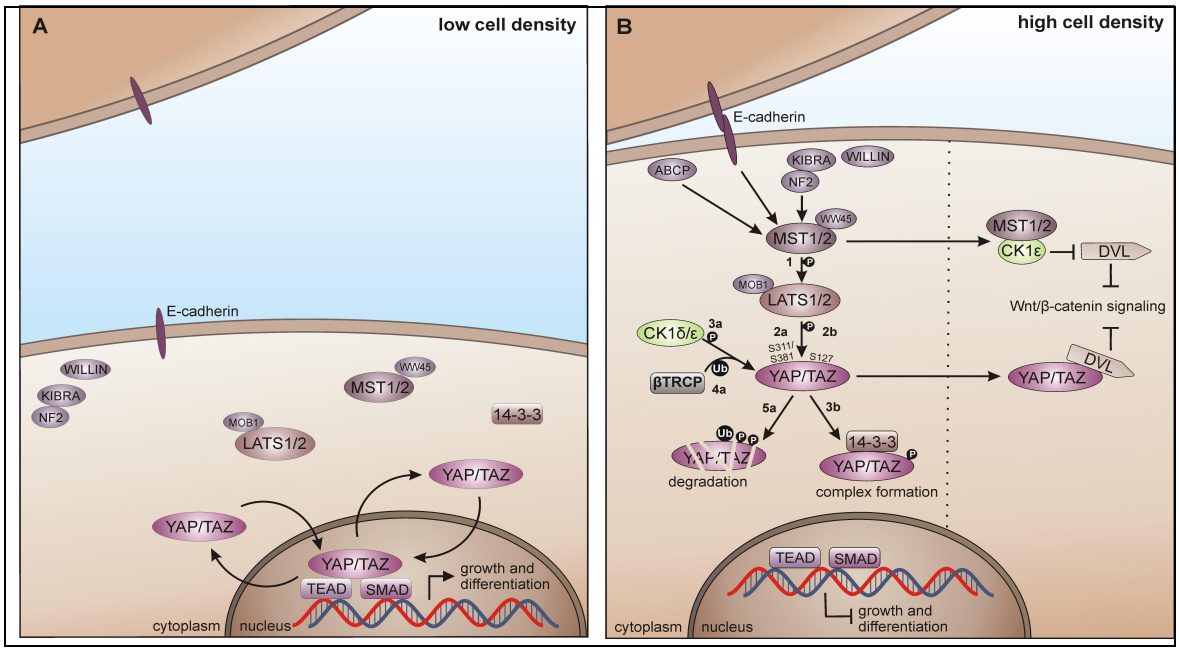

Figure 6: CK1 isoforms in Hpo-signaling. A: Under low cell density, YAP/TAZ can bind to SMADs and TEADs, which will activate Hippo-related genes in the nucleus, and finally leads to tissue growth and cell differentiation. **B**: Under high cell density, several upstream components regulate the high cell-density activated signaling regulation, degradation of YAP/TAZ can suppress YAP/TAZ driven gene transcription by triggering a chain reaction of diverse kinases. Initially, MST1/2 phosphorylates LATS1/2 (1), which can result in the phosphorylation of YAP/TAZ(2a). Then, CK1δ or CK1ε further phosphorylates priming YAP/TAZ (3a), and recruits β-TrCP as well (4a), which will finally result in the degradation of YAP/TAZ (5a). Nevertheless, the formation of 14-3-3-YAP/TAZ-complexes, via the phosphorylation of YAP/TAZ on Ser-127 by LATS1/2 (2a), which prevents YAP/TAZ getting into the nucleus (3b). Inhibition of DVL connects Hippo pathway

and Wnt/β-catenin signalings. Figure obtained from Knippschild et al. [83]. This Figure is licensed under a Creative Commons Attribution 3.0 Generic License. http://creativecommons.org/ licenses /by/3.0/. **Abbreviations**: CK1: casein kinase 1; YAP: Yes-associated protein; TAZ: Tafazzin; SMAD: SMA/mothers against decapentaplegic; TEAD: TEA domain; MST1/2: STE20-like protein kinase 1/2; LATS1/2: large tumor suppressor 1 and 2; β-TrCP: beta-transducin repeat containing protein; DVL: Disheveled

1.2.3.5 CK1 in apoptotic pathways

Apoptosis is a highly regulated process of controlling cell elimination which plays crucial roles in embryonic development and tissue homeostasis. It has been described that several CK1 isoforms are involved in the regulation of apoptotic signal transduction [4].

In the tumor necrosis factor receptor superfamily member 6 (Fas)-mediated apoptotic pathway, CK1 is supposed to phosphorylate the pro-apoptotic protein BH3-interacting domain death agonist (Bid) at amino acids Ser-64 and Ser-66. Once phosphorylated by CK1δ and ε, Bid cannot be processed by initiator caspase 8-mediated proteolysis, thereby Fas-mediated apoptosis is inhibited [35].

CK1 isoforms are involved in additional apoptotic pathways. In the p75-mediated apoptosis, CK1 phosphorylates the p75 neurotrophin receptor (p75NTR), which in turn negatively regulates apoptosis [9]. Furthermore, CK1α has been reported to interact and phosphorylate retinoid X receptor (RXR), one of the retinoic acid receptors, which can regulate cell survival by building heterodimers with nerve growth factor 1B (NGF1B), insulin-like growth factor binding protein 3 (IGFBP-3), and β-catenin. Consequently, RXR agonist-induced apoptosis is inhibited by CK1 activity [104][173]. Moreover, in tumor necrosis factor-related apoptosis inducing ligand (TRAIL)-induced apoptosis, CK1 generates reactive oxygen species (ROS) and activates c-Jun N-terminal kinase (JNK), inducing autophagy mediated by death receptor 5 (DR5), which, consequently, upregulates DR5 finally leading to sensitization of TRAIL and enhancement of TRAIL-induced apoptosis [21].

Additionally, CK1α can phosphorylate Fas-associated protein with death domain (FADD) allowing participation in regulation of non-apoptotic functions of FADD like cell cycle interaction or sensitivity toward chemotherapeutics [1][2].

1.2.3.6 CK1 in the development of different diseases

Due to the involvement of CK1 isoforms in many cellular processes and its interaction with key regulatory proteins of various signal transduction pathways, deregulation or mutations of CK1 isoforms are associated with the pathogenesis of neurological diseases

like Alzheimer's disease (AD), Parkinson's disease (PD) or sleeping disorders, as well as different kinds of cancers [14][38][87][120][122][133][145].

1.2.3.6.1 CK1 in neurodegenerative diseases

Immunohistochemistry and gene expression studies showed that CK1 isoforms are associated with the corresponding specific pathological hallmarks of neurodegenerative diseases, especially tauopathies, such as Alzheimer's disease (AD) [136][171]. AD is an irreversible progressive neurodegenerative disorder characterized by abnormal hyperphosphorylation of the tau protein and increased amyloid-β production. All CK1 isoforms are elevated in the CA1 region of the AD hippocampus, while the CK1δ mRNA level was upregulated more than 30-fold [46][140][171]. CK1δ phosphorylates tau at residues Ser-202/Thr-205 and Ser-396/Ser-404 leading to dissociation of tau from tubulin [34][93]. Moreover, it was demonstrated that CK1 in combination with GSK3 phosphorylates more than 15 sites of paired helicoidal filaments (PHF) tau, which will result in their destabilization and finally in the death of neurons. In addition, overexpression of CK1ε leads to an increase in amyloid-β (Aβ) peptide production, which is accumulated in AD [42].

1.2.3.6.2 CK1 in cancer

Since CK1 family members are involved in various signaling pathways described above, CK1 was considered to exhibit key regulatory functions by modulation key regulatory proteins such as p53, MDM2, and β-catenin. Hence, it is obvious that mutations or deregulation of CK1 is contributing to the development and progression of numerous cancer entities [24][82][83][86] (**Table1**).

As functions of CK1α in tumorigenesis are multi-faceted, it is difficult to classify it as oncogene or tumor suppressor [72][141]. Reduced expression level of CK1α in lymphomas, ovarian, breast, and colon carcinomas, as well as primary melanomas and melanoma metastases was observed compared to the respective benign tissue [141]. Loss of heterozygosity of the CK1α gene causes a highly invasive carcinoma when p53 is inactivated, which indicates that CK1α acts as a tumor suppressor [40]. However, in acute myelogenous leukemia (AML) patients, an increased expression of CK1α was detected, and inhibition of CK1α activity leads to highly selective killing of leukemia stem cells [72].

Overexpression of CK1ε was detected in various cancers like adenoid cystic carcinomas of

the salivary gland, epithelial ovarian cancer, and tumors of brain, head and neck, renal, bladder, lung, prostate, and salivary gland, in leukemia, melanoma, and seminoma [128] [170]. However, the relationship between CK1ε and survival rate is not generalized since it depends on additional factors. Whereas overexpression of CK1ε leads to poor survival in ovarian cancer [128], loss of CK1ε results in shorter survival of patients with oral cancer [94].

It has been shown that CK1δ mRNA is overexpressed in various cancers like breast cancer, kidney cancer, as well as hematopoietic malignancies. The oncogenic features of CK1δ were also confirmed [6][15][112][129]. However, the correlation of expression of CK1δ and the overall survival of patients can lead to different outcomes. While high expression levels of CK1δ are associated with shorter patient`s survival in glioblastoma, lung cancer, and colorectal patients, a high expression of CK1δ correlates with longer patient survival time can be found in breast cancer, chronic lymphocytic leukemia, and astrocytic glioma patients [82].

Table 1: CK1 isoforms in different tumor entities. Adapted from Knippschild et al. 2014. Copyright (2014) Knippschild, Krüger, Richter, Xu, García-Reyes, Peiffer, Halekotte, Bakulev, and Bischof. This table is licensed under a Creative Commons Attribution 3.0 Generic License http://creativecommons.org/licenses/by/3.0/

Isoform	Characteristic feature	Tumor entity	Ref.
CK1α	low/absent expression	lymphomas, ovarian, breast, and colon carcinomas	(Sinnberg et al. 2010)
CK1γ3	altered activity/expression	renal cell carcinoma	(Masuda *et al.* 2003)
CK1δ	increased expression levels	choriocarcinomas	(Stoter et al. 2005)
CK1δ	reduced immunostaining	poorly differentiated breast carcinomas and DCIS	(Knippschild et al. 2005)
CK1δ/ε	elevated protein levels	high-grade ductal pancreatic carcinomas	(Brockschmidt *et al.* 2008)
CK1ε	reduced expression levels	pancreatic ductal adenocarcinoma	(Relles *et al.* 2013)

CK1ε	decreased immunoreactivity	invasive mammary carcinoma	(Fuja *et al.* 2004; Utz *et al.* 2010)
CK1ε	overexpression	breast cancer	(Shin *et al.* 2014)
CK1ε	high gene expression	adenoid cystic carcinoma of the salivary gland	(Frierson *et al.* 2002)
CK1ε	overexpression	epithelial ovarian cancer	(Rodriguez *et al.* 2012)
CK1ε	overexpression	tumors of brain, head and neck, renal, bladder, lung, prostate, leukemia, melanoma, and seminoma	(Yang *et al*. 2008)
CK1ε	loss of cytoplasmic expression	poor prognosis in oral cancer patients	(Lin *et al.* 2014)

1.2.4 CK1 specific inhibitors

Because of the above described involvement of CK1 isoforms in tumorigenesis as well as in neurodegenerative diseases like AD, PD, ALS, and sleeping disorders, interest in the CK1 family as drug targets has increased enormously within the last decade. CK1 inhibitors can be classified into competitive or non-competitive inhibitors depending on the structure of the enzyme-bound antagonist complex [130]. Depending on binding to the active or inactive conformation of the kinase, ATP competitive inhibitors are divided into type I ("DFG-in") and type II ("DFG-out"), which are able to result in lower substrate phosphorylation by binding into the ATP-binding pocket to compete with ATP binding [175]. Type III inhibitors are non-competitive inhibitors, which are also defined as allosteric compounds, because of their binding to a different site of the catalytic cleft next to the ATP-binding pocket. Type IV inhibitors are also non-competitive inhibitors, which can bind covalently and irreversibly to the active site, distant to the ATP-binding pocket of the kinase [130][163]. So far, most of the investigated and characterized CK1 inhibitors belong to ATP-competitive inhibitors and the development of highly effective small molecule inhibitors (SMIs) was the main focus within the last decades. However, as the similarity of CK1δ to other CK1 isoforms (CK1α, γ1- 3, ε) is much high, it is very challenging to design SMIs being specific for CK1δ or ε only.

In 1989, one of the first CK1 inhibitors CKI-7 (N-(2-Aminoethyl)-5-chloroisoquinoline-

8-sulphonamide; IC_{50} ~ 6uM) was developed. However, it did not show any CK1 isoform-specificity, instead it showed some additional effects for CK2 family or even other kinases [25][167]. Later, inhibitor IC261 (3-[(2,4,6- trimethoxyphenyl)-methylidenyl]-indolin-2-one; IC_{50} ~ 1uM) was developed to exhibit a higher potential and selectivity towards CK1δ and ε through binding to the ATP binding pocket [105]. Additionally, it has been demonstrated that the compound has therapeutic potential in xenotransplantation models for pancreatic cancer and neuroblastoma tumors [15][146]. However, unfortunately IC261 has also several off-target effects due to direct binding to microtubles and to block voltage-gated sodium channels [43]. Later, D4476 (4-[4-(2,3-dihydro-benzo[1,4] dioxin-6-yl)-5-pyridin-2-yl-1H-imidazol-2-yl]benzamide), first developed as a transforming growth factor (ALK5) inhibitor, was found to be more selective towards CK1 (IC_{50} ~ 0.3uM) than the well-known IC261 [124].

Based on structure virtual screens, various highly potent CK1-specific inhibitors were identified, among them amino-anthraquinone analogs, roscovitine-, imidazole- and isoxazole- derivatives as well as N6-phenyl-1H-pyrazolo[3,4-d] pyrimidine-3,6-diamine derivatives [115][118][169]. PF-670462 (4-[3-Cyclohexyl-5-(4-fluoro-phenyl)-3H-imidazol-4-yl]-pyrimidin-2-ylamine dihydrochloride), a potent CK1 inhibitor with low isoform selectivity between CK1δ and ε showed positive effects on bipolar disorder, addictive behavior as well as in perturbed circadian behavior [5][81][108]. Moreover, PF-670462 also showed beneficial effects for the treatment of chronic lymphocytic leukemia (CLL) in cells and mouse models, resulting in a longer overall survival [71]. Conversely, PF4800567 (3-(3Chlorophenoxy)methyl]-1-(tetrahydro-2H-pyran-4-yl)-1H-pyrazolo[3,4-D] pyrimidin-4-amine) showed much higher selectivity towards CK1ε than CK1δ with a 22-fold higher inhibition. Stronger inhibition of CK1ε showed anti-proliferative effects in different cell lines [156]. In addition, due to the low IC_{50} value and its ability for brain-penetration, this CK1δ/ε inhibitor showed its potential for treating ALS. Based on its potency in the treatment of ALS, synthesis of small molecule inhibitors has been performed to develop CK1 inhibitors of next-generation.

Additionally, several benzimidazole-based CK1-specific inhibitors have shown their potential and effectiveness to CK1δ and ε, including SR-3029 and SR-2890; Bischof-5 and Bischof-6; Richter-2; IWP-2, IWP-4, and compound 19 [10][11][45][125].

Recently, inhibitors, 3-(2,5-dimethoxyphenyl)-N-(4-(5-(4-fluorophenyl)-2-(methylthio)-

1H-imidazol-4-yl)-pyridin-2-yl)-propanamide (compound 11b) and 4-(2,5-dimethoxyphenyl)-N-(4-5-(4-fluorphenyl)-2-(methylthio)-1H-imidazol-4-yl)-pyridi n-2-yl)-1-methyl-1H-pyrrole-2-carboxamide (compound 16b) were developed as highly selective inhibitors for CK1δ (compound 11b: IC_{50} CK1δ = 4 nM, CK1ε: 25nM ; compound 16b: IC_{50} CK1δ = 8 nM, CK1ε: 81nM), which were also to inhibit proliferation of several pancreatic tumor cell lines [53].

Although most of SMIs are ATP-competitive type I inhibitors, the efficacy of these inhibitors is mediated not only through selective inhibition of CK1δ and ε, but also through the inhibition of CK1α and γ. Interestingly, the inhibition of CK1α seems to have therapeutic effect for myeloid or non-small cell lung cancer (NSCLC) cancer treatment [37][89][149], while activation of CK1α inhibits the pro-oncogenic Wnt-signaling pathway. For CK1γ, some specific inhibitors were also developed, like 2-phenylamino-6-cyano-1H-benzimidazole, which has been identified with an IC_{50} about 140 nM, much lower than for other CK1 isoforms [63].

There are numerous more inhibitors targeting CK1, which are well investigated (**Table 2**) and which have to be explored in the future.

Table2: **Small molecule inhibitors :** IC_{50} values of CK1-inhibitors are listed below and reported in μM. Additional targets of inhibition are also listed. n.p.: not provided.

Inhibitor name	IC_{50} [μM]	ATP [μM]	Additional targets	Reference
CKI-7	CK1 ~ 6-9.5	10	cAPK, CKII, CaM kinase	[25][167]
IC261	CK1 ~ 1	10	mitotic spindle	[105]
D4476	CK1 ~ 0.3	100	ALK5, p38α	[124]
SR-series	CK1 ~ 0.004 -0.260	20	FLT, MYLK, Cdks	[10]
PF-670462	CK1δ: 0.014 CK1ε: 0.008	10	EGFR, SAPK2A/p38	[81][108]
PF-4800567	CK1ε: 0.711 CK1δ: 0.032	10	EGFR	[156]
Bischof-5	CK1δ: 0.040 CK1ε: 0.199	10	CLKs, CK1α, DYRK	[11]
Richter-2	CK1δ: 0.020 CK1ε: 0.210	10	AURK, CLK	[125]
IWP-2	CK1δ: 0.9 CK1ε: 4	10	Porcupine	[45]

11b	CK1δ: 0.004 CK1ε: 0.025	10	n.p.	[53]
16b	CK1δ: 0.008 CK1ε: 0.081	10	n.p.	[53]

1.3 Aim of the study

The highly conserved CK1 family plays crucial regulatory roles in multiple cellular processes from protozoa to human [135]. They are key regulatory enzymes modulating the activity functions and interactions of their target proteins by site-specific phosphorylation. Consequently, dysregulation or mutation of CK1 isoforms within their coding regions contribute to the development of various different pathologies, including severe neurological or proliferative diseases, like cancer [14] [87][122][133][135]. In this contet, CK1 isoforms have become interesting new drug targets.

As a member of the CK1 family, CK1δ was considered as a new drug target because it is often dysregulated in numerous cancers. In addition, numerous human (*hum*) CK1δ mutations were found in human tumour entities, which might contribute to tumour development and progression [91][126][147] (**Figure 7**). One of the investigated mutations of CK1δ is CK1δ^{T67S}, which already showed increased oncogenic potential in colon cancer [126]. However, although lots of CK1δ mutations were found and numerous CK1 inhibitors have been synthesized, it remains challenging to develop inhibitors specific for CK1δ, due to the existence of the highly conserved CK1 isoforms (CK1α, γ1- 3, δ, ε), and for hyperactive CK1δ mutants.

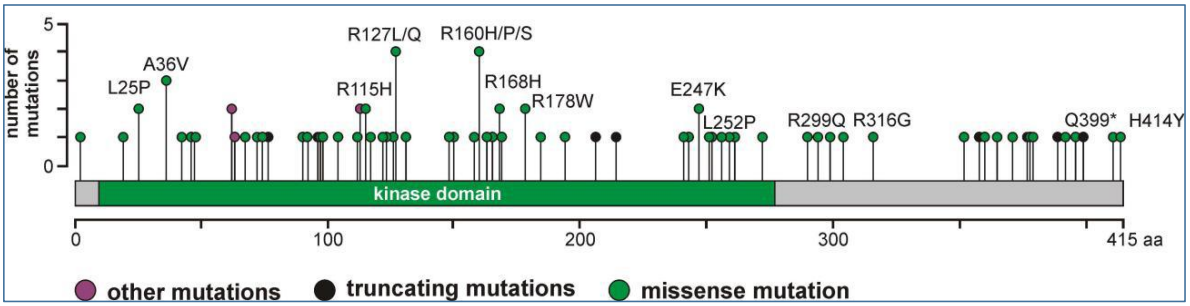

Figure 7: Mutations in CK1δ identified in different types of cancers. (www.cBioPortal.org (Cerami et al., Cancer Discovery (2012); Gao et al., Sci. Signal (2013)). Abbreviations: aa: amino acids, L: leucine; P: proline; A: alanine; V: valine; R: arginine; H: histidine; Q: glutamine; I: isoleucine; M: methionine; S: serine; W: tryptophan; G: glycine; *: stop codon; Y: tyrosine.

Therefore, 17 CK1δ mutants were characterized in regard to their kinase activity and oncogenic potential (**Table 3**).

Table 3: CK1δ mutations identified after a cBioPortal-based search [*Cerami et al., Cancer Discovery (2012); Gao et al., Sci. Signal (2013)***], which have been chosen for further experiments.** CK1δ mutants are listed with the corresponding cancer type where they have been identified. Abbreviations: L: leucine; P: proline; A: alanine; V: valine; R: arginine; H: histidine; Q: glutamine; I: isoleucine; M: methionine; S: serine; W: tryptophan; G: glycine; *: stop codon; Y: tyrosine.

CK1δ mutant	Cancer Type
L25P	Stomach Adenocarcinoma. Lung Adenocarcinoma.
A36V	Colorectal Adenocarcinoma. Esophageal Squamous Cell Carcinoma. Mixed cancer types
R115H	Colorectal Adenocarcinoma. Mixed cancer types. Head and Neck Squamous Cell Carcinoma. Uterine Endometrioid Carcinoma
R127L	Lung Squamous Cell Carcinoma
R127Q	Bladder Urothelial Carcinoma
I148M	Cutaneous Melanoma
R160H	Colorectal Adenocarcinoma. Mixed cancer types
R160P	Colon Adenocarcinoma
R160S	Mixed Cancer Types
R168H	Uterine Endometrioid Carcinoma. Mixed cancer types.Uterine Endometrioid Carcinoma
R178W	Colorectal Adenocarcinoma. Mixed cancer types
E247K	Uterine Endometrioid Carcinoma. Rectal Adenocarcinoma. Uterine Endometrioid Carcinoma
L252P	Mixed Cancer Types
R299Q	Mixed Cancer Types
R316G	Mixed Cancer Types
Q399*	Pancreatic Adenocarcinoma
H414Y	Pancreatic Adenocarcinoma

Within this doctoral thesis, three selected hyperactive mutants, namely CK1δ^{T67S}, CK1δ^{R127Q}, CK1δ^{R168H}, will be characterized.

I. The first part of the doctoral thesis will focus on the screening of established as well as newly designed small molecule compounds as possible selective inhibitors for both, CK1δ wt and CK1δ mutants CK1δ^{T67S}, CK1δ^{R127Q}, CK1δ^{R168H}.

II. Characterization of the susceptibility of these three CK1 mutants to both, known and

newly designed CK1δ inhibitors will allow for the identification of CK1 specific small molecule inhibitors (SMIs) with lower IC_{50} values to the mutants than to *hum*$CK1^{wt}$.

III. Transfection of a CK1δ k.o. Hela cell line with $CK1\delta^{wt}$ and CK1δ mutants will enable the characterization of susceptibility of the transfected cells to both known and newly designed CK1δ inhibitors, and can be used to demonstrate mutant-specific effects of the inhibitors.

2. Materials and Methods

2.1 Materials

2.1.1 Consumables

consumable	manufacturer
Cell culture dish 100 mm	Nunc, USA
Cell culture dish 60 mm	Whatman, England
Cell culture plate 6 well	Sarstedt, Germany
Cell culture plate 12 well	Nunc, USA
Cell culture plate 24 well	Sarstedt, Germany
Cell culture plate 96 well	Sarstedt, Germany
TC Flask T75, standard	Sarstedt, Germany
Cryovials 1.8 ml	Sarstedt, Germany
Filtropur S 0.2 µm (sterile filter)	Sarstedt, Germany
Gelloading tips	Sarstedt, Germany
High performance autoradiography films	GE Healthcare, Germany
Pasteur pipettes	VWR, USA
PCR 8-well-SoftStrips, 0.2 ml	Biozym, Germany
Pipette tips (0.1 – 10 µl)	Eppendorf, Germany
Pipette tips (0.5 – 20 µl)	Eppendorf, Germany
Pipette tips (2 – 200 µl)	Eppendorf, Germany
Pipette tips (100 – 1000 µl)	Eppendorf, Germany
Pipette tips (500 – 5000 µl)	Eppendorf, Germany
Reaction tubes (0.2 ml)	Eppendorf, Germany

Reaction tubes (1.5 ml)	Eppendorf, Germany
Reaction tubes (2 ml)	Eppendorf, Germany
Sarstedt tubes 15 ml	Sarstedt, Germany
Sarstedt tubes 50 ml	Sarstedt, Germany
Serological Stripette® (5 ml)	Corning® Costar, USA
Serological Stripette® (10 ml)	Corning® Costar, USA
Serological Stripette® (25 ml)	Corning® Costar, USA
Whatman® qualitative filter paper	Whatman, England

2.1.2 Chemicals and biochemicals

Chemical	**manufacturer**
Acetic acid	VWR, France
Acrylamide (Rotiphorese® Gel 30)	Carl Roth, Germany
Ampicillin	Carl Roth, Germany
Aprotinin	Sigma-Aldrich, USA
APS	Sigma-Aldrich, USA
ATP	Sigma-Aldrich, USA
[γ-^{32}P]-ATP	Hartmann Analytic GmbH, Germany
Bacto™ Agar	BD Biosciences, USA
Benzamidine	Sigma-Aldrich, USA
Bromphenol blue	Sigma-Aldrich, USA
BSA	Serva, Germany
Coomassie Brilliant Blue R-250	Waldeck/Chroma, Germany
Coumaric Acid	Sigma-Aldrich, USA
DTT	Sigma-Aldrich (Fluka®), USA

DMEM	Gibco® Life Technologies, Scotland
DMSO	Sigma-Aldrich, USA
DPBS	Life Technologies GmbH, Germany
EDTA	Sigma-Aldrich, USA
EGTA	Sigma-Aldrich, USA
Ethanol	Sigma-Aldrich, USA
Ethidium Bromide	Honeywell Fluka, Germany
Fetal bovine serum (FBS)	Biochrom AG, Germany
Formaldehyde	Geyer, Germany
GeneRuler 1kb DNA Ladder	Thermo Scientific, USA
Glutathione Sepharose 4 Fast Flow	GE Healthcare, UK
Glutathione	Sigma-Aldrich, USA
Glycerol	Sigma-Aldrich, USA
Glycine	AppliChem, Germany
G418 sulfate, cell culture	Calbiochem, USA
Hydrochloric acid (HCl, 6 N)	Sigma-Aldrich (Fluka®), USA
IPTG	Fermentas, Germany
Isopropanol	VWR, USA
Luminol	Sigma-Aldrich (Fluka®), USA
Lysozyme	Sigma-Aldrich, USA
L-Glutamine	GE Healthcare, UK
L-Glutathione reduced	Sigma-Aldrich, USA
Methanol	Sigma-Aldrich, USA
Nonfat dry milk	AppliChem, Germany

Nonidet® P 40 (NP40)	Sigma-Aldrich (Fluka®), USA
Penicillin/Streptomycin	Life Technologies GmbH, Germany
Precision Plus Protein™ Standards Dual Color	Bio Rad, Germany
RNase-free H2O	QIAGEN, Germany
Puromycin	Invivogen, France
SDS	Carl Roth, Germany
Silver nitrate	Merck, Germany
Sodium chloride (NaCl)	Sigma-Aldrich, USA
TEMED	Sigma-Aldrich, USA
MTT	Sigma-Aldrich, USA
Tris	USB Europe GmbH, Germany
Trypsin-EDTA	GE Healthcare, UK
Tween-20	Sigma-Aldrich, USA
Yeast extract	Sigma-Aldrich (Fluka®), USA
α-casein	Sigma-Aldrich, USA

2.1.3 Kits

kit	**manufacturer**
AffinityScript Multiple Temperature cDNA Synthesis Kit	Agilent Technologies, USA
Effectene Transfection Reagent	QIAGEN, Germany
Plasmid Plus Midi Kit	QIAGEN, Germany
RNeasy Mini Kit(50)	QIAGEN, Germany

2.1.4 Primers

approach	**primer**	**primer sequence**
His-CK1δ	5'BamH1-His-CK1δ	5'-GGA TCC ATG CAT CAC CAT CAC CAT CAC CCC GGG ATG GAG CTG AGA GTC GGG AAC-3'

	3'EcoR1-CK1δTV1	5'-GAA TTC TCA TCG GTG CAC GAC AGA CTG A-3'
	3'BamH1-CK1δTV2	5'-GGA TCC CTA CTT GCC GTG GTG TTC GAA A-3'

All primers were ordered at Eurofins Genomics, Germany.

2.1.5 Devices

device	**manufacturer**
Biofuge stratos	Heraeus Instruments, Germany
BioMax Autoradiography Cassette	Kodak, USA
BioMetra OV5	Thermo Scientific, USA
CAWOMAT 2000 IR	CAWO, Germany
Centrifuge 5810R	Eppendorf, Germany
Centrifuge 5415R	Eppendorf, Germany
Centrifuge 5417C	Eppendorf, Germany
CERTOMAT® BS-1 Bacterial incubator	Sartorius Group, Germany
CK2 Inverted Microscope	Olympus, Japan
Diaphragm vacuum pump	Vacuubrand GmbH + Co. KG, Germany
Heraeus HeraCell incubator	Thermo Scientific, USA
HERAsafe	Heraeus Instruments, Germany
IKA® KS 260 basic shaker	IKA® Werke GmbH &Co. KG, Germany
Labcycler	SensoQuest, Germany
Liquid scintillation counter LC6000IC	Beckman Coulter, Germany
LUNA™ Automated Cell Counter	Logos Biosystems, Südkorea
Megafuge 1.0R	Heraeus Instruments, Germany
Mini-Protean® Tetra Cell System for SDS-PAGE	BioRad Laboratories, Inc,USA
MP220 pH-meter	Mettler Toledo GmbH, Germany
Pipettes (from 0.1-2.5 µl to 500-5000 µl)	Eppendorf AG, Germany
Pipet boy	Integra Bioscience AG, Switzerland

Plateshake	Wallac,
Power Supply, Model 1000/500	BioRad, Germany
QIAxpert	QIAGEN, Germany
Savant™ Refrigerated Vapor Traps	Thermo Savant, USA
SGD2000 Slab gel dryer	Thermo Savant, USA
Sonifier 250, Branson	Fisher Scientific, USA
Stuart™ Scientific roller mixer SRT1	Sigma-Aldrich, USA
Thermomixer comfort	Eppendorf, Germany
TriStar^2 LB 942 Microplate Reader	Berthold Technologies, Germany
UV bench	Syngene, UK
Water bath W80	Labortechnik Medingen, Germany

2.1.6 Software, online tools and databases

term	**company/URL**
cBioportal	Cbioportal.org
ClustalW	genome.jp/tools-bin/clustalw
GraphPad Prism 6	GraphPad Software
ImageJ	ImageJ Software
MS-Office Package	Microsoft

2.2 Methods

2.2.1 Purification of Glutathione S Transferase (GST) tagged proteins

Expression and purification of GST tagged proteins was performed for producing (*hum)*TV1-CK1δ^{wt}, (*hum)*CK1δ^{R127Q}, (*hum)*CK1δ^{R168H}, (*hum)*TV2-CK1δ^{wt} and (*hum)*CK1δ^{T67S} as recombinant proteins in recombinant Escherichia coli by ITPG.

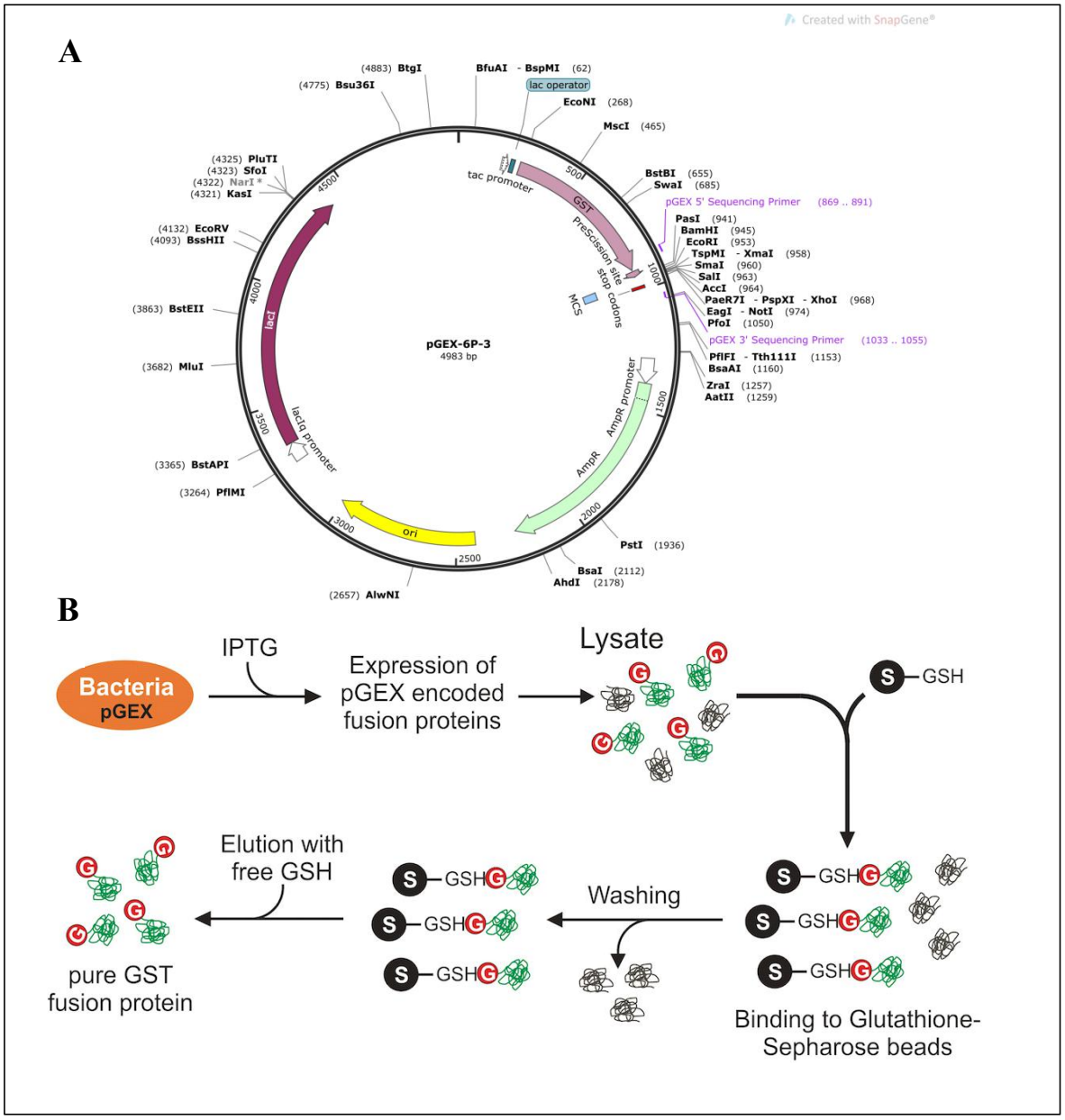

Figure 8: Purification of Glutathione S Transferase (GST)-tagged proteins A: Map of pGEX-6P-3 vector. GST: gens for glutathione-S-transferase (GST), AmpR: gene for ampicillin resistance, MCS: multiple cloning site, ori: origin of replication [http://www.snapgene.com/resources]. B: Flow diagram of the expression and purification of GST-fusion proteins from recombinant bacteria.

XL-1 Blue bacteria previously having been transformed with the respective pGEX expression vector, which was coding for the protein of interest. On the first day,

recombinant bacteria was first inoculated in 50 ml LB-medium (containing 100 µg/ml ampicillin), which was then incubated in the shaking incubators overnight (37°C, 125 rpm). The next day, 400 ml LB-medium (containing 100 µg/ml ampicillin) were added before incubating them for about 1 hour to obtain an optical density (OD) of 0.7 – 0.9 (37°C, 125 rpm).

To induce protein production, 450 µl 0.5 M IPTG was added into the bacteria suspension, activating the Lac promoter and initializing the expression of the fusion protein for 2h at 37°C. However, for expression of CK1 isoforms the bacteria suspension was incubated overnight to reduce inhibiting autophosphorylation (15°C, 125 rpm). Next, the culture was centrifuged at 4000 rpm for 10 min at 4°C. The supernatant was discarded and the pellet was stored at -80 °C for 20 min or overnight. Then, the bacterial pellets were resuspended with 10 ml fresh NP-40 lysis buffer, and transferred into Sorvall tubes. The solution was incubated on ice for 30 min after adding 2.5 mg lysozyme.

After incubating, 10 ml NP-40 lysis buffer were added and cell lysates were sonicated for 2 seconds to break the bacterial DNA, which were later centrifuged for 30 min at 4°C and 10000 rpm. The supernatant was transferred into 50 ml falcon tubes, and 600 µL of PBS/Glutathione Sepharose (1:1) were added. Tubes were rotated for 2h or overnight at 4°C. After rotation, Glutathione sepharose beads with the attached GST-tagged protein were collected by centrifugation for 2 min at 4°C and 3000 rpm. After centrifugation, the pellets were resuspended with 1 ml washing buffer 1 and collected into 1.5 ml Eppendorf tubes. Therefore, the supernatant was discarded and the pellet was washed three times with 1 ml washing buffer 1 and additional two times with washing buffer 2. For washing step, tubes were centrifuged at 14000 rpm for 30 seconds at 4°C. The expressed GST-tagged proteins were then solved in 600 µl elution buffer containing free reduced glutathione and rotated for 20 min at 4°C to increase the elution efficiency of the GST-tagged protein. After rotation, the solution was centrifuged for 1 min at 4°C and 14000 rpm, and the supernatant was transferred into a fresh 1.5 ml Eppendorf tube and stored on ice. To increase the elution efficiency of the GST-tagged protein, this elution step was repeated twice with 300 µl and 150 µl of elution buffer, respectively. The supernatants were all combined and GST-p53$^{1-64}$ and GST-β-catenin$^{1-181}$ proteins were dialyzed in the dialysis solution overnight at 4°C by using dialysis membranes, for a kinase, dialysis was not needed. At last, 10 % glycerol was added to expressed protein before they were shock-frozen in liquid nitrogen and stored at -80 °C.

LB medium	10 g/l NaCl, 5 g/l yeast extract, 10 g/l peptone, sterilized by autoclaving, supplemented with 100 µg/ml ampicillin
NP-40 Lysis buffer	20 mM Tris-HCl [pH 7.6], 150 mM NaCl, 10 % (v/v) glycerol, 0.5% (v/v) NP-40, 1 mM EDTA, 1 mM EGTA, 50 µM benzamidine, 25 µg/ml aprotinin，1 mM DTT,
Washing buffer 1	lysis buffer with 0.2 mM NaCl
Washing buffer 2	20 mM Tris-HCl [pH 7.6], 50 mM NaCl, 10 % (v/v) glycerol, 1 mM EDTA, 25 µg/ml aprotinin
Elution buffer	50 mM Tris-HCl [pH 7.0], 0.1 % (w/v) reduced glutathione, 1 mM EDTA, 25 µg/ml aprotinin
Dialysis solution	50 mM Tris-HCl [pH 7.0], 1 mM EDTA

The concentrations of the purified proteins were analyzed by Coomassie staining (for substrates) or silver staining (for kinases).

2.2.2 Sodium dodecyl sulfate-polyacrylamide gel electrophoresis (SDS-PAGE)

To separate proteins, 12.5 % acrylamide gels, consisting of upper and lower gel, were prepared by using Bio-Rad plates and combs with a thickness of 0.75 mm and SDS-PAGE was performed according to their molecular weight.

Protein samples were prepared with 3 ml 5x SDS loading buffer, then denatured after 5 min at 99 °C and shortly centrifuged to remove condensed liquid from the lid. The samples, as well as the Dual Color standard (1:3 in H_2O) were loaded into the gel pockets. The gel was then placed in an electrophoresis chamber with 1 x electrophoresis running buffer. Electrophoresis separation was started with 80 V for 20 minutes and increased up to 180 V until the end of the run. Afterward, the part of the gel containing the bands of interest was stained either by Coomassie or silver staining.

Upper gel	300 mM Tris-HCl [pH 6.8], 0.19 % (w/v) SDS, 4.4 % (w/v) acrylamide; just before casting the gels 0.06 % (w/v) APS and 0.19 % (v/v) TEMED were added
Lower gel	310 mM Tris-HCl [pH 8.8], 0.19 % (w/v) SDS, 10.0 % / 12.5 % (w/v) acrylamide; just before casting the gels 0.09 % (w/v) APS and 0.063 % (v/v) TEMED were added
Running buffer	250 mM Tris-HCl, 1.9 M glycine, 1 % (w/v) SDS
5x SDS-loading buffer	250 mM Tris-HCl [pH 6.8], 25 % (v/v) β-mercaptoethanol (MSH), 50 % (v/v) glycerol, 10 % (w/v) SDS, 0.5 % (w/v) bromphenol blue

2.2.3 Coomassie staining

In order to quantify and visualize proteins, proteins were stained with Coomassie. After separation of proteins by SDS-PAGE, the gel was stained in Coomassie Brilliant Blue R-250 solution under shaking conditions for 15-20 min. Afterward, gels were transferred to destaining solution for 45 min until unspecifically bound of Coomassie Brilliant Blue was washed out and protein bands were clearly visible. The gel was shortly washed in water before being vacuum dried on a Whatman paper using a gel dryer connected to a cooling trap and a diaphragm vacuum pump at 80°C for 60 min.

Coomassie staining solution	45 % (v/v) isopropanol, 9 % (v/v) acetic acid, 3.0 g Coomassie Brilliant Blue R-250 solved in 1 L dH_2O
Coomassie destaining solution	10 % (v/v) isopropanol, 10 % (v/v) acetic acid in dH_2O

2.2.4 Silver staining

Because of the high sensitivity of proteins to silver ions, silver staining was applied to visualize and determine the concentrations of proteins like GST-CK1δ. For SDS-PAGE, 5 and 10 µl of each purified GST-CK1 solution and 1 µl of the protein ladder Precision Plus Protein™ Standards Dual Color (1:3 in dH_2O) were loaded into the gel pockets. As standard protein dilutions of BSA was loaded also. After electrophoresis, gels were incubated for 1 h in fixation solution 1 and then in fixation solution 2 overnight. After washing 3 times with dH_2O, silver salt-impregnation was performed for 30 min. To remove excess of silver ions, gels were washed in 2.5 % sodium-carbonate solution for 1 min. Subsequently, the gels were developed in developing solution for 5-10 min. the reaction was stopped by adding stop solution whenever the protein bands became clearly visible. After another 3 times of washing with water, gels were conserved in 3 % glycerol for 1 h. Finally, the dried gels were scanned and analyzed by using ImageJ.

fixation solution 1:	30 % ethanol (v/v), 10 % acetic acid (v/v) in dH_2O
fixation solution 2:	0.2 M sodium acetate, 30 % ethanol (v/v), 1.43 ml glutardialdehyde , 400 µl thiosulfate solution (2 %) in dH_2O
silver nitrate solution:	0.2 % silver nitrate (w/v), 25 µl of 37 % formaldehyde in dH_2O
developing solution:	2.5 % sodium carbonate (w/v), 40 µl of 37 % formaldehyde, 40 µl

	thiosulfate solution (2 %) in dH_2O
stop solution:	1 % glycine in dH_2O
conservation:	3 % glycerol in dH_2O

2.2.5 Determination of kinase activity *in vitro*

In vitro kinase assays were performed to verify the kinases' capacity to phosphorylate the respective substrate. For each reaction, GST-CK1α, γ, δ , or ε served as enzyme and α-casein as substrate. The kinase buffer contained 10 µM ATP and 2 µCi [γ-^{32}P]-ATP. After mixing all reagents, reactions were incubated at 30°C for 30 min and stopped with 3 µl of 5x-SDS-loading buffer. Then the samples were heated at 95°C for 5 min and shortly centrifuged before loading into the gel pockets and separating by SDS-PAGE. Gels have been stained with Coomassie staining and dried with a gel dryer as described in chapters 2.2.2 and 2.2.3. Thereafter, dried gels were exposed to an X-ray film until the radioactively labeled substrate bands became highly visible depending on the kinases and substrates. The phosphorylated substrate bands were cut, and put into scintillation tubes to perform Cherenkov counting. The resulting data were analyzed and evaluated by the software GraphPad Prism 6.

Kinase buffer with ATP (10x)	250 mM Tris-HCl [pH 7.5], 100 µM ATP, 100 mM $MgCl_2$, 1 mM EDTA
5x SDS-loading buffer	250 mM Tris-HCl [pH 6.8], 25 % (v/v) β-mercaptoethanol (MSH), 50 % (v/v) glycerol, 10 % (w/v) SDS, 0.5 % (w/v) bromphenol blue

2.2.6 Determination of inhibitory effects of CK1 specific inhibitors *in vitro*

In vitro kinase assays were performed to detect the effects of inhibitors on the purified GST-CK1 isoforms (α, γ_3, δ, and ε) and various GST-CK1δ mutants. Inhibitors IWP2, IWP4 (Cayman Chemical, Ann Arbor, USA), 11b, 16b (Hakelotte et al., 2018), Richter-2 (Richter et al., 2014), Bischof-5 (Bischof et al., 2012), LKP-091, LKP-104, LKP-105, LKP-106, LKP-112, LKP-114, LKP-115, LKP-116 (provided by Prof. Christian Peifer, Kiel, Germany, see **table 4**) as well as DMSO control were used. IC_{50} values of selected inhibitors were tested on CK1δ wt by using different concentrations of the tested compound.

2 µl of each inhibitor dilution was laid on the bottom of the 1.5 ml reaction tube. 3 µl of the respective kinase was pipetted on the rear edge of the reaction tube. At last, 10 µl of the Master Mix (MM: 1.5 µl 10 x kinase buffer with 100 µM ATP, 0.4 µl -casein, 0.2µl [γ–^{32}P]-ATP and 7.9 µl dH_2O) was pipetted at the front edge of the reaction tube (**Figure 9**).

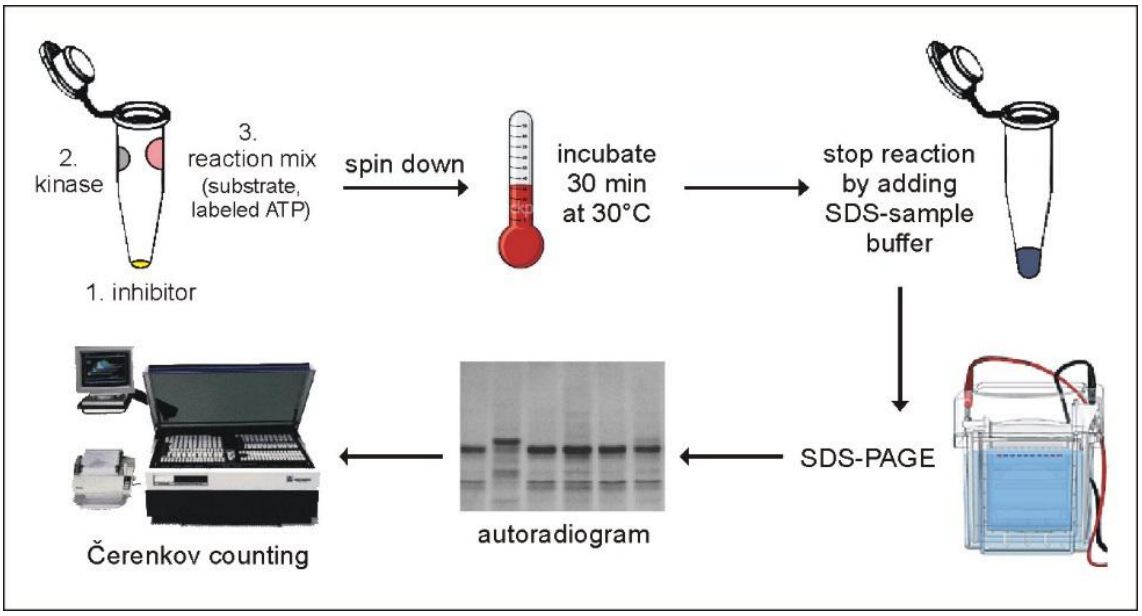

Figure 9: Procedure of *in vitro* kinase reaction for *in vitro* kinase assay. Kinase, inhibitor, and reaction mix were added to a 1.5 ml reaction tube separated from each other and mixed by short centrifugation. The reaction was stopped after incubation for 30 minutes at 30°C by addition of SDS loading buffer. Subsequently, reactions are separated by SDS-PAGE, exposed to X-ray film, and transfer of radioactive phosphate into substrate proteins is quantified by Čherenkov counting.

Thereafter, the reaction was started after spinning down all reagents by centrifugation. Afterward, the same incubation, staining and drying as well as analysis procedures were performed as described in chapter 2.2.5.

Table 4: Chemical structures of the newly designed inhibitors. Structures are modified from [96], CC BY 4.0, https://creativecommons.org/licenses/by/4.0/

Code	Structure	Code	Structure
LKP-091	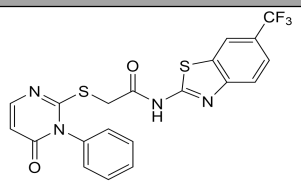	LKP-112	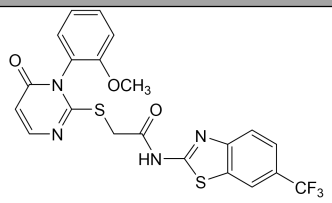
LKP-104	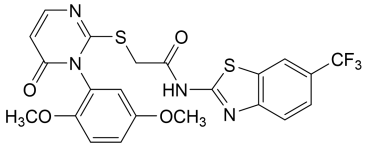	LKP-114	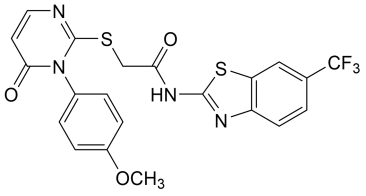

LKP-105	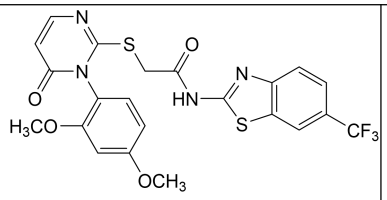	LKP-115	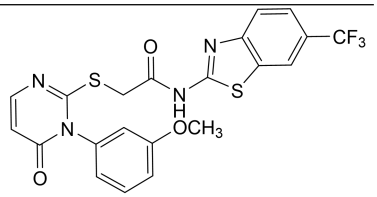
LKP-106	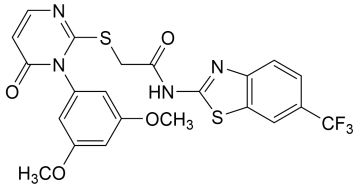		

2.2.7 Determination of IC_{50} values

To determine the IC_{50} values of an inhibitor for GST-CK1 isoforms kinase assays were performed by using the respective compound in serial dilutions ranging from 5 nM to 10 µM and DMSO as control (**Table 5**).

Then the experiment continued as described above and the resulting data was analyzed using GraphPad Prism 6. The sigmoidal dose-response (variable slope) function was selected to obtain the respective IC_{50} value after normalizing the data.

Table 5: Inhibitors serial dilutions

Final concentration (End volume 15 µl)	working dilutions	#
10.00 µM	2 µl 10 mM + 266.66 µl DMSO	1
5.00 µM	50 µL #1 + 50 µL DMSO	2
2.50 µM	50 µL #2 + 50 µL DMSO	3
1.25 µM	50 µL #3 + 50 µL DMSO	4
625 nM	50 µL #4 + 50 µL DMSO	5
313 nM	50 µL #5 + 50 µL DMSO	6
156 nM	50 µL #6 + 50 µL DMSO	7
78 nM	50 µL #7 + 50 µL DMSO	8
39 nM	50 µL #8 + 50 µL DMSO	9
20 nM	50 µL #9 + 50 µL DMSO	10
10 nM	50 µL #10 + 50 µL DMSO	11
5 nM	50 µL #11 + 50 µL DMSO	12

2.2.8 Cell lines and cell culture

Hela$^{CK1\delta-/-}$ cells (CSNK1D Knockout Hela Cell Line catalogue no. CL0012906502A, EdiGene, China) were grown in Dulbecco's modified eagle medium (DMEM), supplemented with 10 % (v/v) fetal calf serum (FCS), 100 units/ml penicillin and 100

µg/ml streptomycin and additional 1µg/ml Puromycin. Cells were cultured in 100 mm cell culture dishes, respectively, and placed in an incubator with 5 % carbon dioxide (CO_2) at 37°C. Cells were passaged each 2-3 days whenever the cells gained about 80 % confluence. Cells were washed with Dulbecco's Phosphate Buffered Saline (DPBS) and treated with trypsin for 5 min at 37°C. The reaction was stopped by adding fresh medium. A ratio of 1:4 - 1:6 was selected for a subcultivation and seeded in 100 mm cell culture dishes with fresh medium.

2.2.9 G418 selection

G418 is routinely used in gene selections to screen for resistant mammalian cells which express the neo gene. First, Hela$^{CK1\delta-/-}$ (EdiGene, China) cells were seeded in a 6-well plate at the density of 100,000 cells/ml and incubated for 24 h at 37°C. After incubation, the medium was gently removed and 1.5 ml medium containing varying concentrations of G418 (0, 0.1, 0.2, 0.3, 0.4, 0.5, 1.0, 1.5, 2.0, 2.5, 3.0, 3.5 mg/ml) was added. Thereafter, cells were further incubated at 37°C. The selective medium was refreshed every 3-4 days until determining the lowest concentration of G418 that kills a large majority of the cells within 14 days.

2.2.10 Transfection

The transfection of TV1-CK1δ^{wt}, TV2-CK1δ^{wt}, CK1δ^{R127Q}, CK1δ^{R168H}, CK1δ^{T67S} in Hela$^{CK1\delta-/-}$ cells was performed by using Effectene (QIAGEN, Germany) as transfection reagent. Vector pcDNA^{TM} 3.1/V5-His TOPO was selected because of bearing neomycin and kanamycin resistance, allowing selecting of possible clones.

On the day before transfection, 2-8*10^5 cells were seeded in 60 mm dish with 5 ml appropriate growth medium containing serum and antibiotics. Incubate the cells under normal growth conditions (37 ℃ and 5% CO_2) until the transfection day when the cells gained approximately 40 - 80 % confluence.

The day of transfection, diluted 1 µg of the desired DNA with buffer EC to get a final volume of 150 µl. Then 8 µl Enhancer was added into the Eppendorf tube and vortexed for 1 s. After 2-5 min incubation at room temperature, the DNA-enhancer mixture was centrifuged for 10s to remove drops from the top of the tube. Hereafter, add 25 µl Effectene transfection reagent into the mixture and mixed by vertexing for 10 s. Then the samples were incubated for another 5 min to allow transfection-complex formation. While

complex formation took place, the consumed medium was aspirated from the plate and 4 ml fresh growth medium was added after cells had been washed once with 4 ml PBS. After incubation, 1 ml growth medium was added into the tube containing the transfection complexes and mixed by pipetting up and down twice, instantly transferring the transfection complexes drop-wise onto the cells. Finally, the dishes were gently swilled to ensure uniform distribution of the transfection complexes. Transfected cells were then grown under normal growth conditions. After 48 h, transfected cells were passaged 1:5 in 100 mm dishes with the appropriate selective G418 containing medium (DMEM supplemented with 10 % (v/v) Fetal Calf Serum (FCS), 1 % penicillin (10000 units/ml), 1 % streptomycin (10000 µg/ml) and additionally 0.6 mg/ml G418 for Hela cells). Change the selection medium 2-3 times a week until clones appeared.

2.2.11 Picking of stably transfected clones

When a single cell clone had been formed, cells were rinsed with 7 ml PBS after gently aspirating the medium. After marking the single clone place with a marker pen, a yellow pipette tip was used to oblique scrap and suck the cells as well as to transfer them into 96-wells plate containing the appropriate selective medium. After picking up and transferring the transfected cells into a 96-wells plate, cells were incubated at 37 °C and 5% CO_2 conditions until 80% confluence was contained in each well. The procedure of splitting cells for transferring them to the next larger plate, which passed from 96 well-plate to 24 well-plate, 12 well-plate, 6 well-plate and 60 mm cell culture dishes up to 100 mm cell culture dishes is described in chapter 2.2.9.

cell culture vessels	Medium [ml]	DPBS [ml]	trypsin/EDTA [µl]
96 well-plate	0.2	0.1	50
24 well-plate	0.5	0.5	250
12 well-plate	1	1	250
6 well-plate	2	2	250
60mm cell culture dish	4	3	500
100mm cell culture dish	10	7	1000

2.2.12 Purification of total RNA

RNeasy Mini Kit (QIAGEN, Germany) was used for purification of total RNA. After harvesting cells with a number of $7*10^6$, the cell pellet was solved in buffer RLT, which was then pipetted into a QIAshredder spin column to homogenize the cell lysate under centrifugation for 2 min at full speed. After mixing the homogenized lysate with 600µl of 70% ethanol, the mixture was transferred into a RNeasy spin column to perform a centrifugation for 15 s at ≥ 10,000 rpm. Afterward, the flow-through after centrifuging for 15 s was discarded. The pellet was washed once with buffer RW1 and twice with buffer RPE. In each case after centrifugation, the supernatant was discarded. Finally, to elute the total RNA, 50 µl RNase-free water was added into the RNeasy spin column, which was placed in a 1.5 ml collection tube and centrifuged for 1 min at full speed. The QIAxpert (QIAGEN, Germany) was used to detect the concentration of purified total RNA.

2.2.13 First-strand cDNA synthesis

The first-strand cDNA synthesis reaction in a microcentrifuge tube was prepared by adding the following components in order:

1 µg of total RNA
1 µl of oligo(dT) primer (0.5 ug/ul)
RNase-free water to total volume 15,7 µl

The reactions were incubated for 5 min at 65 °C after a short low-speed centrifugation, which was later cooled down to room temperature to allow primers to anneal to the RNA. Before starting the cDNA program by using Labcycler (SensoQuest, Germany), the following components were added into the reaction for a final volume of 20 µl.

2.0 µl of 10 x Affinity script RT Buffer
0.8 µl of dNTP mix (25 mM each dNTP)
0.5 µl of RNase Block Ribonuclease Inhibitor (40 U/µl)
1 µl of Affinity Script Multiple Temperature RT

The program cDNA performed:

Temperature (°C)	Time (min)
42	5
55	60
70	15

Finally, the first-strand cDNA synthesis reactions were completed and stored at -20 °C.

2.2.14 Polymerase chain reaction (PCR)

In order to amplify the destination sequence, PCR was performed as below. 1 µl of template DNA and 24 µl of master mix were used to get a total volume of 25 µl. 2.5 µl of 10x PCR buffer, 250 µM of dNTPs, 100 nM of forward primers and reverse primers, and 2.5 U of Taq DNA polymerase were contained in each master mix solution. All reactions were transferred to Labcycler (SensoQuest, Germany) after briefly mixing and low-speed centrifugation, then a PCR program was performed with the cycling parameters given in **Table 6**.

Table 6: PCR cycling parameters

product	primers	PCR conditions		
		temperature	duration	cycles
CK1δ full length	5'BamH1-His-CK1δ 3'EcoR1-CK1δTV1 or 3'BamH1-CK1δTV2	94°C	10 min	
		94°C 62°C 72°C	1 min 1 min 1 min	35x
		72°C	10 min	
		4°C	∞	

The amplified cDNA samples were loaded into the well of 1% agarose gel, which was separated at 80 V for 1.5 h. UV light system and UV bench were used to visualize DNA fragments.

2.2.15 Preparation of cell extracts

In order to detect protein by Western blot analysis, pre-cooled DPBS were used to wash the stably transfected cells twice. After adding NP40 lysis buffer, cells were then scraped from

the culture dish and transferred into a 1.5 ml Eppendorf tube, which should keep on ice and incubate for 30 min. The supernatant was collected after cell lysates were centrifuged for 15 min at 14,000 rpm and 4 °C, which was used for the corresponding experiment.

NP40 lysis buffer	50 mM Tris-HCl [pH 8.0], 120 mM NaCl, 0.5 % NP40, 10 % glycerol, 5 mM DTT, 1 mM EGTA, 1 mM benzamidine, 25 µg/ml aprotinin

2.2.16 Determination of protein concentrations

Protein concentrations of cell lysate were determined by Pierce® BCA Protein Assay kit (Thermo Scientific, Germany) after lysing cellsby NP40 lysis buffer. First of all, dilute the BSA protein stock to prepare 0.1, 0.3, 0.5, and 0.7 µg/µl protein standards. Then cell lysates were diluted in 1:20 with dH_2O. After adding 10 µl of H_20/BSA/sample dilution and 200 µl of the A: B (50:1) solution in the appropriate well (96-well plate), incubate the 96-well plate for 30 min at 37 °C. The measurement of the protein concentration was performed after incubation by using the Berthold Tristar and analysis with BCA-template excel file.

Table 7: Pipetting scheme-Berthold Tristar

H_2O	0.1	0.3	0.5	0.7	Sample 1	Sample 2	Sample 3	Sample 4	Sample 5	Sample 6	Sample 7
H_2O	0.1	0.3	0.5	0.7	Sample 1	Sample 2	Sample 3	Sample 4	Sample 5	Sample 6	Sample 7
H_2O	0.1	0.3	0.5	0.7	Sample 1	Sample 2	Sample 3	Sample 4	Sample 5	Sample 6	Sample 7
Sample 8	Sample 9	Sample 10	Sample 11	Sample 12	Sample 13	Sample 14	Sample 15	Sample 16	Sample 17	Sample 18	Sample 19
Sample 8	Sample 9	Sample 10	Sample 11	Sample 12	Sample 13	Sample 14	Sample 15	Sample 16	Sample 17	Sample 18	Sample 19
Sample 8	Sample 9	Sample 10	Sample 11	Sample 12	Sample 13	Sample 14	Sample 15	Sample 16	Sample 17	Sample 18	Sample 19
Sample 20	Sample 20	Sample 20	Sample 21	Sample 21	Sample 21	Sample 22	Sample 22	Sample 22	Sample 23	Sample 23	Sample 23
Sample 24	Sample 24	Sample 24	Sample 25	Sample 25	Sample 25	Sample 26	Sample 26	Sample 26	Sample 27	Sample 27	Sample 27

2.2.17 Western Blot analysis

In each case 20 µg of the respective protein extract as well as positive and negative control were first separated by SDS-PAGE as described in chapter 2.2.2 and blotted to a pre-activated PVDF membrane in a wet blot Western blot system (BioRad Laboratories, Hercules, USA), filled with 1x transfer buffer, for 1.5 hours at 60 V and 4°C. Thereafter, incubate the transferred PVDF membrane 1 h at room temperature with 5 % (w/v) milk in TBS-Tween (TBST) to block unspecific binding sites. The membrane was probed with the appropriate primary antibodies (diluted in blocking solution) and incubated overnight at

4°C. After three times washing with TBST for 5 min, the membrane was incubated 1 h at room temperature with the secondary antibod. After another three times washing for 5 min with TBST, ECL (enhanced chemiluminescence) solution (solution A: solution B in ratio of 1:1) was prepared to detect proteins on the membrane, while a radiographic film was used to expose the detected proteins.

10x TBS:	200 mM Tris-HCl [pH 8.0], 1.4 M NaCl in dH_2O
TBS-Tween:	0.1 % (v/v) Tween-20 in 1x TBS
Blocking solution	5% milk powder in TBST
ECL solution A	100 mM Tris-HCl [pH 8.5], 2.5 mM luminol, 400 µM coumaric acid
ECL solution B	100 mM Tris-HCl [pH 8.5], 13 mM H_2O_2
10x Transfer buffer	500 mM Tris, 780 mM glycine in dH_2O

Table 8: Antibodies

Primary	**Manufacturer**
β-actin monoclonal antibody	Sigma-Aldrich, St. Louis, USA
His-Tag Polyclonal Antibody	Cell Signaling Technology, Frankfurt, Germany
Secondary	**Manufacturer**
Anti-rabbit IgG, HRP-linked Antibody	Cell Signaling Technology, Frankfurt, Germany
Anti-mouse IgG, HRP-linked Antibody	Cell Signaling Technology, Frankfurt, Germany

2.2.18 MTT viability assay

To determine cell viability, MTT viability assays were performed. The MTT assay is a colorimetric assay, based on the reduction of the yellow tetrazole dye in the purple formazan.

Under sterile conditions, 200 µl PBS were added to the two external rows and cells ($5*10^4$ cells/well) were seeded in 96-wells plates according to **Figure 10** and incubated overnight at 37 °C and 5 % CO_2. Replace the old medium with fresh medium with desired inhibitor for treatments and cells were incubated another 48 h (**Figure 10**). After adding 10 µl filtered, sterile MTT reagent (5 mg/ml, diluted in PBS) into each well, the cells were incubated for 4 h at 37 °C and 5 % CO_2. 100 µl of acidic isopropanol (180 ml isopropanol + 20 ml 1N HCl) was added into each well after the medium was removed. Then, the plates were covered with aluminum paper and shaken at room temperature for 30 min. TriStar^2 LB 942 Microplate Reader (Berthold Technologies, Bad Wildbad, Germany) plate

reader was used for measurement of absorbance, while GraphPad Prism 6 was used for the resulting data analysis.

MTT solution	5 mg/ml MTT in PBS
Acidic isopropanol	90 % (v/v) isopropanol, 10 % (v/v) 1N HCl

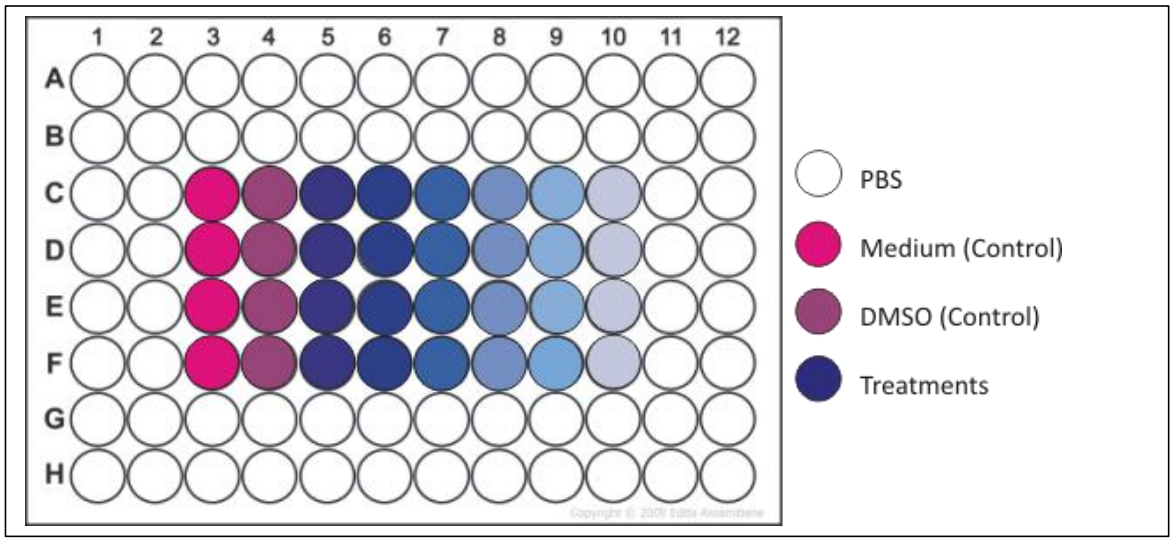

Figure 10: Management for 96-well plate: 200µl PBS was added to the two external rows, in the middle rows, respective medium, DMSO and treatments were added. **Abbreviations**: PBS: Phosphate Buffered Saline; DMSO: dimethyl sulfoxide.

3. Results

Since expression and/or activity of CK1δ are often deregulated in tumors, CK1δ is a new potential target for the development of highly specific inhibitors, which could be used for therapeutic purposes. Although interests in small molecule inhibitors (SMIs) against CK1δ has increased, it is still very challenging to develop highly isofprm-specific SMIs, due to the high similarity of CK1δ to other CK1 isoforms (CK1α, $\gamma_{1\text{-}3}$, ε). Therefore, a set of newly designed CK1-specific inhibitors was screened for their effects on CK1 isoforms. Furthermore, based on the cBioPortal database, human hyperactive CK1δ mutants were identified in various tumor entities and may have an oncogenic potential. Therefore, three tumor-derived mutations detected within the kinase domain of CK1δ were selected and used to identify small molecule inhibitors exhibiting a higher affinity to CK1δ mutants than to wt CK1δ.

3.1 Introduction of selected mutations into *hum*CK1 δ on pcDNA™ 3.1/V5-His TOPO®

First, human CK1δ mutants CK1δ^{R127Q} and CK1δ^{R168H} were introduced into the full length human CK1δ transcription variant 1 (TV1) while the human CK1δ mutant CK1δ^{T67S} was introduced into the full length human CK1δ transcription variant 2 (TV2) by site-directed mutagenesis as described in Material and Methods. Success of mutagenesis was confirmed by sequencing. An alignment of wt and mutant CK1δ proteins of the outlined sequence is shown in **Figure 11**.

CK1δ variants	Sequence (aa 51-100)
CK1δ_TV2_T67S	IESKIYKMMQGGVGIPS IRWCGAEGDYNVMVMELLGPSLE DLFNFCSRKF
CK1δ_TV2_wt	IESKIYKMMQGGVGIPT IRWCGAEGDYNVMVMELLGPSLEDLFNFCSRKF
	********** ********** ********** **********
	Sequence (aa 101-150)
CK1δ_TV1_R127Q	SLKTVLLLADQMISRIEYIHSKNFIHQDVKPDNFLMGLGKKGNLVYIIDF
CK1δ_TV1_R168H	SLKTVLLLADQMISRIEYIHSKNFIHRDVKPDNFLMGLGKKGNLVYIIDF
CK1δ_TV1_wt	SLKTVLLLADQMISRIEYIHSKNFIHRDVKPDNFLMGLGKKGNLVYIIDF
	********** ********** ********** **********
	Sequence (aa 151-200)
CK1δ_TV1_R168H	GLAKKYRDARTHQHIPYHENKNLTGTARYASINTHLGIEQSRRDDLESLG
CK1δ_TV1_R127Q	GLAKKYRDARTHQHIPYRENKNLTGTARYASINTHLGIEQSRRDDLESLG
CK1δ_TV1_wt	GLAKKYRDARTHQHIPYRENKNLTGTARYASINTHLGIEQSRRDDLESLG

********** **********

Figure 11 : Protein sequence alignment of human CK1δ variants (aa 51-200). The alignment was performed using the online tool ClustalW. The position of the desired mutations is highlighted and the mutated amino acid is marked in red. **Abbreviations**: CK1: casein kinase 1; wt: wild type; TV: transcription variant; aa: amino acid.

3.2 Expression and purification of recombinant GST fusion proteins

For further comparison of the kinase activity and features of CK1δ wt and mutants, (*hum*)TV1-CK1δ^{wt}, (*hum*)TV2-CK1δ^{wt} and (*hum*)CK1δ^{R127Q}, (*hum*)CK1δ^{R168Q} as well as (*hum*)CK1δ^{T67S} were expressed as GST fusion proteins in *E. coli*, purified by affinity chromatography and eluted by addition of reduced glutathione as described in Material and Methods. The concentrations of purified CK1δ wt and mutants were determined densitometrically with ImageJ software after performing SDS-PAGE and silver staining. Besides, for protein quantification, a BSA standard curve was generated (**Figure 12**).

Because of the differences in the phosphorylation states of the different GST-(*hum*)CK1δ proteins, there are two bands with different intensity between 73 and 75 kDa (**Figure 12**). The concentrations determined for GST-(*hum*)CK1δ wt and mutants are displayed in **Table 9**.

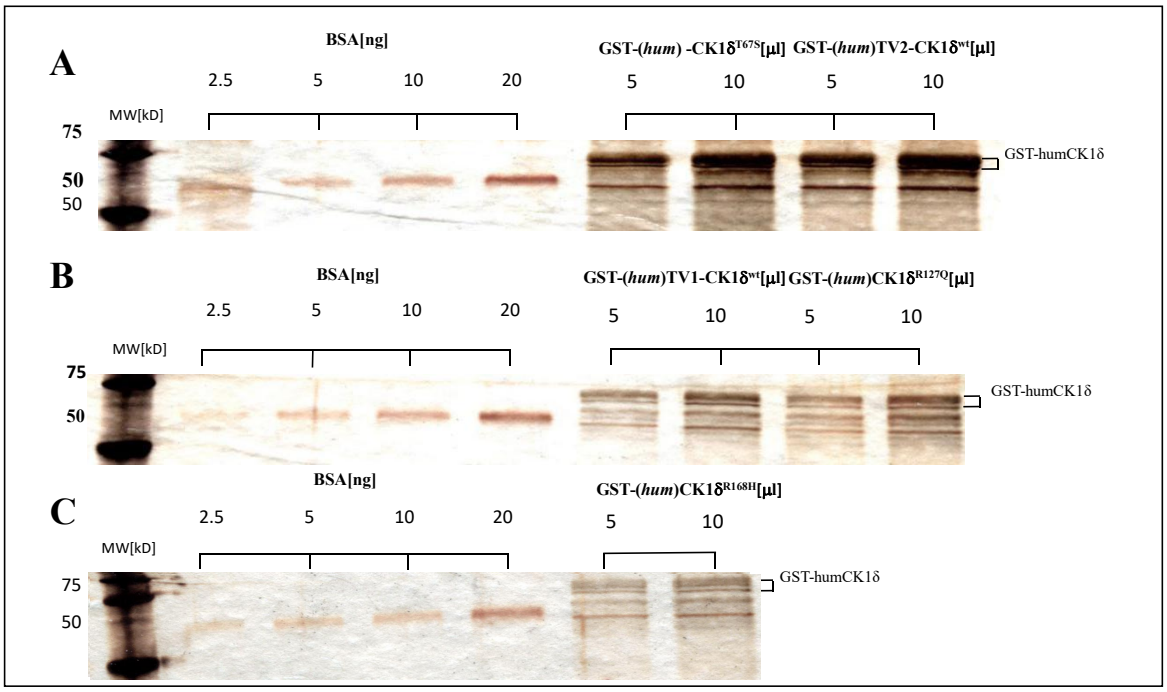

Figure 12 : Densitometric quantification of GST-CK1δ variants after silver staining. Silver staining was performed as described in Material and Methods to determine the concentration of purified GST-(*hum*)CK1δ proteins separated by SDS-PAGE. BSA standard dilutions are visible at the size of

~ 69 kDa, while GST-CK1δ variants show two bands between 73 kDa to 75 kDa due to differences in their degree of site-specific phosphorylation. **A**: GST-CK1δ variants: BSA standard with amounts of 2.5 ng, 5 ng, 10 ng and 20 ng, GST-(*hum*)CK1^{T67S} and GST-(*hum*)TV2-CK1δ^{wt} with volumes of 5µl and 10µl are used. **B**: GST-CK1δ variants: BSA standard with amounts of 2.5 ng, 5 ng, 10 ng and 20 ng, GST-(*hum*)TV1-CK1δ^{wt} and GST-(*hum*)CK1δ^{R127Q} with volumes of 5µl and 10µl are used. **C**: GST-CK1δ variants: BSA standard with amounts of 2.5 ng, 5 ng, 10 ng and 20 ng, GST-(*hum*)CK1δ^{R168H} with volumes of 5µl and 10µl are used. Molecular Weight (MW): Precision Plus Protein^{TM} Standards Dual Color (10-250 kDa). **Abbreviations**: CK1: casein kinase 1; TV: transcription variant; GST: glutathione S transferase; MW: molecular weight; SDS-PAGE: sodium dodecyl sulfate-polyacrylamide gel electrophoresis; hum: human; kDa: kilo Dalton; BSA: bovine serum albumin.

Table 9: Concentrations of purified GST-(*hum*)CK1 proteins as determined by ImageJ analysis.

Kinases	concentration [ng/µl]
GST-(*hum*)TV1-CK1δ^{wt}	1.009
GST-(*hum*)CK1δ^{R127Q}	1.115
GST-(*hum*)CK1δ^{R168H}	1.399
GST-(*hum*)TV2-CK1δ^{wt}	3.271
GST-(*hum*)CK1δ^{T67S}	4.786

3.3 Effects of small molecule inhibitors on the activity of (*hum*)CK1δ wild type and mutants.

Since it has been shown that several CK1δ mutants contribute to tumor development due to their higher oncogenic potential compared to CK1δ wt, interest in identifying small molecule inhibitors with higher affinity against CK1δ mutants than against CK1δ wt has increased enormously. Therefore, the inhibitory capacity of the CK1δ specific inhibitors **Richter-2** (Richter et, al., 2014), **Bischof-5** (Bischof, J, et, al., 2012), **11b** and **16b** (Halekotte J, et al., 2016), **IWP-2** and **IWP-4** (Garcia-Rheyes et al., 2018) against CK1δ wt and mutants were compared in *in vitro* kinase assays at their IC_{50} concentrations previously determined for GST-(*hum*)TV1-CK1δ^{wt} using α-casein as substrate.

A

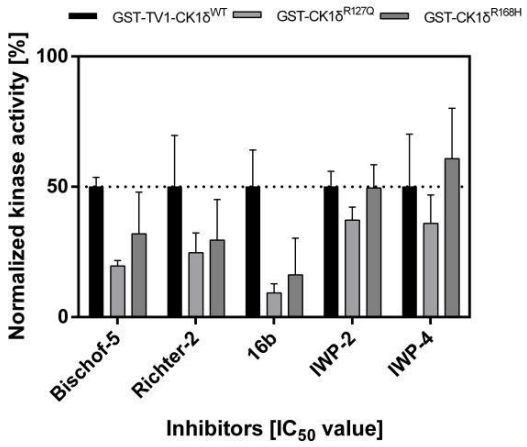

B

#	Residual kinase activity (%)		
	GST-(hum)TV1-CK1δ^{wt}	GST-(hum)CK1δ^{R127Q}	GST-(hum)CK1δ^{R168H}
Bischof-5	50 ± 4	20 ± 2	32 ± 15
Richter-2	50 ± 20	25 ± 8	30 ± 16
16b	50 ± 14	9 ± 4	16 ± 14
IWP-2	50 ± 6	37 ± 5	50 ± 9
IWP-4	50 ± 20	36 ± 11	61 ± 19

C

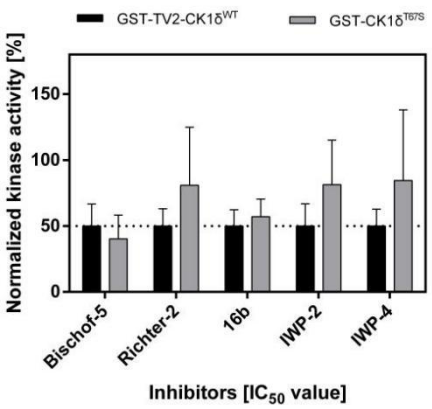

D

#	Residual kinase activity (%)	
	GST-(*hum*)TV2-CK1δ^{wt}	GST-(*hum*)CK1δ^{T67S}
Bischof-5	50 ± 17	40 ± 18
Richter-2	50 ± 13	80 ± 43
16b	50 ± 12	57 ± 13
11b	50 ± 33	62 ± 50
IWP-2	50 ± 17	81 ± 34
IWP-4	50 ±13	84 ± 54

Figure 13：Inhibitory effects of the compounds Richter-2; Bischof-5; 16b; 11b, IWP-2, and IWP-4 on GST-(*hum*)CK1δ wt and GST-(*hum*)CK1δ mutants: *In vitro* kinase assays were performed to determine the effects of selected compounds on GST-(*hum*)TV1-CK1δ^{wt} and GST-(*hum*)CK1δ mutants GST-(*hum*)CK1δ^{R127Q} and GST-(*hum*)CK1δ^{R168H} (**A, B**) as well as on GST-(*hum*)TV2-CK1δ^{wt} and GST-(*hum*)CK1δ^{T67S} (**C, D**). Samples were separated by SDS-PAGE. Coomassie stained and phosphate incorporation into α-casein was determined by Cherenkov counting. Results were normalized to the DMSO control (100%) using Prism 6. Bar graphs represent the mean and the standard deviation (SD) of the triplicates. **B:** Residual kinase activity of GST-(*hum*)TV1-CK1δ wt and mutants after treatment with inhibitors. **D:** Residual kinase activity of GST-(*hum*)TV2-CK1δ wt and mutants after treatment with inhibitors. Modified from [96], CC BY 4.0. https://creativecommons.org/licenses/by/4.0/ **Abbreviations**: CK1: casein kinase 1; TV: transcription variant; hum: human; GST: glutathione S transferase; SDS-PAGE: sodium dodecyl sulfate-polyacrylamide gel electrophoresis; DMSO: dimethyl sulfoxide; SD: standard deviation.

The results presented in Figure 14 A and B indicate that GST-(*hum)*CK1 δ ^{R127Q} was stronger inhibited by all tested inhibitors compared to GST-(*hum*)TV1-CK1δ^{wt}, thereby displaying 20 %, 25%, 36%, 9%, 37%, 36% residual activities, respectively. In contrast, only **Bischof-5**, **Richter-2** and **16b** inhibited GST-(*hum*)CK1δ^{R168H} stronger than GST-(*hum*)TV1-CK1δ^{wt}, with residual activities of 32%, 30% and 16%, respectively. Compared to GST-(*hum*)TV2-CK1δ^{wt}, GST-(*hum*)CK1δ^{T67S} was only stronger inhibited by **Bischof-5**, resulting in a residual activity of 40% compared to 50% obtained for GST-(*hum*)TV2-CKδ^{wt} (**Figure 13**).

3.4 Determination of IC50 values against GST-(*hum*)CK1δ wt and GST-(*hum*)CK1δ mutants

Since the initial screening results indicated that **Bischof-5** and **16b** had a much higher inhibitory effect on GST-(*hum*)CK1δ^{R168H} and GST-(*hum*)CK1δ^{R127Q} than on GST-(*hum*)TV1-CK1δ^{wt}, the IC_{50} values of these two compounds were determined using a serial inhibitor dilution in each case ranging from 5 nM to 10 µM (**Figure 14**). GST-(*hum*)TV1-CK1δ wt and GST-(*hum*)CK1δ mutants were used as source of enzyme and α-casein as substrate (0.8 µg/reaction) in the presence of 2 µCi [γ-^{32}P]-ATP, 10 µM ATP, and the specific CK1δ inhibitors **Bischof-5** or **16b**.

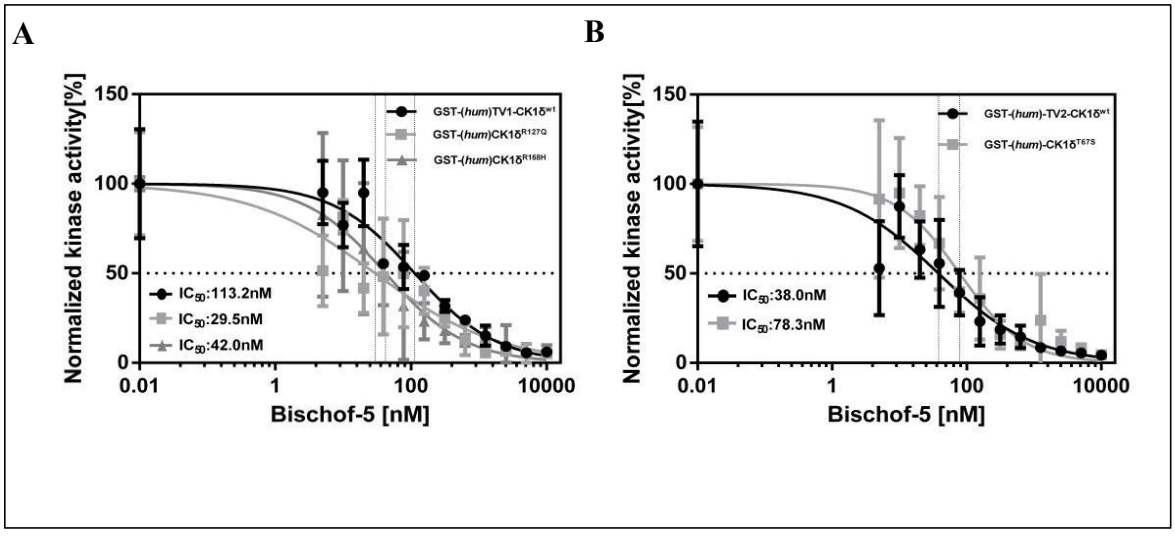

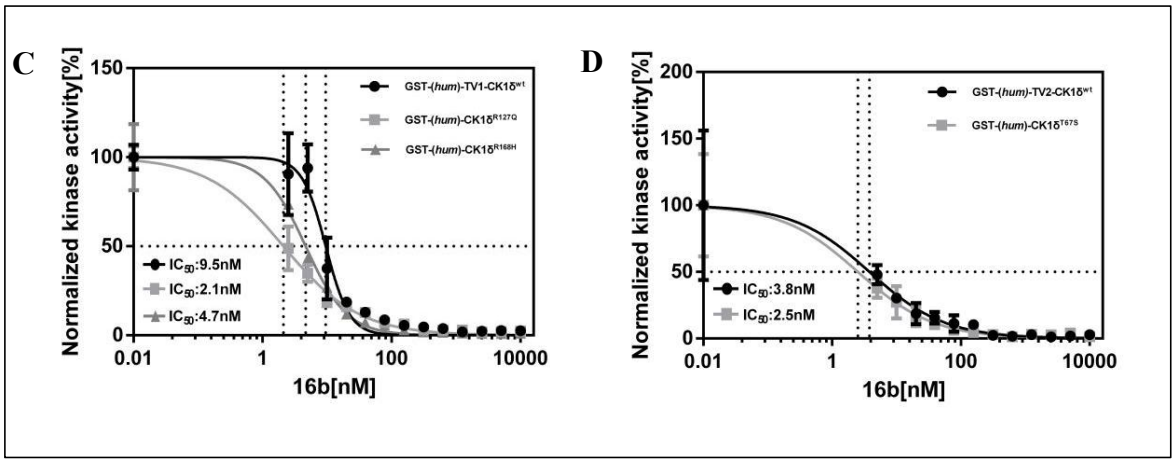

Figure 14: Determination of the IC_{50} values of Bischof-5 (A, B) and 16b (C, D) for GST-(hum)CK1δ wt and mutants. Serial dilutions ranging from 5 nM to 10 µM of **Bischof-5** and **16b** were used to determine the 50% inhibitory concentration (IC_{50}) for GST-(hum)CK1δ wt and mutants. **A:** IC_{50} value of **Bischof-5** for GST-(*hum*)TV1-CK1δ^{wt}, GST-(*hum*)CK1δ^{R127Q} and GST-(*hum*)CK1δ^{R168H}. **B:** IC_{50} value of **Bischof-5** for GST-(*hum*)TV2-CK1δ^{wt} and GST-(*hum*)CK1δ^{T67S}. **C:** IC_{50} value of **16b** for GST(*hum*)TV1-CK1δ^{wt}, GST-(*hum*)CK1δ^{R127Q} and GST-(*hum*)CK1δ^{R168H}. **D:** IC_{50} value of **16b** for GST(*hum*)TV2-CK1δ^{wt} and GST-(*hum*)CK1δ^{T67S}. Phosphorylated samples were separated by SDS-PAGE, stained with Coomassie. Phosphate incorporation into α-casein was quantified by Cherenkov counting. Results were normalized to the DMSO control (100%) using Prism 6. Bar graphs represent the mean and the standard deviation (SD) of the triplicates. Modified from [96], CC BY 4.0. https://creativecommons.org/licenses/by/4.0/ **Abbreviations**: CK1: casein kinase 1; TV: transcription variant; hum: human; SDS-PAGE: sodium dodecyl sulfate-polyacrylamide gel electrophoresis; DMSO: dimethyl sulfoxide; GST: glutathione S transferase; IC_{50}: 50% inhibitory concentration.

In **Figure 14**, IC_{50} values of **Bischof-5** and **16b** against GST-(*hum*)TV1-CK1δ^{wt}, GST-(*hum*)CK1δ^{R127Q}, GST-(*hum*)CK1δ^{R168H}, GST-(*hum*)TV2-CK1δ^{wt} and GST-(*hum*)CK1δ^{T67S} are presented. **Bischof-5** showed a higher inhibitory effect on both TV1-CK1δ mutants compared to GST-(*hum*)TV1-CK1δ^{wt}, while the highest inhibitory effect was observed on GST-(*hum*)CK1δ^{R127Q}, resulting in an approximately 3-fold lower IC_{50} value than that of GST-(*hum*)TV1-CK1δ^{wt}. In addition, **16b** also inhibited both TV1-CK1δ mutants stronger than GST-(*hum*)TV1-CK1δ^{wt}. The determined IC_{50} values were 4.5-fold reduced for GST-(*hum*)CK1δ^{R127Q} and 2-fold reduced for GST-(*hum*)CK1δ^{R168H} compared to GST-(*hum*)TV1-CK1δ^{wt} (**Figure 14** and **Table 10**). For both inhibitors, no stronger inhibition of GST-(*hum*)CK1δ^{T67S} than GST-(hum)-TV2-CK1δ^{wt} was observed.

Table 10: IC_{50} values of compounds Bischof-5 and 16b for GST-(*hum*)TV1-CK1δ^{wt}, GST-(*hum*)CK1δ^{R127Q} and GST-(*hum*)CK1δ^{R168H} are presented in nM with their respective standard deviation (SD).

Compounds	GST-(*hum*)-TV1-CK1δ^{wt}	GST-(*hum*)CK1δ^{R127Q}	GST-(*hum*)CK1δ^{R168H}
Bischof-5	113.2 nM ± 0.08	42.2nM ± 0.14	71.1 ± 0.09
16b	9.5 nM ± 0.04	2.1 nM ± 0.05	4.7 ± 0.02

3.5 Validation of newly designed CK1 small molecule inhibitors

Although numerous CK1δ inhibitors have been already developed, there is still the need for improving their selectivity for CK1δ, especially for more specifically inhibiting highly oncogenic CK1δ mutants, as well as improving their chemical stability, and cell permeability. In this chapter, several newly synthesized small molecule inhibitors, designed and developed by the working group of our cooperation partner Prof. Peifer (University of Kiel) will be characterized and analyzed. Their chemical structures are shown in **Table 4**. Due to the strong effects of IWP-derivatives on the CK1δ gatekeeper mutant (García et al., 2018), new IWP-derivatives have been tested for these hyperactive mutants (T67S (Richter et al., 2015), R127Q, R168H). These compounds were tested for *in vitro* selectivity for CK1 isoforms, potency for inhibiting CK1δ mutants and regarding their ability to inhibit proliferation of tumor cell lines. The results are presented in the following chapters.

3.5.1 *In vitro* effects of LKP_compounds on CK1 isoforms activity

The inhibitory potency of **LKP**_compounds against four CK1 isoforms has been first screened using 10 µM of each compound in *in vitro* kinase assays. CK1α, γ, δ, and ε were used as a source of enzyme and α-casein as substrate (0.8 µg/reaction) in the presence of 2µCi [γ-^{32}P]-ATP, 10 µM ATP, and 10 µM of the tested compound. Kinase activities of four CK1 isoforms (CK1α, γ, δ and ε) in the absence and presence of the indicated **LKP**_compounds are shown in **Figure 15**.

A

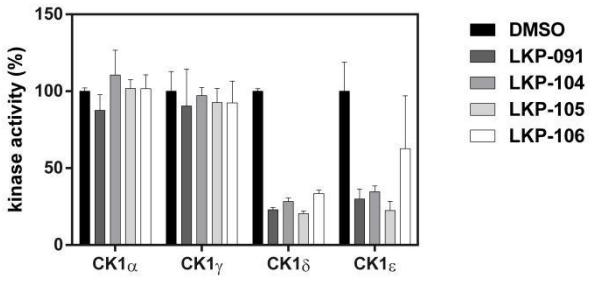

B

#	Residual kinase activity (%)			
	CK1α	**CK1γ**	**CK1δ**	**CK1ε**
LKP-091	87.5 ± 3.4	90.4 ± 8.0	23.0 ± 0.5	29.9 ± 2.2
LKP-104	90.4 ± 8.0	97.2 ± 1.7	28.3 ± 0.8	34.7 ± 1.3
LKP-105	101.8 ± 1.9	92.7 ± 3.0	20.4 ± 0.6	22.4 ± 2.0
LKP-106	101.7 ± 3.0	92.4 ± 4.7	33.5 ± 0.8	42.8 ± 0.7

Figure 15: Inhibitory effects of LKP_compounds against CK1 isoforms. **A:** *In vitro* kinase assays were performed to determine the effects of **LKP**_compounds **LKP-091**, **LKP-104**, **LKP-105**, and

LKP-106 against CK1α, γ, δ, and ε isoforms to verify their specificity as well as potency for CK1δ and ε. Phosphorylated samples were separated by SDS-PAGE, and stained with Coomassie. Phosphate incorporation into α-casein was determined by Cherenkov counting. Results were normalized to the DMSO control (100%) using Prism 6. Bar graphs represent the mean and the standard deviation of the triplicates. **B:** Residual activity of four CK1 isoforms after treatment is summarized. Modified from [96], CC BY 4.0. https://creativecommons.org/licenses/by/4.0/ **Abbreviations**: CK1: casein kinase 1; SDS-PAGE: sodium dodecyl sulfate-polyacrylamide gel electrophoresis; DMSO: dimethylsulfoxide; SD: standard deviation.

All newly designed **LKP**_compounds showed strong inhibitory effects on CK1δ and ε, but almost no inhibitory effects on CK1α and γ (**Figure 15A** and **B**). Moreover, highest inhibitory effects were observed on CK1δ kinase activity, which was inhibited more than 67-80 %, while CK1ε kinase activity was inhibited from 58% to 78 % (**Figure 15B**).

3.5.2 Determination of IC_{50} values of LKP_compounds against GST-(*hum*)CK1δ

Regarding to its strong inhibitory effects against CK1δ, IC_{50} values of **LKP**_compounds for CK1δ were determined using a serial inhibitor dilution in each case ranging from 5 nM to 10 µM as described in Materials and Methods. GST-(*hum*)TV1-CK1δ^{wt} was used as a source of enzyme (1µg/reaction), while α-casein was used as substrate (0.8 µg/reaction) in the presence of 2 µCi [γ-^{32}P]-ATP and 10 µM ATP.

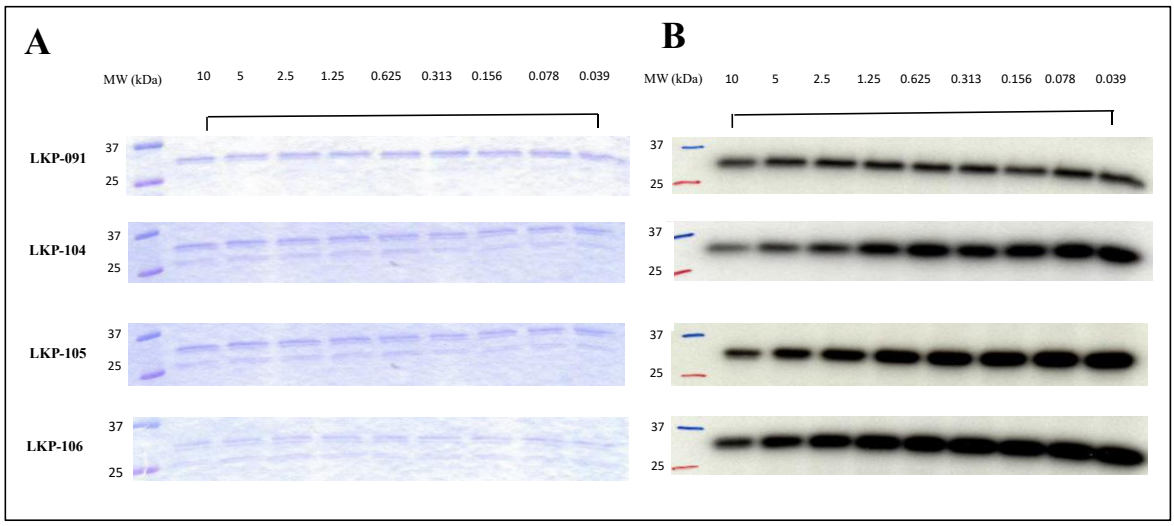

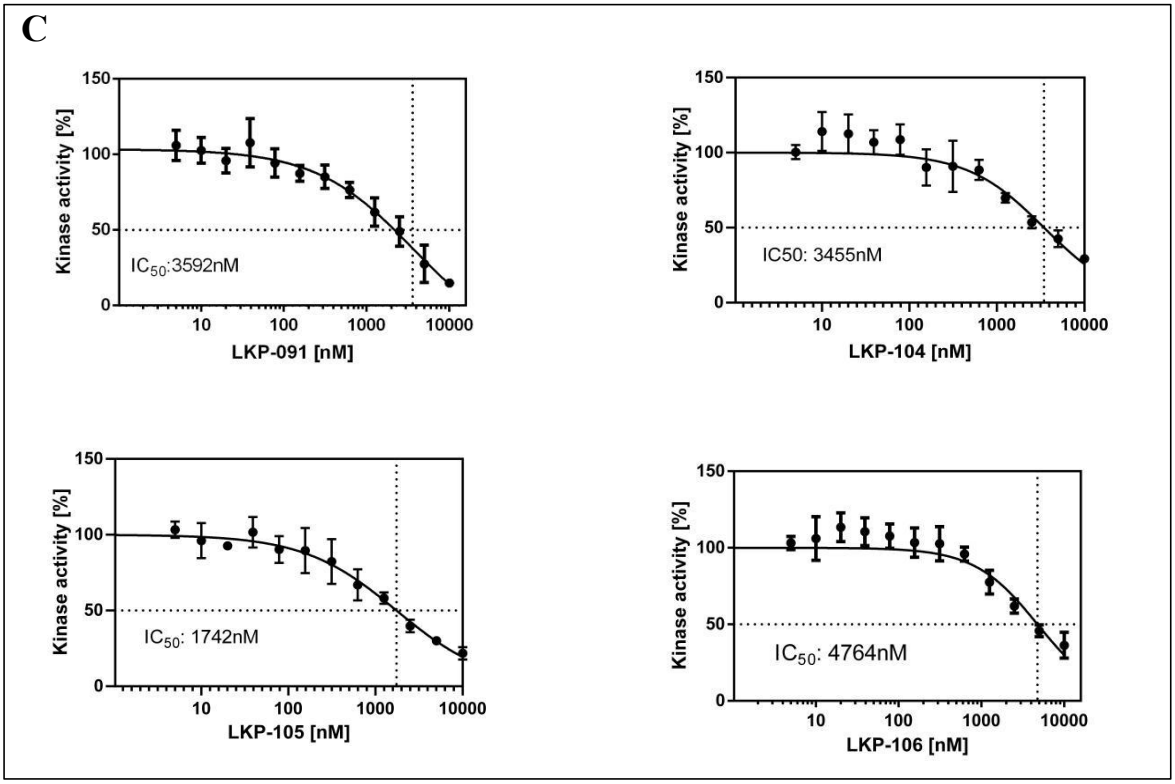

Figure 16: IC_{50} values of LKP-091, 104, 105, 106 against CK1δ. Serial dilutions ranging from 5 nM to 10 μM of **LKP-091, LKP-104, LKP-105, LKP-106** were used to determine the 50% inhibitory concentration (IC_{50}) for CK1δ as described in Materials and Methods. **A:** Coomassie stained SDS-gels with α-casein as substrate (~28 kDa). **B:** Corresponding autoradiography with α-casein as substrate (~28 kDa). MW: Precision Plus Protein™ Standards Dual Color (10-250 kDa). **C:** IC_{50} values of **LKP-091, LKP-104, LKP-105, LKP-106**. Results were normalized towards the DMSO control and the analysis was performed by using GraphPad Prism 6. Bar graphs represent the mean and the standard deviation (SD) of the triplicates. **Abbreviations**: CK1: casein kinase 1; MW: molecular weight; kDa: kilo Dalton; SDS-PAGE: sodium dodecyl sulfate-polyacrylamide gel electrophoresis; DMSO: dimethyl sulfoxide; SD: standard deviation.

All **LKP**_compounds showed strong inhibitory effects against CK1δ with low IC_{50} values (**Figure 16**), which are displayed in **Table 12**, while the highest inhibition was observed for **LKP-105** exhibiting the lowest IC_{50} value.

Table 12: IC_{50} values of LKP-091, 104, 105, 106 compounds for CK1δ

Compounds	CK1δ IC_{50}[nM]
LKP-091	3592 nM
LKP-104	3455 nM
LKP-105	1742 nM
LKP-106	4764 nM

3.5.3 Effects of LKP_compounds on the activity of (*hum*)CK1δ wild type and mutants

Due to its strong effects against CK1δ and higher selectivity towards CK1δ compared to the other CK1 isoforms, further experiments were performed to compare the inhibitory effects of **LKP_** compounds between CK1δ mutants and CK1δ wild type.

A

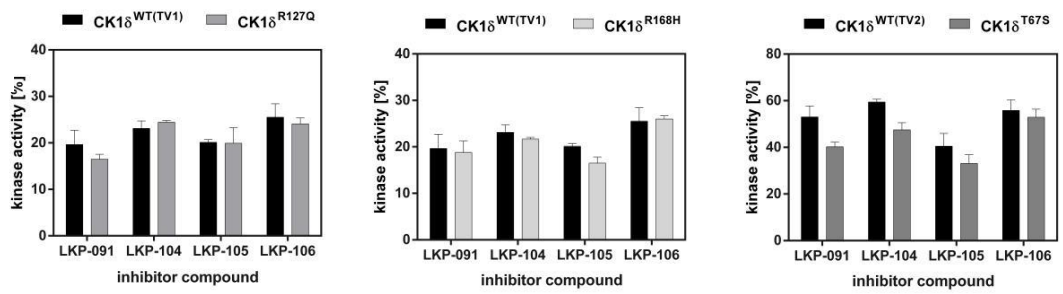

B

#	Residual kinase activity (%)				
	GST-(*hum*)TV1-CK1δ^{wt}	GST-(*hum*)CK1δ^{R127Q}	GST-(*hum*)CK1δ^{R168H}	GST-(*hum*)TV2-CK1δ^{wt}	GST-(*hum*)CK1δ^{T67S}
LKP-091	19.6 ± 3.0	16.5 ± 1.0	18.8 ± 2.5	53.1 ± 4.7	40.2 ± 2.0
LKP-104	23.1 ± 1.6	24.4 ± 0.3	21.6 ± 0.4	59.4 ± 1.2	47.5 ± 3.1
LKP-105	20.1 ± 0.6	19.9 ± 3.4	26.0 ± 1.3	40.5 ± 5.5	33.1 ± 3.7
LKP-106	25.5 ± 3.0	24.1 ± 1.3	16.5 ± 0.7	55.8 ± 4.6	52.9 ± 3.5

Figure 17：Inhibitory effects of LKP_compounds on GST-(*hum*)-CK1δ wt and mutants. *In vitro* kinase assays were performed in the absence and presence of the indicated LKP compounds as described in Materials and Methods. In (**A**), phosphorylated samples were separated by SDS-PAGE and stained with Coomassie. Phosphate incorporation into α-casein was determined by Cherenkov counting. Results were normalized towards the DMSO control. Experiments were performed in triplicate and GraphPad Prism 6 was used for the analysis. Bar graphs represent the mean and the standard deviation (SD) of the triplicates. (**B**) Residual activities of GST-(*hum*)TV1-CK1δ^{wt}, GST-(*hum*)-CK1δ^{R127Q}, GST-(*hum*)-CK1δ^{R168H}, GST-(*hum*)TV2-CK1δ^{wt} and GST-(*hum*)-CK1δ^{T67S} after treatment with different **LKP_**compounds were summarized. **Abbreviations**: CK1: casein kinase 1; TV: transcription variant; GST: glutathione S transferase; hum: human; DMSO: dimethyl sulfoxide; SD: standard deviation.

LKP-091 inhibited GST-(*hum*)-CK1δ^{R127Q} slightly more than GST-(*hum*)TV1-CK1δ^{wt}, whereas **LKP-104** and **LKP-106** showed stronger inhibition for GST-(*hum*)-CK1δ^{R168H}. Similar inhibition of GST-(*hum*)-CK1δ^{R168H} and GST-(*hum*)TV1-CK1δ^{wt} were observed in the presence of **LKP-091** and **LKP-105** as well as for GST-(*hum*)-CK1δ^{R127Q} and GST-(*hum*)TV1-CK1δ^{wt} in the presence of **LKP-104** and **LKP-105** (**Figure 17**). The results presented in **Figure 18** also show that the four **LKP_**compounds reduced the kinase activity of GST-(*hum*)TV2-CK1δ^{wt} to a residual activity between 40.5 and 59.4%, whereby **LKP-106** exhibited the strongest effects (residual activity 40.5 %). GST-(*hum*)CK1δ^{T67S} was inhibited by **LKP-091**, **LKP-104**, **LKP-105,** and **LKP-106** to 19% stronger than GST-(*hum*)TV2-CK1δ^{wt} (**Figure 17**).

3.5.4 *In vitro* effects of second generation set of LKP_compounds on CK1 isoforms activity

The inhibitory potency of a second generation set of three **LKP**_compounds (**LKP-112, LKP-114, LKP-115**) against four CK1 isoforms (CK1α, γ, δ, and ε) has also been first screened using 10 μM of each compound in *in vitro* kinase assays. CK1α, γ, δ and ε were used as a source of enzyme, while α-casein was used as substrate (0.8 μg/reaction) in the presence of 2 μCi [γ-^{32}P]-ATP, 10 μM ATP and 10 μM of the tested compound. Kinase activities of four CK1 isoforms (CK1α, γ, δ and ε) in the absence and presence of the indicated **LKP_** compounds are shown in **Figure 18.**

A

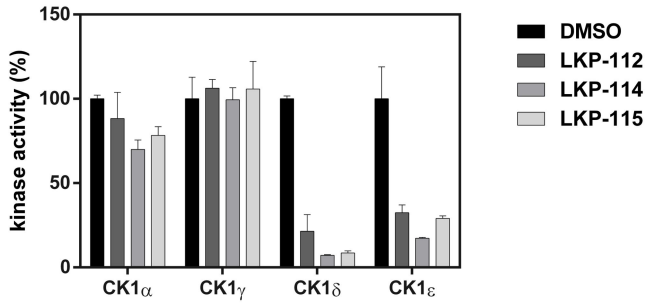

B

#	Residual kinase activity (%)			
	CK1α	**CK1γ**	**CK1δ**	**CK1ε**
LKP-112	88.2 ± 15.5	106.2 ± 5.1	21.5 ± 9.8	32.4 ± 4.7
LKP-114	69.9 ± 5.6	99.4 ± 7.1	7.1 ± 0.5	17.4 ± 0.4
LKP-115	78.7 ± 5.2	105.8 ± 16.4	8.6 ± 1.3	29.1 ± 1.5

Figure 18: Inhibitory effects of the newly designed LKP_compounds (LKP-112, LKP-114, LKP-115) on CK1 isoforms: LKP-112, LKP-114, LKP-115 were tested against CK1α, γ, δ and ε isoforms to verify their specificity as well as potency for CK1δ and ε. *In vitro* kinase assays were performed as described in Materials and Methods. In (**A)** results were normalized towards the DMSO control. Experiments were performed in triplicates and GraphPad Prism 6 was used for the analysis. Bar graphs represent the mean and the standard deviation (SD) of the triplicates. Grouped method was performed as a statistical analysis to compare the inhibitory effects of each compound to DMSO control. **B:** Residual activity of four CK1 isoforms after each treatment with different **LKP**_compounds is summarized. **Abbreviations**: CK1: casein kinase 1; TV: transcription variant; DMSO: dimethyl sulfoxide; SD: standard deviation.

All three **LKP**_compounds (**LKP-112, LKP-114, LKP-115**) showed strong inhibitory effects on CK1δ and ε, whereas highest inhibitory effects were observed on CK1δ kinase activity, which was inhibited more than 79 to 93 %, while CK1ε kinase activity was inhibited from 68% to 83%. All **LKP**_compounds displayed almost no inhibition of CK1α and CK1γ (**Figure 18A** and **B**).

3.5.5 Determination of IC_{50} values of second generation set of LKP_compounds against GST-(*hum*)CK1δ

Due to its strong effects against CK1δ and higher selectivity towards CK1δ, IC_{50} values of **LKP-112, LKP-114, LKP-115** were determined as described in Materials and Methods. Therefore, serial dilutions ranging from 5 nM to 10 µM of the compounds **LKP-112, LKP-114, LKP-115** were used. GST-(*hum*)TV1-CK1δ^{wt} was used as a source of enzyme, while α-casein was used as substrate (0.8 µg/reaction) in the presence of 2 µCi [γ-^{32}P]-ATP and 10 µM ATP.

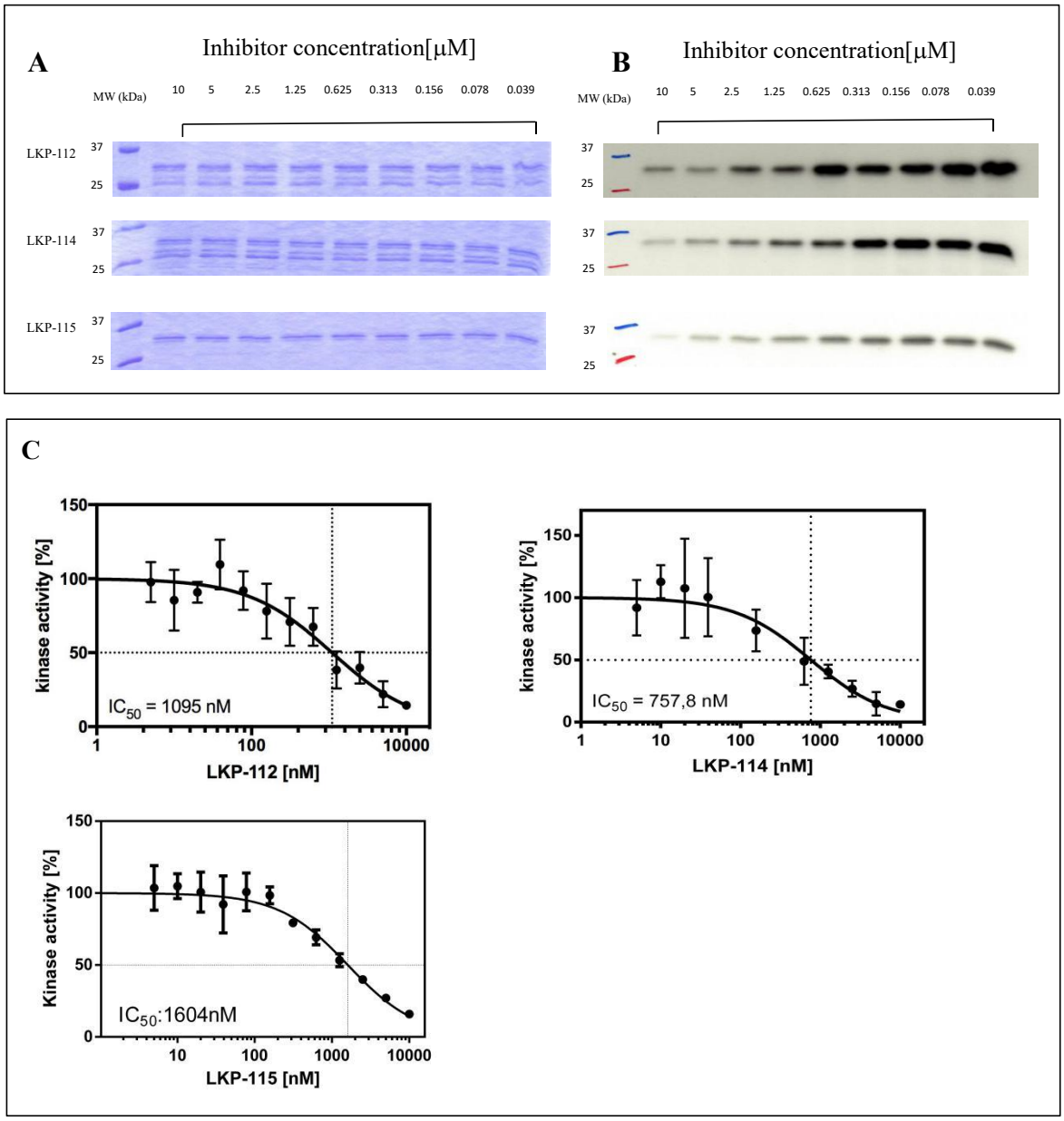

Figure 19: IC_{50} values of LKP-112, LKP-114, LKP-115 against CK1δ. Serial dilutions ranging from 5 nM to 10 µM of **LKP-112, LKP-114, LKP-115** were used to determine the 50% inhibitory concentration (IC_{50}) for CK1δ as described in Materials and Methods. **A:** Coomassie stained

SDS-gels with α-casein as substrate (~28 kDa). **B:** Corresponding autoradiography with α-casein as substrate (~28 kDa). MW: Precision Plus Protein™ Standards Dual Color (10-250 kDa). **C:** IC_{50} values of **LKP-112, LKP-114, LKP-115**. Results were normalized towards the DMSO control (100%) and the analysis was performed using GraphPad Prism 6. Bar graphs represent the mean and the standard deviation (SD) of the triplicates. **Abbreviations**: CK1: casein kinase 1; TV: transcription variant; MW: molecular weight; kDa: kilo Dalton; DMSO: dimethyl sulfoxide; SD: standard deviation

LKP-112, LKP-114, LKP-115 all showed strong inhibitory effects against CK1δ with low IC_{50} values, which are displayed in **Table 13**, while the highest inhibition was observed for LKP-114 with lowest IC_{50}.

Table 13: IC_{50} values of LKP-112, LKP-114, LKP-115 compounds for CK1δ

Compound	CK1δ IC_{50}[nM]
LKP-112	1095 nM
LKP-114	757.8 nM
LKP-115	1604 nM

In summary, from *in vitro* results, the analyzed **LKP**_compounds showed strong effects and high selectivity towards CK1δ. Furthermore, higher inhibition capability of **LKP**_compounds was observed against some CK1δ mutants when comparing to wt CK1δ. Accordingly, cell-based MTT assays were performed to detect cellular permeability of these compounds, which will be displayed in the following chapters.

3.6 Establishment of new Hela$^{CK1\delta-/-}$ cell lines stably expressing either wt CK1δ wt or CK1δ mutants

In order to compare the inhibition of newly designed **LKP**_compounds on both CK1δ wt and mutants in cell-based assays, a CK1δ knockout Hela (Hela$^{CK1\delta\,-/-}$) cell line was used and stably transfected with pcDNA™3.1/V5-His TOPO® plasmids either encoding wt CK1δ variants or CK1δ mutants (generated by Bischof et al.) as described in Materials and Methods.

The following five CK1δ wt and mutants were transfected into Hela$^{CK1\delta\,-/-}$ cels: TV1-CK1δ^{wt}, CK1δ^{R127Q}, CK1δ^{R168H}, TV2-CK1δ^{wt}, CK1δ^{T67S} as described in Materials and Methods. Stable clones were established after selection with G418 at a concentration of 0.6 mg/ml and expression of the respective CK1δ variant/mutant was verified by PCR and Western blot analysis.

3.6.1 Experimental proof of successful transfection of Hela$^{CK1\delta\,-/-}$ cells on RNA level by Polymerase chain reaction (PCR)

In order to confirm the successful transfection of Hela$^{CK1\delta\,-/-}$ cells with the respective CK1δ variant/mutant, total RNA from the respective cell lysate was purified and transcribed into cDNA as described in Material and Methods. Thereafter, PCR for the detection of the desired His-CK1δ variants/mutants was performed. The results are displayed in **Figure 20.**

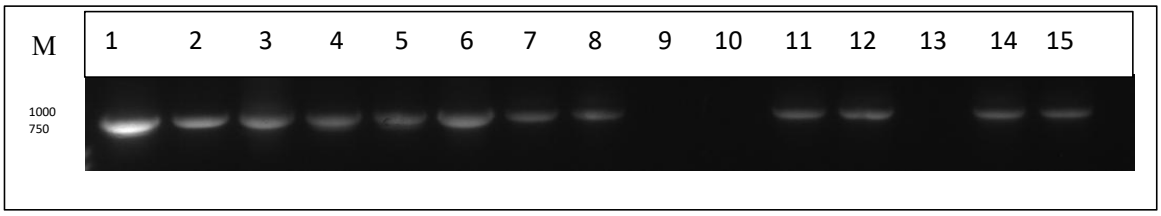

Figure 20: Agarose gels of His-CK1δ PCR reactions: RNA was purified from lysates of Hela$^{CK1\delta\,-/-}$ clones stably expressing CK1δ wild type or mutants CK1δ^{R127Q}, CK1δ^{R168H}, CK1δ^{T67S}, respectively, and transcribed into cDNAs, which were used as templates to amplify CK1δ wild type or mutants by PCR with specific primers. Samples were separated by agarose gel electrophoresis and visualized under UV light. M: GeneRuler^{TM} 1kb DNA Ladder (250-10000bp). 1: TV2-CK1δ^{wt} (colony 1); 2: TV2-CK1δ^{wt} (colony 2); 3: positive control; 4: CK1δ^{T67S} (colony 1); 5: CK1δ^{T67S} (colony 2); 6: positive control; 7: TV1-CK1δ^{wt} (colony 1); 8: TV1-CK1δ^{wt} (colony 2); 9: positive control; 10: negative control; 11: CK1δ^{R127Q} (colony 1); 12: CK1δ^{R127Q} (colony 2); 13: positive control; 14: CK1δ^{R168H} (colony 1); 15: CK1δ^{R168H} (colony 2). Positive control: plasmids, negative control: RNase free water. **Abbreviations:** CK1: casein kinase 1; PCR: polymerase chain reaction; wt: wild type; UV: ultraviolet M: marker; bp: base pairs; kb: kilo base pairs.

The results of PCR for the His-CK1δ gene are presented in **Figure 20**, while 10 lanes of product bands were revealed. The PCR reactions of TV1-CK1δ^{wt} and TV2-CK1δ^{wt}-expressing colonies as well as the mutants CK1δ^{T67S}, CK1δ^{R127Q} and CK1δ^{R168H}-expressing colonies showed clear bands at the height of approximately 900 bp, which is equal to the size of the His-CK1δ fragment which can be obtained by using the above mentioned primers. The positive controls in lanes 3 and lane 6 also displayed bands of this size, which supports this result. Nevertheless, transfection of Hela$^{CK1\delta-/-}$ cells with TV2-CK1δ^{wt}, CK1δ^{T67S}, TV1-CK1δ^{wt}, CK1δ^{R127Q}, and CK1δ^{R168H} could successfully be demonstrated on RNA level.

3.6.2 Experimental proof of successful transfection of Hela$^{CK1\delta-/-}$ cells on protein level by Western Blot analysis

The transfected vectors encoding CK1δ variants and mutants are equipped with a His-tag, which enables the detection of the translated proteins. On the protein level, Western Blot

analysis was used to confirm the successful transfection of Hela$^{CK1\delta-/-}$ cells. Protein concentration of Hela$^{CK1\delta-/-}$ cells and Hela$^{CK1\delta-/-}$ clones expressing CK1δ variants/mutants was determined by Pierce® BCA Protein Assay kit (Thermo Scientific, Germany) as described in Material and Methods. His-Tag polyclonal antibody (Cell Signaling Technology, Germany) was used as the primary antibody, which specifically recognizes the His-CK1δ-specific 72 kDa band and anti-rabbit (Cell Signaling Technology, Germany) was used as the secondary antibody. 20 µg of the respective protein extract and control were used and separated by SDS-PAGE as described in Materials and Methods. The detected His-CK1δ-specific protein bands of all clones expressing CK1δ wt and mutants are shown in **Figure 21**.

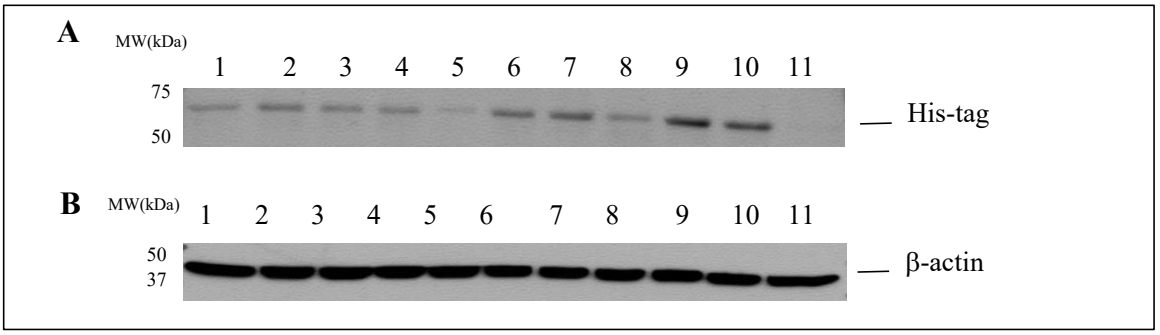

Figure 21：Detection of His-CK1δ by Western Blot Analysis: Cell lysates from untransfected and transfected Hela$^{CK1\delta-/-}$ cells were separated by SDS-PAGE and transferred to a PVDF membrane, which was probed with antibodies, incubated in ECL solution and finally exposed to a X-ray film. **A:** His-tag polyclonal antibody was selected as primary antibody while anti-rabbit was used as secondary antibody, CK1δ was detected by Western Blot analysis. **B:** β-actin monoclonal antibody was selected as primary antibody while anti-mouse was used as the secondary antibody. 1,2: TV2-CK1δ^{wt}; 3,4: CK1δ^{T67S}; 5,6: TV1-CK1δ^{wt}; 7,8: CK1δ^{R127Q}; 9,10: CK1δ^{R168H}; 11: Hela$^{CK1\delta-/-}$. MW: Precision Plus Protein^{TM} Standards Dual Color (10-250 kDa). **Abbreviations:** CK1: casein kinase 1; hum: human; MW: molecular weight; kDa: kilo Dalton.

In summary, PCR and Western Blot analysis confirmed the successful transfection of Hela$^{CK1\delta-/-}$ cells with CK1δ wt and CK1δ mutants.

After the successful establishment of Hela$^{CK1\delta-/-}$ cells stably expressing either CK1δ wt or CK1δ mutants, cell-based MTT assays were performed to characterize the effects of newly designed **LKP_** compounds on cell viability.

3.7 Effects of newly designed LKP_compounds on the viability of Hela cell lines

Newly synthesized LKP_compounds have been tested for these hyperactive mutants (T67S (Richter et al., 2015), R127Q and R168H) on cell-based MTT assay, which will be

displayed in following chapters.

Effects of **LKP**_compounds on cell viability of parental Hela cells, untransfected Hela$^{CK1\delta-/-}$ cells as well as Hela$^{CK1\delta\ -/-}$ cells stably transfected with TV1-CK1δ^{wt} were first tested with an inhibitor concentration of 50 µM and 25 µM (**Figure 22**).

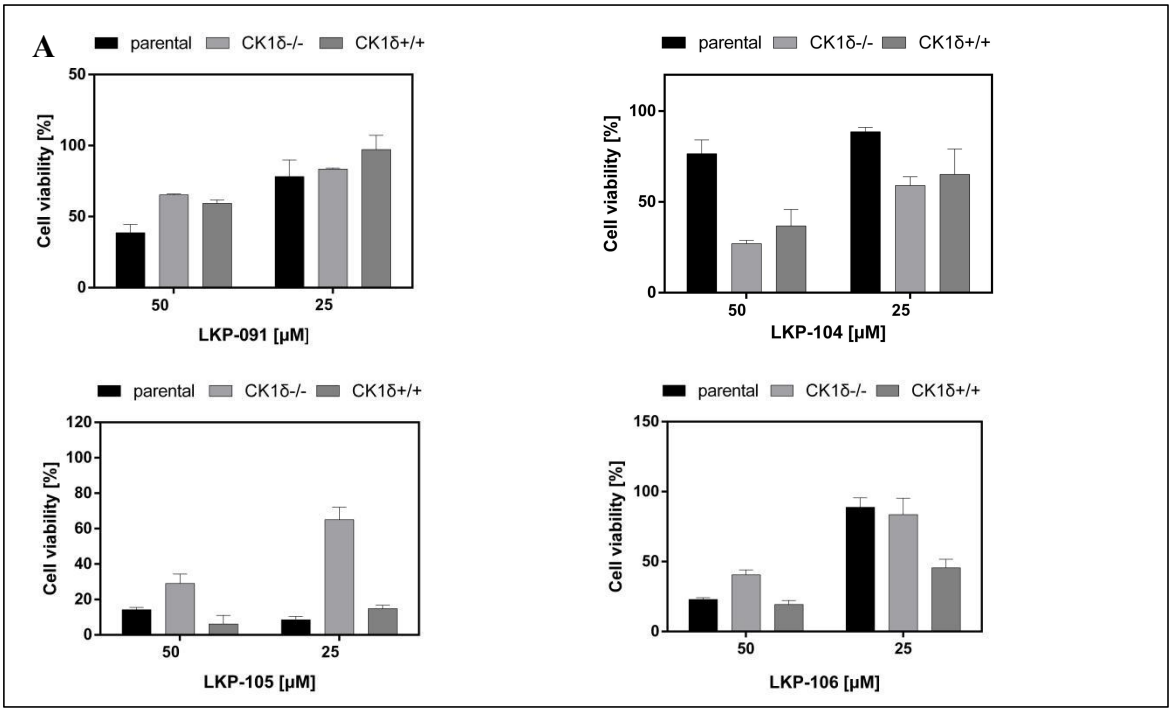

B

LKP_compounds [µM]		Residual cell viability (%)		
		Hela^{parental}	Hela$^{CK1\delta-/-}$	Hela$^{CK1\delta-/-,\ TV1\text{-}CK1\delta wt}$
LKP-091	**50**	38.7 ± 5.8	65.4 ± 0.6	59.3 ± 2.6
	25	78.2 ± 11.7	83.4 ± 0.7	97.2 ± 9.9
LKP-104	**50**	76.5 ± 7.7	27.2 ± 1.8	36.8 ± 9.0
	25	88.6 ± 2.4	59.9 ± 4.9	65.2 ± 13.9
LKP-105	**50**	14.3 ± 1.3	29.3 ± 5.3	6.2 ± 4.9
	25	8.5 ±1.9	65.8 ± 7.0	14.9 ± 1.9
LKP-106	**50**	22.9 ± 1.3	40.6 ± 3.5	19.3 ± 2.9
	25	88.9 ± 6.7	83.5 ± 11.8	45.5 ± 6.2

Figure 22：Viability screening of LKP_compounds for parental Hela cell line as well as untransfected and transfected Hela$^{CK1\delta-/-}$ cells lines. A: Viability of parental Hela cell line as well as untransfected and transfected Hela$^{CK1\delta-/-}$ cells lines was first screened by MTT viability assay after treatment with 50 µM and 25 µM of **LKP**_compounds as described in Material and Methods. **B:** Residual cell viability of parental Hela cell line as well as untransfected and transfected Hela$^{CK1\delta-/-}$ cells lines after treatment with **LKP**_compounds are summarized. Results have been normalized towards the DMSO control (100 %) and bars of normalized data were obtained using GraphPad 6, with their respective standard deviation (SD) as error bars. Modified from [96], CC BY 4.0. https://creativecommons.org/licenses/by/4.0/ **Abbreviations:** CK1: casein kinase; DMSO: dimethyl sulfoxide.

The results presented in **Figure 22** clearly show that **LKP-105** reduced cell viability of Hela$^{CK1\delta-/-,\ TV1\text{-}CK1\delta wt}$ 4.5-fold more compared to the CK1δ depleted Hela$^{CK1\delta-/-}$ cell line, which seems to indicate that **LKP-105** specifically targets CK1δ in cell-based assays. Similar effects were observed for **LKP-106**, which reduced cell viability of Hela$^{CK1\delta-/-,\ TV1\text{-}CK1\delta wt}$ cells 2-fold more compared to CK1δ depleted Hela$^{CK1\delta-/-}$ cells, but effects observed for **LKP- 106** were much lower than **LKP-105**.

To confirm the effects of **LKP-105** on cell viability of Hela$^{CK1\delta-/-}$ cells and Hela$^{CK1\delta-/-,\ TV1\text{-}CK1\delta wt}$ cells, EC_{50} values were determined and are shown in **Figure 23**.

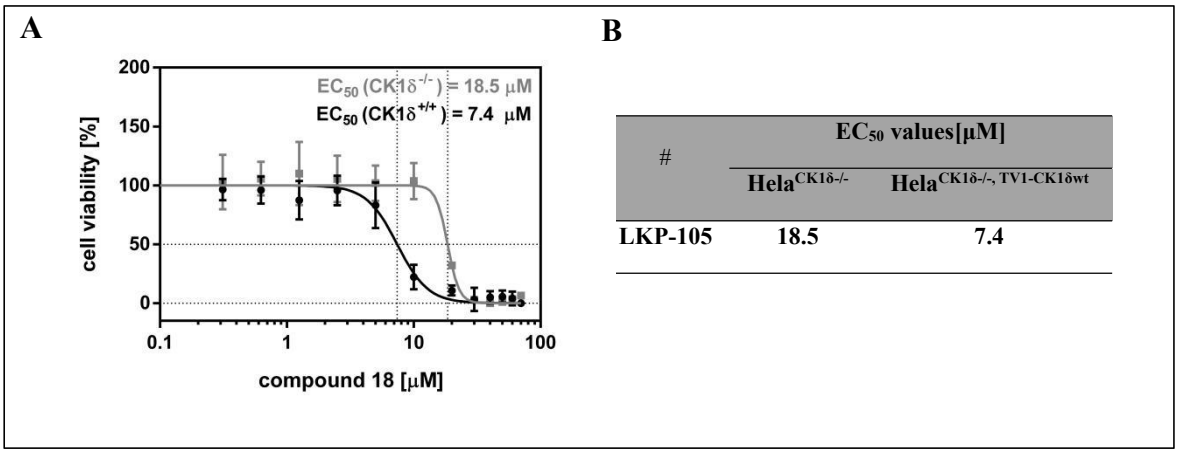

#	EC_{50} values[µM]	
	Hela$^{CK1\delta-/-}$	Hela$^{CK1\delta-/-,\ TV1\text{-}CK1\delta wt}$
LKP-105	**18.5**	**7.4**

Figure 23：EC_{50} values of LKP-105 for Hela$^{CK1\delta-/-}$ and Hela$^{CK1\delta-/-,\ TV1\text{-}CK1\delta wt}$. MTT assay was performed as described in Material and Methods using the serial dilution ranging from 70 µM to 0.3125 µM of **LKP-105** and DMSO as control. After treating cells with MTT-solution and incubating for 4 h, the absorption coefficient was measured at 570 nm. **A:** Results have been normalized towards the DMSO control (100 %) and bars of normalized data were obtained using GraphPad 6, with their respective standard deviation (SD) as error bars. **B:** EC_{50} values of **LKP-105** on Hela$^{CK1\delta-/-}$ and Hela$^{CK1\delta-/-,\ TV1\text{-}CK1\delta wt}$. Modified from [96], CC BY 4.0. https://creativecommons.org/licenses/by/4.0/ **Abbreviations:** CK1: casein kinase 1; DMSO: dimethyl sulfoxide; SD: standard deviation.

More than 2-fold increased EC_{50} value of **LKP-105** against Hela$^{CK1\delta-/-}$ than for Hela$^{CK1\delta-/-,\ TV1\text{-}CK1\delta wt}$ was observed, which indicates stronger effects on cell viability of **LKP-105** on Hela$^{CK1\delta-/-,\ TV1\text{-}CK1\delta wt}$ cell line.

Afterward, further experiments were performed to compare the inhibitory effects of **LKP**_compounds on CK1 δ wt and CK1 δ mutants in cell culture.**LKP-105** showed stronger effects on cell viability of Hela$^{CK1\delta-/-,\ CK1\delta R127Q}$ cells compared to Hela$^{CK1\delta-/-,\ TV1\text{-}CK1\delta wt}$ cells at the concentrations of 10 and 20 µM. Slightly stronger effects on cell viability of Hela$^{CK1\delta-/-,\ CK1\delta R168H}$ cells in comparison to Hela$^{CK1\delta-/-,\ TV1\text{-}CK1\delta wt}$ were observed in the presence of **LKP-105** (**Figure 24**). For Hela$^{CK1\delta-/-,\ CK1\delta T67S}$ cells, no stronger effects on cell viability were observed comparing to Hela$^{CK1\delta-/-,\ TV2\text{-}CK1\delta wt}$ cells.

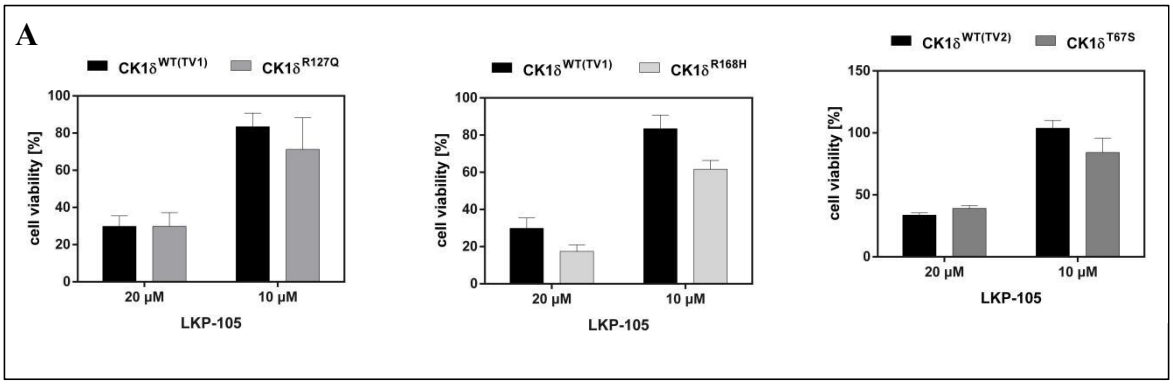

B

#	Concentration [µM]	Residual cell viability (%)				
		$Hela^{CK1\delta-/-,\ TV1\text{-}CK1\delta wt}$	$Hela^{CK1\delta-/-,\ CK1\delta R127Q}$	$Hela^{CK1\delta-/-,\ CK1\delta R168H}$	$Hela^{CK1\delta-/-,\ TV2\text{-}CK1\delta wt}$	$Hela^{CK1\delta-/-,\ CK1\delta T67S}$
LKP-105	**20**	29.9 ± 6.7	17.5 ± 3.4	27.6 ± 9.7	33.7 ± 1.7	39.0 ± 2.4
	10	83.4 ± 13.4	61.6 ± 4.7	65.8 ± 25.8	103.8 ± 6.2	84.2 ± 11.6

Figure 24：Viability screening of LKP-105 for $Hela^{CK1\delta-/-}$ cells lines transfected with either CK1δ wt or mutant CK1δ. A: Viability of $Hela^{CK1\delta-/-,\ TV1\text{-}CK1\delta wt}$, $Hela^{CK1\delta-/-,\ CK1\delta R127Q}$, $Hela^{CK1\delta-/-,\ CK1\delta R168H}$ as well as $Hela^{CK1\delta-/-,\ TV2\text{-}CK1\delta wt}$ and $Hela^{CK1\delta-/-,\ CK1\delta T67S}$ cells were first screened by MTT viability assay after treatment with **LKP-105** as described in Material and Methods. **B:** Residual cell viability of $Hela^{CK1\delta-/-,\ TV1\text{-}CK1\delta wt}$, $Hela^{CK1\delta-/-,\ CK1\delta R127Q}$, $Hela^{CK1\delta-/-,\ CK1\delta R168H}$ as well as $Hela^{CK1\delta-/-,\ TV2\text{-}CK1\delta wt}$ and $Hela^{CK1\delta-/-,\ CK1\delta T67S}$ cells after treatment with different concentrations of **LKP-105** are summarized. Results have been normalized towards the DMSO control (100 %) and bars of normalized data were obtained using GraphPad 6, with their respective standard deviation (SD) as error bars. Modified from [96], CC BY 4.0, https://creativecommons.org/licenses/by/4.0/ **Abbreviations:** wt: wild type; TV: transcription variant; CK1: casein kinase 1.

Afterward, effects of **LKP-112, LKP-114 and LKP-115** on cell viability of $Hela^{parental}$, $Hela^{CK1\delta-/-}$, as well as $Hela^{CK1\delta-/-,\ TV1\text{-}CK1\delta wt}$ were also tested at a concentration of 25 µM and 50 µM (**Figure 25**).

A

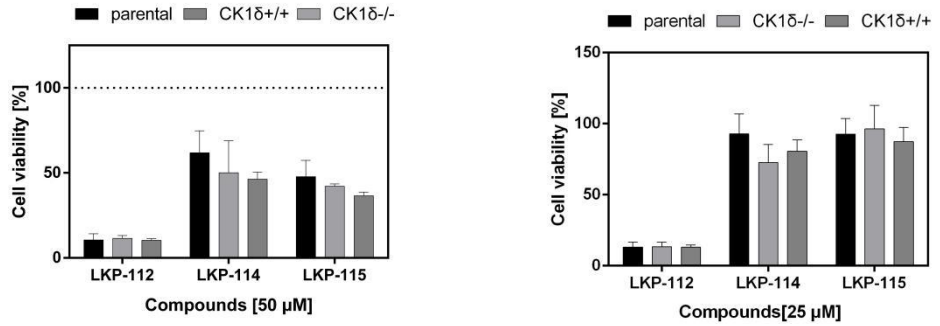

B

Compounds	Concentration [µM]	Residual cell viability (%)		
		Hela^{parental}	**Hela$^{CK1δ-/-}$**	**Hela$^{CK1δ-/-, TV1-CK1δwt}$**
LKP-112	**50**	10.6 ± 3.6	11.5 ± 1.7	10.3 ± 1.1
	25	27.3 ± 2.0	28.8 ± 1.9	18.3 ± 0.2
LKP-114	**50**	61.8 ± 12.9	50 ± 18.8	46.4 ± 4.1
	25	98.4 ± 1.5	98.0 ± 15.1	81.4 ± 10.8
LKP-115	**50**	47.7 ± 9.6	42.1 ± 1.4	36.5 ± 2.1
	25	109.9 ± 3.6	106.9 ± 15.5	92.6 ± 14.6

Figure 25： Viability screening of LKP_compounds for Hela^{parental}, Hela$^{CK1δ-/-}$ as well as Hela$^{CK1δ-/-, TV1-CK1δwt}$ cell lines. A: Viability of Hela^{parental}, Hela$^{CK1δ-/-}$ as well as Hela$^{CK1δ-/-, TV1-CK1δwt}$ cell lines were first screened by MTT viability assay after treatment with 50 µM and 25 µM concentration of **LKP-112, LKP-114, LKP-115** as described in Material and Methods. Results have been normalized towards the DMSO control (100 %) and bars of normalized data were obtained using GraphPad 6, with their respective standard deviation (SD) as error bars. **B:** Residual cell viability of Hela^{parental}, Hela$^{CK1δ-/-}$ as well as Hela$^{CK1δ-/-, TV1-CK1δwt}$ cells after treatment with **LKP-112, LKP-114, LKP-115** are summarized. **Abbreviations:** wt: wild type; TV: transcription variant; CK1: casein kinase; DMSO: dimethyl sulfoxide.

The observed results clearly indicate that **LKP-112, LKP-114 and LKP-115** all slightly stronger inhibited the cell viability of Hela$^{CK1δ-/-, TV1-CK1δwt}$ cells compared to the CK1δ depleted Hela$^{CK1δ-/-}$ cell line. Afterward, MTT-assays were performed to compare the inhibitory effects of **LKP-112, LKP-114 and LKP-115** against CK1 δ wt and CK1 δ mutants in cell culture as described in Materials and Methods.

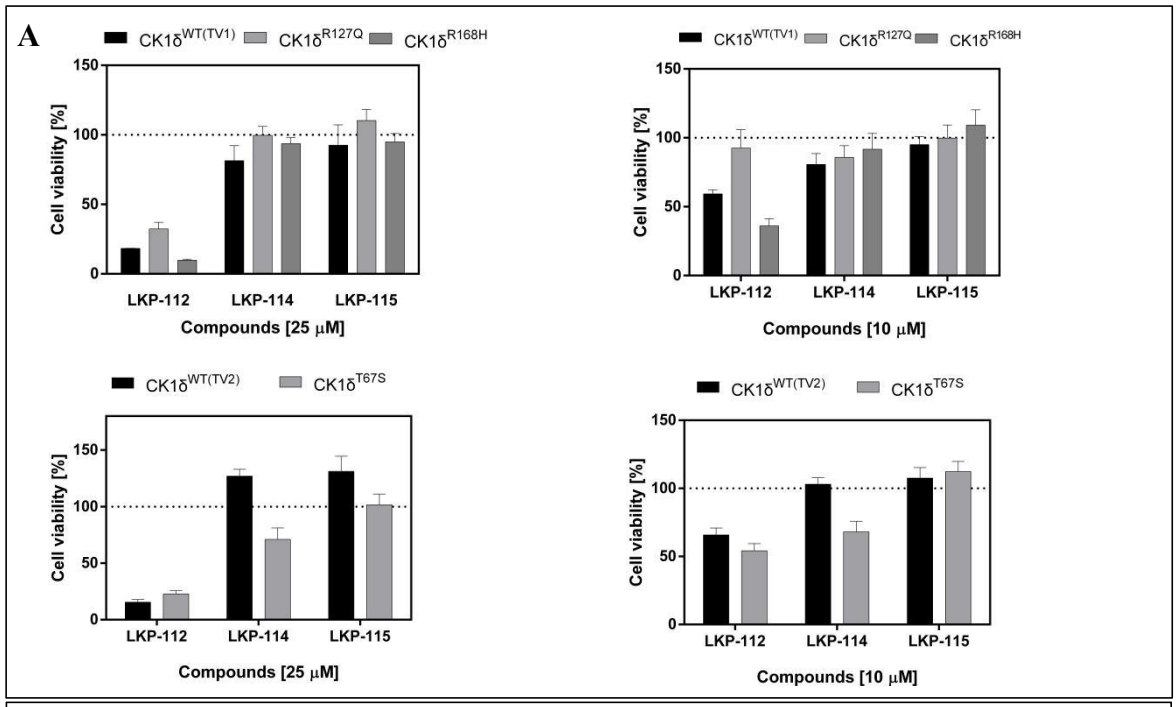

B

#	Concentration[μM]	Residual cell viability (%)				
		$Hela^{CK1δ-/-,\ TV1-CK1δwt}$	$Hela^{CK1δ-/-,\ CK1δR127Q}$	$Hela^{CK1δ-/-,\ CK1δR168H}$	$Hela^{CK1δ-/-,\ TV2-CK1δWT}$	$Hela^{CK1δ-/-,\ CK1δT67S}$
LKP-112	**25**	18.3 ± 0.2	32.3 ± 4.8	9.8 ± 0.7	15.6 ± 2.3	22.9 ± 2.9
	10	59.3 ± 3.0	92.6 ± 13.4	36.0 ± 5.2	65.8 ± 5.2	54.2 ± 5.3
LKP-114	**25**	81.4 ± 10.7	99.7 ± 6.4	93.6 ± 4.5	126.9 ± 6.0	71.1 ± 9.9
	10	80.7 ± 7.8	85.8 ± 8.4	91.7 ± 11.5	103.1 ± 4.7	68.1 ± 7.7
LKP-115	**25**	92.6 ± 14.6	110.3 ± 7.9	94.9 ± 6.0	131.2 ± 13.2	101.5 ± 9.5
	10	95.1 ± 5.8	99.8 ± 9.5	109.2 ± 11.0	107.6 ± 7.7	112.3 ± 7.5

Figure 26: Viability screening of LKP-112, LKP-114, LKP-115 for $Hela^{CK1δ-/-}$ cells lines transfected with both CK1δ wt and mutants. A: Viability of $Hela^{CK1δ-/-,\ TV1-CK1δwt}$, $Hela^{CK1δ-/-,\ CK1δR127Q}$, $Hela^{CK1δ-/-,\ CK1δR168H}$ as well as $Hela^{CK1δ-/-,\ TV2-CK1δwt}$ and $Hela^{CK1δ-/-,\ CK1δT67S}$ cell lines were first screened by MTT viability assay after treatment with **LKP-1112, LKP-114, LKP-115** as described in Material and Methods. Results have been normalized towards the DMSO control (100 %) and bars of normalized data were obtained using GraphPad 6, with their respective standard deviation (SD) as error bars **B:** Residual cell viability of $Hela^{CK1δ-/-,\ TV1-CK1δwt}$, $Hela^{CK1δ-/-,\ CK1δR127Q}$, $Hela^{CK1δ-/-,\ CK1δR168H}$ as well as $Hela^{CK1δ-/-,\ TV2-CK1δwt}$ and $Hela^{CK1δ-/-,\ CK1δT67S}$ cells lines after treatment with different concentrations of **LKP-112, LKP-114, LKP-115** are summarized. **Abbreviations:** wt: wild type; TV: transcription variant; CK1: casein kinase 1; SD: standard deviation.

The results indicated that **LKP-112** showed 2-fold stronger effects on cell viability of $Hela^{CK1δ-/-,\ CK1δR168H}$ cells in comparison to $Hela^{CK1δ-/-,\ TV1-CK1δwt}$ cells. Stronger effects on cell viability of $Hela^{CK1δ-/-,\ CK1δT67S}$ cells in comparison to $Hela^{CK1δ-/-,\ TV2-CK1δwt}$ cells were observed after treatment with **LKP-114**. No obvious stronger effects against CK1δ mutant-expressing compared to CK1δ wild type-expressing cells were observed in cell-based assays after treatment with **LKP_**compounds (**Figure 26**).

Due to its higher inhibitory effects on CK1δ^{R168H} compared to CK1δ wild type in cell-based assays, EC_{50} values of **LKP-112** in both, Hela$^{CK1δ-/-,\ TV1\text{-}CK1δwt}$ and Hela$^{CK1δ-/-,\ CK1δR168H}$ cells were performed. Furthermore, EC_{50} values of **LKP-114** in both, Hela$^{CK1δ-/-,\ TV2\text{-}CK1δwt}$ and Hela$^{CK1δ-/-,\ CK1δT67S}$ were determined (**Figure 27**).

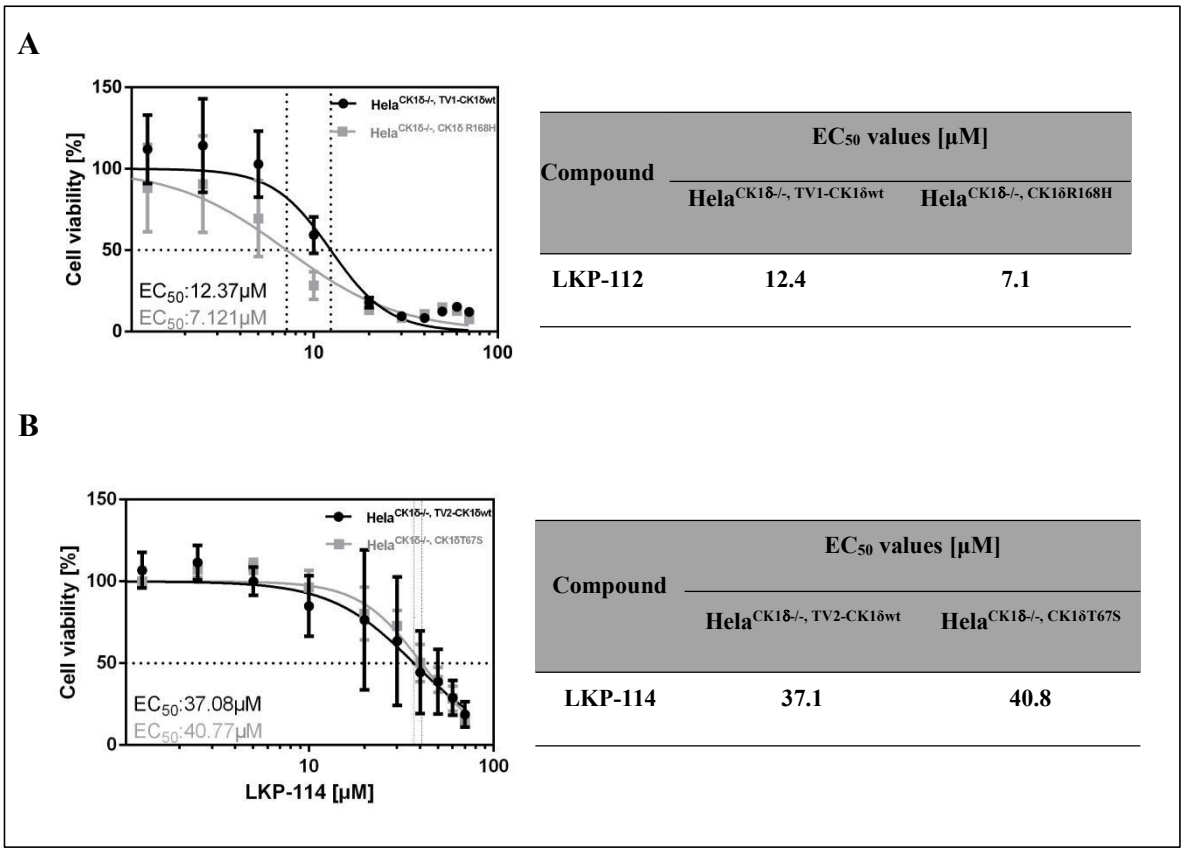

Compound	EC_{50} values [µM]	
	Hela$^{CK1δ-/-,\ TV1\text{-}CK1δwt}$	Hela$^{CK1δ-/-,\ CK1δR168H}$
LKP-112	**12.4**	**7.1**

Compound	EC_{50} values [µM]	
	Hela$^{CK1δ-/-,\ TV2\text{-}CK1δwt}$	Hela$^{CK1δ-/-,\ CK1δT67S}$
LKP-114	**37.1**	**40.8**

Figure 27: Determination of EC_{50} values of LKP-112 and LKP-114 in Hela$^{CK1δ-/-,\ CK1δwt}$ as well as in Hela$^{CK1δ-/-,\ CK1δ\ mutants}$ cell lines. MTT assays were performed as described in Material and Methods with ta serial dilution of **LKP-112** and **LKP-114** ranging from 70 µM to 0.3125 µM**.** DMSO served as control. After treating cells with MTT-solution and incubating for 4 h, the absorption coefficient was measured at 570 nm. **A:** EC_{50} value of **LKP-112** in Hela$^{CK1δ-/-,\ TV1\text{-}CK1δwt}$ and Hela$^{CK1δ-/-,\ CK1δR168H}$ cell lines. Results have been normalized towards the DMSO control (100 %) and bars of normalized data were obtained using GraphPad 6, with their respective standard deviation (SD) as error bars. **B:** EC_{50} value of **LKP-114** in Hela$^{CK1δ-/-,\ TV2\text{-}CK1δwt}$, and Hela$^{CK1δ-/-,\ CK1δT67S}$ cell lines. **Abbreviations:** wt: wild type; TV: transcription variant; CK1: casein kinase; DMSO: dimethyl sulfoxide; SD: standard deviation.

Determination of EC_{50} values of **LKP-112** in both, Hela$^{CK1δ-/-,\ TV1\text{-}CK1δwt}$ and Hela$^{CK1δ-/-,\ CK1δR168H}$ cell lines indicated that **LKP-112** showed higher inhibitory effects on mutant CK1δ^{R168H} than on wild type CK1δ in cell-based assays. However, determination of EC_{50} values of **LKP-114** in Hela$^{CK1δ-/-,\ TV2\text{-}CK1δwt}$ and Hela$^{CK1δ-/-,\ CK1δT67S}$ indicated that no obvious difference was observed between the inhibition of cell viability of Hela$^{CK1δ-/-,\ TV2\text{-}CK1δwt}$ and Hela$^{CK1δ-/-,\ CK1δT67S}$ cell lines after treatment with **LKP-114**.

4. Discussion

Since a wide range of substrates are phosphorylated by CK1, CK1 family members play crucial roles in the regulation of tumor suppressor functions and multiple cellular processes, like membrane trafficking, cell differentiation and proliferation, DNA repair, Wnt-, Hedgehog-, and Hippo- signalling pathways. Moreover, dysregulation or mutations of CK1 isoforms within their coding regions were found to result in the development of various different pathologies, like neurodegenerative diseases and cancer development, which suggests the therapeutic potential of CK1-specific inhibitors in the treatment of these diseases [11][120]. However, although several mutations of CK1 were found in different human tumor entities, knowledge about the role of the respective mutants is limited.

Thus, this thesis focusses on three hyperactive CK1δ mutants found in human tumour entities, namely: $CK1\delta^{T67S}$, $CK1\delta^{R127Q}$, $CK1\delta^{R168H}$.

The main results within this study are:

1) Mutants $CK1\delta^{R127Q}$ and $CK1\delta^{R168H}$ exhibit increased susceptibility to inhibitors Bischof-5 and 16b compared to CK1δ wt.

2) Newly optimized and synthesized LKP_compounds showed CK1δ–specific inhibition, indicated by stronger inhibition of wild type and mutant CK1δ compared to other CK1 isoforms in *in vitro* kinase assays.

3) Stably transfected $Hela^{CK1\delta-/-}$ cell lines expressing CK1δ wt or CK1δ mutants have been established successfully. **LKP-105** seems to have a CK1δ-dependent effect on the cell viability and displays higher inhibitory effects on $CK1\delta^{R127Q}$ than on wt CK1δ in cell-based assay, while **LKP-112** shows therapeutic potential specifically for the hyperactive, highly oncogenic CK1δ mutant $CK1\delta^{R168H}$ in cell culture.

These results will be discussed in detail within the following chapters.

4.1 CK1-specific inhibitors have altered effects on CK1δ variants

Members of the CK1 family play regulatory roles in tumor suppressor functions. Moreover, because of the steric changes in the structure, mutations of CK1δ can result in altered expression levels and kinase activity, for example, abnormal expression levels and

activities have been found in choriocarcinomas and pancreatic carcinomas, which can contribute to the development of cancer [83]. Moreover, mutation of CK1δ can result in increased binding properties of inhibitor compounds compared to wild type CK1δ [11][99] . For instance, the highly oncogenic mtCK1δ^{T67S} shown increased kinase activity and increased the sensitivity to the ATP-competitive CK1δ-specific inhibitors due to the more flexible ATP binding after mutation [126]. Based on software-based chemical modeling, identification of compounds specifically inhibiting CK1δ wt and CK1δ mutants can be performed faster and more efficient. Such inhibitors can be synthesized to target CK1δ mutants with increased oncogenic potential, thereby preventing tumor development and progression.

As ATP-competitive inhibitor, compound Bischof-5 showed specific inhibition of kinase activity of CK1δ and effects on cell viability of several tumor cell lines. Moreover, in spite of the ‘‘closed gate’’, the inhibitory effects of Bischof-5 against activity of CK1δ^{M82F} was stronger than that against CK1δ wt because of the π-hydrogen bond between the benzimidazole moiety of Bischof-5 and phenylalanine 82 [11]. **Bischof-5** was then selected to compare the sensitivity of CK1δ wt and CK1δ mutants to CK1δ inhibitors. *In vitro* kinase assays were performed in the presence of **Bischof-5** at the determined IC_{50} concentration, while GST-(*hum*)TV1-CK1δ^{wt} or GST-(*hum*)CK1δ^{R127Q} or GST-(*hum*)CK1δ^{R168H} were used as the source of enzyme. Stronger inhibitory effects against GST-(*hum*)CK1δ^{R127Q} and GST-(*hum*)CK1δ^{R168H} were observed, which were approximately 30% and 18% stronger than for GST-(*hum*)TV1-CK1δ^{wt} being incubated with **Bischof-5**. Stronger inhibition was confirmed by determination of IC_{50} values ($IC_{50\,(CK1\delta R127Q)}$ = 42.2 nM, $IC_{50\,(CK1\delta R168H)}$ = 71.1 nM, $IC_{50\,(TV1\text{-}CK1\delta wt)}$ = 113.2 nM).

Compound **16b** has been synthesized with highly specific potential toward CK1δ, caused by formation of hydrogen bonds to Lys38 and Asp149 of CK1δ [53]. In presence of compound **16b**, *in vitro* initial screenings were performed by using GST-(*hum*)TV1-CK1δ^{wt} or GST-(*hum*)CK1δ^{R127Q} or GST-(*hum*)CK1δ^{R168H} as the source of enzyme and α-casein as substrate. Both CK1δ mutants, GST-(*hum*)CK1^{R127Q} and GST-(*hum*)CK1^{R168H}, were inhibited stronger compared to GST-(*hum*)TV1-CK1δ^{wt}, while GST-(*hum*)CK1^{R127Q} was inhibited more than 5-fold stronger than GST-(*hum*)TV1-CK1δ^{wt} and GST-(*hum*)CK1^{R168H} was inhibited more than 3-fold stronger than GST-(*hum*)TV1-CK1δ^{wt}. Subsequent determination of the more reliable IC_{50} ($IC_{50\,(CK1\delta R127Q)}$

= 2.1nM, $IC_{50\ (CK1\delta R168H)}$ = 4.7nM, $IC_{50\ (TV1\text{-}CK1\delta wt)}$ = 9.5nM) values demonstrated the significantly stronger inhibition of CK1δ mutants compared to wt CK1δ.

The stronger inhibition of GST-(*hum*)CK1δ^{R127Q} may be caused by the changed electrical charge of the protein, which changed amino acid 127 from positively charged (R: arginine) to polar uncharged (Q: glutamine) after mutation. Meanwhile, point mutations were observed to affect the catalytic efficacy and sensitivity to CK1δ-specific inhibitors due to effects on flexibility of ATP binding after mutation [125][172], which may explain the higher sensitivity of GST-(*hum*)CK1^{R168H} to **Bischof-5** and **16b**. Thus, both *in vitro* kinase assays and IC_{50} values indicate higher selectivity of **Bischof-5** and **16b** for CK1δ mutants R127Q and R168H compared to CK1δ wt.

These results are in line with previous results, showing that Richter-2 inhibits CK1δ^{T67S} 2.4-fold stronger than wt CK1δ, and that the CK1δ gatekeeper mutant M82F is inhibited 28-fold stronger by IWP-2 than wt CK1δ [45][124]. Once these residues are mutated, the phosphorylation of substrate, as well as the interaction and selectivity of CK1δ-specific inhibitors can be affected [39].

4.2 Effects of newly optimized and synthesized CK1δ inhibitors on CK1δ wt and mutants in in vitro kinase assays and cell-based assays

Due to the strong inhibitory effects on kinase activity with low IC_{50} values and the strong inhibition of proliferation and cell growth, IWP-derivatives showed high potency and selectivity for CK1δ in *in vitro* kinase assays and cell-based assays. Moreover, IWP-derivatives showed higher affinity towards the gatekeeper mutant CK1δ^{M82F} than to CK1δ wt because of the additional π hydrogen bonding to phenylalanine 82. Therefore, IWP-derivatives were considered as interesting scaffolds for developing new drugs with high specificity toward CK1δ and hyperactive CK1δ mutants [45]. Based on IWP-derivatives, newly optimized LKP_compounds have been designed and characterized for CK1δ wt and selected hyperactive mutants. Seven LKP_compounds were initially analyzed in *in vitro* kinase assays for inhibition of the activity of CK1 isoforms using α-casein as substrate to investigate CK1 isoform selectivity. An initial screening analysis indicated that all LKP_compounds could strongly inhibit both, CK1δ and ε with low IC_{50}

values, but almost no inhibition on CK1α and CK1γ could be observed, which was in line with reports about previously designed compounds [11][45][125]. Moreover, comparing to other LKP_compounds, compounds **LKP-112, 114, 115** showed increased selectivity towards CK1δ than towards CK1ε. Among them, **LKP-115** inhibited CK1δ more than 3-fold stronger than CK1ε. Deletion of a methoxy group, which could increase the binding properties to CK1δ might explain the increased selectivity towards CK1δ than towards CK1ε. Because of the significantly improved binding properties, compounds **LKP-112,114,115** might be highly specific inhibitors for CK1δ.

Once high inhibitory effects of a compound were observed in *in vitro* kinase assays, its cellular membrane permeability needs to be tested. As an ideal cell culture model, a CSNK1D knockout Hela cell line was used to characterize the effects of LKP_compounds on CK1δ wt and CK1δ mutants in cell culture. $Hela^{parental}$ cells express wild type CK1δ transcription variants, while CK1δ is depleted in $Hela^{CK1\delta-/-}$cells, which had already previously been used to successfully characterize CK1-specific cellular functions [119]. Moreover, transfection of $Hela^{CK1\delta-/-}$ cells with CK1δ wt or the hyperactive CK1δ mutants (TV1-$CK1\delta^{wt}$, TV2-$CK1\delta^{wt}$ and mutants $CK1\delta^{R127Q}$, $CK1\delta^{R168H}$, $CK1\delta^{T67S}$), can ensure the cells only express the selected CK1δ variants and no endogenous CK1δ. This makes it an ideal model for revealing the effects of LKP_compounds on cell viability and the inhibitory effects of LKP_compounds on CK1 δ wt and CK1 δ mutants in cell-based assays.

Newly synthesized and optimized LKP_compounds were used to perform cell-based MTT assays to compare the affinity of these inhibitory compounds towards CK1δ wt and mutants in cell culture. An initial screen of LKP_compounds on untransfected and transfected $Hela^{CK1\delta-/-}$ as well as $Hela^{parental}$ cell lines was performed. The results showed that compound LKP-105 inhibited the cell viability of transfected $Hela^{CK1\delta-/-,\ TV1\text{-}CK1\delta wt}$ much more compared to the untransfected $Hela^{CK1\delta-/-}$ cell line, which seems to indicate that LKP-105 specifically targets CK1δ also in cell-based assays. These results were confirmed by determination of EC_{50} values ($EC_{50(HelaCK1\delta-/-)}$ = 18.3 μM, $EC_{50(HelaCK1\delta-/-,\ TV1\text{-}CK1\delta wt)}$ = 6.0 μM), which revealed that cell viability was affected if CK1δ is present, but less affected once CK1δ is depleted ($Hela^{CK1\delta-/-}$). Moreover, compound LKP-105 showed stronger inhibition against $CK1\delta^{R127Q}$ than against TV1-$CK1\delta^{wt}$ in cell-based assays. Interestingly,

LKP-112 showed approximately three-fold higher selectivity towards Hela $^{CK1\delta-/-,\ CK1\delta R168H}$ cells than towards Hela $^{CK1\delta-/-,\ TV1\text{-}CK1\delta wt}$ cells. This is indicated by its EC_{50} values of 7.1 μM and 12.4μM, respectively. Differences among the impact of LKP_compounds on CK1δ wt and CK1δ mutants indicate the different affinities of these inhibitors to the ATP-binding pocket because of the possible conformational changes after mutation. Many residues in CK1δ have been verified to be important for substrate binding. For instance, Arg-178, Asn-172, Thr-176, and Gly-215 in CK1δ influence substrate recognition by forming the binding site [100]. However, although the structures and molecular weights of all the LKP_compounds are semilar, different kinase affinity and cellular membrane permeability could be observed in both *in vitro* kinase assays and cell-based assays, which might be caused by differences in 3D-structures of the different compounds. Additionally, in the cellular context, more parameters are influencing on the inhibitory effects of an inhibitor, for example, the higher intracellular ATP concentration might influence the binding of an inhibitor to the specific kinase [11][125]. Moreover, the CK1 inhibitor might be able to bind to the ATP-binding pockets of other kinases as well, which will result in off-target effects of CK1 inhibitors [32][153].

In summary, these findings suggest that newly designed LKP_compounds specifically inhibit CK1δ and ε, and that compounds **LKP-105** and **LKP-112** show their high cell membrane permeability and therapeutic potential the highly hyperactive CK1δ mutant R127Q and R168H. Due to the higher affinity to CK1δ mutants, these compounds could serve as leading structure for the development of new drugs for hyperactive CK1δ mutants, and the development of optimized LKP_compounds may lead to the establishment of novel therapeutics for personalized cancer treatment.

In the future, additional experiments like colony-formation assay, wound-healing assays, migration assays and animal models (e.g. mouse xenotransplantation models) should be performed to get insights into the relevance or importance of the potential CK1δ wt and mutant variants with respect to properties like proliferative or invasive potential and thereby, novel therapeutics for personalized cancer treatment could be established with the development of optimized LKP_compounds.

5. Summary

Members of the CK1 (formerly named casein kinase 1) family belong to the group of serine/threonine specific protein kinases, which are evolutionaily highly conserved and ubiquitously expressed in all eukaryotes. The increasing number of substrates phosphorylated by CK1 indicates that CK1 is involved in the regulation of multiple cellular processes like cell metabolism and differentiation, transcription, cell cycle progression, apoptosis, proliferation, DNA-processing and repair as well as inflammatory diseases and tumor diseases. Since CK1δ is often deregulated in various tumor entities and since numerous CK1δ mutants exhibit high oncogenic potential, the interest in targeting CK1δ and CK1δ mutants has increased. In the past years, the development of highly specific small molecule inhibitors (SMIs) against wild type and especially mutant CK1δ has begun to broaden the therapeutic window for CK1δ-overexpressing or -mutated tumors. Nevertheless, there is still high demand for improvements of CK1δ-specific inhibitors, retaining limited off-target effects, high specificity and cellular membrane permeability.

So far, several CK1δ inhibitors have been identified and proven of their specificity to CK1δ. Based on the cBioPortal research, three hyperactive CK1δ mutants: CK1δ^{R127Q}, CK1δ^{R168H} and CK1δ^{T67S} were selected for characterization in course of the present study. This study first concentrates on the effects of established CK1δ inhibitors on CK1δ wt and selected mutants *in vitro*. After mutagenesis and purifications procedures, an initial screening was performed for CK1δ wt and mutants. Among all the inhibitors and CK1δ transcription variants, the sensitivity of CK1δ^{R127Q} and CK1δ^{R168H} to inhibitors Bischof-5 and 16b was higher than that of TV1-CK1δ^{wt}, as indicated by the respective IC_{50} values. However, the sensitivity of the highly oncogenic CK1δ^{T67S} mutant to selected CK1δ inhibitors revealed no significant difference compared to the corresponding wild type TV2-CK1δ^{wt}. In conclusion, established CK1δ inhibitors, Bischof-5 and 16b, showed selectivity towards CK1δ and stronger effects for mutants CK1δ^{R127Q} and CK1δ^{R168H}, compared to CK1δ wt.

Furthermore, newly developed small molecule inhibitors from our long-time collaboration partner, have been synthesized based on IWP-derivates scaffolds and subsequently have been characterized for their effects on selected CK1δ wt and hyperactive mutants. Initially,

these compounds were assayed *in vitro* to check for their special inhibition on CK1δ and ε isoforms. In *in vitro* kinase assays, all LKP_compounds showed much higher potency against CK1δ than against CK1α and γ, while LKP-112, 114 and 115 showed higher specificity towards CK1δ than towards CK1ε. However, not all LKP_compounds could show strong effects on cell viability, which might be caused by the poor cellular permeability. In cell-based assays, LKP-105 seems to specifically target CK1δ. This could be demonstrated by comparing effects on transfected Hela$^{CK1\delta-/-,\ TV1\text{-}CK1\delta wt}$ and CK1δ–depleted Hela$^{CK1\delta-/-}$ cell lines, which resulted in EC_{50} values of 8.2 μM and 18.3 μM, respectively. Furthermore, LKP-105 also showed stronger effects on Hela$^{CK1\delta-/-,\ CK1\delta R127Q}$ than Hela$^{CK1\delta-/-,\ TV1\text{-}CK1\delta wt}$. LKP-112 showed more remarkable effects and approximately three-fold higher selectivity towards Hela$^{CK1\delta-/-,\ CK1\delta R168H}$ than towards Hela$^{CK1\delta-/-,\ TV1\text{-}CK1\delta wt}$. Nevertheless, further cell-based assays and xenograft animal models will be needed to reveal the connection between CK1δ mutants and tumorigenesis. Moreover, 3D-strucure analysis of CK1δ should be established by modeling studies in order to verify how each mutation affects the inhibitor binding affinity. Thereby, insight to diseases affected by kinase dysregulation could be improved. In conclusion, new CK1δ-specific inhibitor compounds with high cellular permeability and higher inhibitory potential towards the hyperactive, highly oncogenic CK1δ mutants CK1δ^{R127Q} and CK1δ^{R168H} were successfully characterized in the present study, which may lead to the establishment of novel therapeutics for personalized cancer treatment.

6. References:

[1] Alappat EC, Feig C, Boyerinas B, Volkland J, Samuels M, Murmann AE, Thorburn A, Kidd VJ, Slaughter CA, Osborn SL, Winoto A, Tang WJ, Peter ME. Phosphorylation of FADD at serine 194 by CKI alpha regulates its nonapoptotic activities. Mol Cell 19: 321–332 (2005).

[2] Alappat EC, Volkland J, Peter ME. Cell cycle effects by C-FADD depend on its C-terminal phosphorylation site. J Biol Chem 278: 41585–41588 (2003).

[3] Apionishev, S, Katanayeva NM, Marks SA, Kalderon D, Tomlinson A. Drosophila Smoothened phosphorylation sites essential for Hedgehog signal transduction. Nat Cell Biol 7: 86-92 (2005).

[4] Ashkenazi A. Targeting the extrinsic apoptotic pathway in cancer: lessons learned and future directions. J Clin Invest 125: 487–489 (2015).

[5] Badura L, Swanson T, Adamowicz W, Adams J, Cianfrogna J, Fisher K, Holland J, Kleiman R, Nelson F, Reynolds L, St Germain K, Schaeffer E, Tate B, Sprouse J. An inhibitor of casein kinase I epsilon induces phase delays in circadian rhythms under free-running and entrained conditions. J Pharmacol Exp Ther 322: 730-738 (2007).

[6] Bar I, Merhi A, Larbanoix L, Constant M, Haussy S, Laurent S, Canon JL, Delrée P. Silencing of casein kinase 1 delta reduces migration and metastasis of triple negative breast cancer cells. Oncotarget 9: 30821-30836 (2018).

[7] Beachy P.A, Karhadkar S.S, Berman D.M. Tissue repair and stem cell renewal in carcinogenesis. Nature 432: 324-331 (2004).

[8] Behrend L, Stöter M, Kurth M, Rutter G, Heukeshoven J, Deppert W, Knippschild U. Interaction of casein kinase 1 delta (CK1delta) with post-Golgi structures, microtubules and the spindle apparatus. Eur J Cell Biol 79: 240-251 (2000).

[9] Beyaert R,Vanhaesebroeck B, DeclercqW, Van Lint J, Vandenabele P, Agostinis P, Vandenheede JR, Fiers W. Casein kinase-1 phosphorylates the p75 tumor necrosis factor receptor and negatively regulates tumor necrosis factor signaling for apoptosis. J Biol Chem 270: 23293–23299 (1995).

[10] Bibian M, Rahaim RJ, Choi JY, Noguchi Y, Schürer S, Chen W, Nakanishi S, Licht K, Rosenberg LH, Li L, Feng Y, Cameron MD, Duckett DR, Cleveland JL, Roush WR. Development of highly selective casein kinase 1δ/1ε (CK1δ/ε) inhibitors with potent antiproliferative properties. Bioorg Med Chem Lett 23: 4374–4380 (2013).

[11] Bischof J, Leban J, Zaja M, Grothey A, Radunsky B, Othersen O, Strobl S, Vitt D, Knippschild U. 2-Benzamido-N-(1H-benzo[d]imidazol-2-yl)thiazole-4 -carboxamide derivatives as potent inhibitors of CK1δ/ε. Amino Acids 43: 1577–1591 (2012).

[12] Bischof J, Randoll SJ, Sussner N, Henne-Bruns D, Pinna LA, Knippschild U. CK1delta kinase activity is modulated by Chk1-mediated phosphorylation. PLoS One 8: e68803 (2013).

[13] Braune EB, Seshire A, Lendahl U. Notch and Wnt Dysregulation and Its Relevance for Breast Cancer and Tumor Initiation. Biomedicines 6: 101 (2018).

[14] Brennan KC, Bates EA, Shapiro RE, Zyuzin J, Hallows WC, Huang Y, Lee HY, Jones CR, Fu YH, Charles AC, Ptáček LJ. Casein kinase I delta mutations in familial migraine and advanced sleep phase. Sci Transl Med 5: 1-11 (2013).

[15] Brockschmidt C, Hirner H, Huber N, Eismann T, Hillenbrand A, Giamas G, Radunsky B, Ammerpohl O, Bohm B, Henne-Bruns D, Kalthoff H, Leithäuser F, Trauzold A, Knippschild U. Anti-apoptotic and growth-stimulatory functions of CK1 delta and epsilon in ductal adenocarcinoma of the pancreas are inhibited by IC261 in vitro and in vivo. Gut 57: 799-806 (2008).

[16] Brunati AM, Marin O, Bisinella A, Salviati A, Pinna LA: Novel consensus sequence for the Golgi apparatus casein kinase, revealed using proline-rich protein-1 (PRP1)-derived peptide substrates. Biochem J 351: 765-768 (2000).

[17] Carballo GB, Honorato JR, de Lopes GPF, Spohr TCLSE. A highlight on Sonic hedgehog pathway. Cell Commun Signal. 16: 11 (2018).

[18] Cegielska A, Gietzen KF, Rivers A, Virshup DM. Autoinhibition of casein kinase I epsilon (CKI epsilon) is relieved by protein phosphatases and limited proteolysis. J Biol Chem 273: 1357-1364 (1998).

[19] Chang CH, Kuo CJ, Ito T, Su YY, Jiang ST, Chiu MH, Lin YH, Nist A, Mernberger M, Stiewe T, Ito S, Wakamatsu K, Hsueh YA, Shieh SY, Snir-Alkalay I, Ben-Neriah Y. CK1a ablation in keratinocytes induces p53-dependent, sunburn-protective skin hyperpigmentation. Proc Natl Acad Sci 114: 8035-8044 (2017).

[20] Chartier M, Chénard T, Barker J, Najmanovich R. Kinome Render: a stand-alone and web-accessible tool to annotate the human protein kinome tree. PeerJ 1: 126 (2013).

[21] Chen L, Meng Y, Sun Q, Zhang Z, Guo X, Sheng X, Tai G, Cheng H, Zhou Y. Ginsenoside compound K sensitizes human colon cancer cells to TRAIL-induced apoptosis via autophagy-dependent and -independent DR5 upregulation. Cell Death Dis 7: e2334 (2016).

[22] Chen J, Wu X, Lin J, Levine AJ. mdm-2 inhibits the G1 arrest and apoptosis functions of the p53 tumor suppressor protein. Mol Cell Biol 16: 2445-2452 (1996).

[23] Cheong JK, Nguyen TH, Wang H, Tan P, Voorhoeve PM, Lee SH, Virshup DM. IC261 induces cell cycle arrest and apoptosis of human cancer cells via CK1δ/ε and Wnt/β-catenin independent inhibition of mitotic spindle formation. Oncogene 30: 2558-2569 (2011).

[24] Cheong JK, Virshup DM. Casein kinase 1: Complexity in the family. Int J Biochem Cell Biol 43: 465–469 (2011).

[25] Chijiwa TM, Hagiwara M, Hidaka H. A newly synthesized selective casein kinase I inhibitor, N-(2-aminoethyl)-5-chloroisoquinoline-8-sulfonamide, and affinity purification of casein kinase I from bovine testis. J Biol Chem 264: 4924-4927 (1989).

[26] Cobb MH, Rosen OM: Description of a protein kinase derived from insulin-treated 3T3-L1 cells that catalyzes the phosphorylation of ribosomal protein S6 and casein. J Biol Chem 258: 12472-12481 (1983).

[27] Cohen P. The role of protein phosphorylation in human health and disease. The Sir Hans Krebs Medal Lecture. Eur J Biochem 268: 5001-5010 (2001).

[28] Cozza G, Gianoncelli A, Montopoli M, Caparrotta L, Venerando A, Meggio F, Pinna LA, Zagotto G, Moro S. Identification of novel protein kinase CK1 delta (CK1delta) inhibitors through structure-based virtual screening. Bioorg Med Chem Lett 18: 5672–5675 (2008).

[29] Cruciat CM. Casein kinase 1 and Wnt/β-catenin signaling. Curr Opin Cell Biol :46-55 (2014).

[30] Dahlberg CL, Nguyen EZ, Goodlett D, Kimelman D. Interactions between Casein kinase Iepsilon (CKI epsilon) and two substrates from disparate signaling pathways reveal mechanisms for substrate-kinase specificity. PLoS One 4: e4766 (2009).

[31] Davidson G, Wu W, Shen J, Bilic J, Fenger U, Stannek P. Casein kinase 1 gamma couples Wnt receptor activation to cytoplasmic signal transduction. Nature 438: 867–872 (2005).

[32] Defert O, Boland S. Kinase profiling in early stage drug discovery: sorting things out. Drug Discov Today Technol 18: 52-61 (2015).

[33] Denef N, Neubuser D, Perez L, Cohen SM. Hedgehog induces opposite changes in turnover and subcellular localization of patched and smoothened. Cell 102: 521–531 (2000).

[34] Derkinderen P, Scales TM, Hanger DP, Leung KY, Byers HL, Ward MA, Lenz C, Price C, Bird IN, Perera T, Kellie S, Williamson R, Noble W, Van Etten RA, Leroy K, Brion JP, Reynolds CH, Anderton BH. Tyrosine 394 is phosphorylated in Alzheimer's paired helical filament tau and in fetal tau with c-Abl as the candidate tyrosine kinase. J Neurosci 25: 6584-6593 (2005).

[35] Desagher, S., Osen-Sand, A., Montessuit, S., Magnenat, E., Vilbois, F., Hochmann, A., Journot, L., Antonsson, B., and Martinou, J.C. Phosphorylation of bid by casein kinases I and II regulates its cleavage by caspase 8. Mol Cell 8: 601-611 (2001).

[36] Dumaz N, Milne DM, Meek DW. Meek, Protein kinase CK1 is a p53-threonine 18 kinase which requires prior phosphorylation of serine 15. FEBS Lett 463: 312-316 (1999).

[37] Ebert BL, Krönke J. Inhibition of Casein Kinase 1 Alpha in Acute Myeloid Leukemia. N Engl J Med 379: 1873-1874 (2018).

[38] Ebisawa T, Uchiyama M, Kajimura N, Mishima K, Kamei Y, Katoh M, Watanabe T, Sekimoto M, Shibui K, Kim K, Kudo Y, Ozeki Y, Sugishita M, Toyoshima R, Inoue Y, Yamada N, Nagase T, Ozaki N, Ohara O, Ishida N, Okawa M, Takahashi K, Yamauchi T. Association of structural polymorphisms in the human period3 gene with delayed sleep phase syndrome. EMBO Rep 2: 342-346 (2001).

[39] Elphick LM, Lee SE, Gouverneur V, Mann DJ. Using chemical genetics and ATP analogues to dissect protein kinase function. ACS Chem Biol 2: 299–314 (2007).

[40] Elyada E, Pribluda A, Goldstein RE, Morgenstern Y, Brachya G, Cojocaru G, Snir-Alkalay I, Burstain I, Haffner-Krausz R, Jung S, Wiener Z, Alitalo K, Oren M, Pikarsky E, Ben-Neriah Y. CKI alpha ablation highlights a critical role for p53 in invasiveness control. Nature 470: 409–413 (2011).

[41] Fish KJ, Cegielska A, Getman ME, Landes GM, Virshup DM. Isolation and characterization of human casein kinase I epsilon (CKI), a novel member of the CKI gene family. J Biol Chem 270: 14875-14883 (1995).

[42] Flajolet M, He G, Heiman M, Lin A, Nairn AC, Greengard P. Regulation of Alzheimer's disease amyloid-beta formation by casein kinase I. Proc Natl Acad Sci U S A 104: 4159-4164 (2007).

[43] Föhr KJ, Knippschild U, Herkommer A, Fauler M, Peifer C, Georgieff M, Adolph O. State-dependent block of voltage-gated sodium channels by the casein-kinase 1 inhibitor IC261. Invest New Drugs 35: 277-289 (2017).

[44] Manning G, Whyte DB, Martinez R, Hunter T, Sudarsanam S. The protein kinase complement of the human genome. Science 298: 1912-1934 (2002).

[45] García-Reyes B, Witt L, Jansen B, Karasu E, Gehring T, Leban J, Henne-Bruns D, Pichlo C, Brunstein E, Baumann U, Wesseler F, Rathmer B, Schade D,6, Peifer C, Knippschild U. Discovery of Inhibitor of Wnt Production 2 (IWP-2) and Related Compounds As Selective ATP-Competitive Inhibitors of Casein Kinase 1 (CK1) delta/epsilon. J Med Chem 61: 4087-4102 (2018).

[46] Ghoshal N, Smiley JF, DeMaggio AJ, Hoekstra MF, Cochran EJ, Binder LI, Kuret J. A new molecular link between the fibrillar and granulovacuolar lesions of Alzheimer's disease. Am J Pathol 155: 1163-1172 (1999).

[47] Giamas G, Hirner H, Shoshiashvili L, Grothey A, Gessert S, Kühl M, Henne-Bruns D, Vorgias CE, Knippschild U. Phosphorylation of CK1delta: identification of Ser370 as the major phosphorylation site targeted by PKA in vitro and in vivo. Biochem J 406: 389-398 (2007).

[48] Gietzen KF, Virshup DM. Identification of inhibitory autophosphorylation sites in casein kinase I epsilon. J Biol Chem 274: 32063-32070 (1999).

[49] Graves PR, Haas DW, Hagedorn CH, DePaoli-Roach AA, Roach PJ: Molecular cloning, expression, and characterization of a 49-kilodalton casein kinase I isoform from rat testis. J Biol Chem 268:6394-6401 (1993).

[50] Graves PR, Roach PJ. Role of COOH-terminal phosphorylation in the regulation of casein kinase I delta. J Biol Chem 270. 21689-21694 (1995).

[51] Gross SD, Anderson RA: Casein kinase I: spatial organization and positioning of a multifunctional protein kinase family. Cell Signal 1998, 10:699-711.

[52] Grozav AG, Chikamori K, Kozuki T, Grabowski DR, Bukowski RM, Willard B, Kinter M, Andersen AH, Ganapathi R, Ganapathi MK. Casein kinase I delta/epsilon phosphorylates topoisomerase II alpha at serine-1106 and modulates DNA cleavage activity. Nucleic Acids Res 37: 382-392 (2009).

[53] Halekotte J, Witt L, Ianes C, Krüger M, Bührmann M, Rauh D, Pichlo C, Brunstein E, Luxenburger A, Baumann U, Knippschild U, Bischof J, Peifer C. Optimized 4,5-Diarylimidazoles as Potent/Selective Inhibitors of Protein Kinase CK1δ and Their Structural Relation to p38α MAPK. Molecules 22:522 (2017).

[54] Hammond EM, Denko NC, Dorie MJ, Abraham RT, Giaccia AJ. Hypoxia links ATR and p53 through replication arrest. Mol Cell Biol 22: 1834-1843 (2002).

[55] Hammond EM, Dorie MJ, Giaccia AJ. ATR/ATM targets are phosphorylated by ATR in response to hypoxia and ATM in response to reoxygenation. J Biol Chem 278: 12207-12213 (2003).

[56] Hanks SK, Hunter T. The eukaryotic protein kinase superfamily: kinase (catalytic) domain structure and classification. FASEB J 9: 576-596 (1995).

[57] Harvey KF, Zhang X, Thomas DM. The Hippo pathway and human cancer. Nat Rev Cancer 13: 246-257 (2013).

[58] Hathaway GM, Traugh JA: Casein kinases--multipotential protein kinases. Curr Top Cell Regul 21:101-127 (1982).

[59] Heallen T, Zhang M, Wang J, Bonilla-Claudio M, Klysik E, Johnson RL, Martin JF. Hippo pathway inhibits Wnt signaling to restrain cardiomyocyte proliferation and heart size. Science 332: 458-461 (2011).

[60] Heretsch P, Tzagkaroulaki L, Giannis A. Modulators of the hedgehog signaling pathway. Bioorg Med Chem 18: 6613-6624 (2010).

[61] Hirner H, Günes C, Bischof J, Wolff S, Grothey A, Kühl M, Oswald F, Wegwitz F, Bösl MR, Trauzold A, Henne-Bruns D, Peifer C, Leithäuser F, Deppert W, Knippschild U. Impaired CK1 delta activity attenuates SV40-induced cellular transformation in vitro and mouse mammary carcinogenesis in vivo. PLoS One 7: e29709 (2012).

[62] Honaker Y, Piwnica-Worms H. Casein kinase 1 functions as both penulti- mate and ultimate kinase in regulating Cdc25A destruction. Oncogene 29: 3324–3334 (2010).

[63] Hua Z, Huang X, Bregman H, Chakka N, DiMauro EF, Doherty EM, Goldstein J, Gunaydin H, Huang H, Mercede S, Newcomb J, Patel VF, Turci SM, Yan J, Wilson C, Martin MW. 2-Phenylamino-6-cyano-1H-benzimidazole-based isoform selective casein kinase 1 gamma (CK1gamma) inhibitors. Bioorg Med Chem Lett 22: 5392-5395 (2012).

[64] Huart AS, MacLaine NJ, Narayan V, Hupp TR. Exploiting the MDM2-CK1alpha protein-protein interface to develop novel biologics that induce UBL-kinase-modification and inhibit cell growth. PLoS One 7: e43391 (2012).

[65] Huart AS, MacLaine NJ, Meek DW, Hupp TR. CK1alpha plays a central role in mediating MDM2 control of p53 and E2F-1 protein stability. J Biol Chem 284: 32384-32394 (2009).

[66] Hunter T: Protein kinase classification. Methods Enzymol 200:3-37 (1991).

[67] Ianes C, Xu P, Werz N, Meng Z, Henne-Bruns D, Bischof J, Knippschild U. CK1delta activity is modulated by CDK2/E- and CDK5/p35-mediated phosphorylation. Amino Acids 48: 579-592 (2016).

[68] Ingham PW, McMahon AP: Hedgehog signaling in animal development: paradigms and principles. Genes Dev 15: 3059-3087 (2001).

[69] Inuzuka H, Tseng A, Gao D, Zhai B, Zhang Q, Shaik S, Wan L, Ang XL, Mock C, Yin H, Stommel JM, Gygi S, Lahav G, Asara J, Xiao ZX, Kaelin WG Jr, Harper JW, Wei W. Phosphorylation by casein kinase I promotes the turnover of the Mdm2 oncoprotein via the SCF(beta-TRCP) ubiquitin ligase. Cancer Cell 18: 147-159 (2010).

[70] Issinger OG: Casein kinases: pleiotropic mediators of cellular regulation. Pharmacol Ther 59: 1-30 (1993).

[71] Janovska P, Verner J, Kohoutek J, Bryjova L, Gregorova M, Dzimkova M, Skabrahova H, Radaszkiewicz T, Ovesna P, Vondalova Blanarova O, Nemcova T, Hoferova Z, Vasickova K, Smyckova L, Egle A, Pavlova S, Poppova L, Plevova K, Pospisilova S, Bryja V. Casein kinase 1 is a therapeutic target in chronic lymphocytic leukemia. Blood 131: 1206-1218 (2018).

[72] Järås M, Miller PG, Chu LP, Puram RV, Fink EC, Schneider RK, Al-Shahrour F, Peña P, Breyfogle LJ, Hartwell KA, McConkey ME, Cowley GS, Root DE, Kharas MG, Mullally A, Ebert BL. Csnk1a1 inhibition has p53-dependent therapeutic efficacy in acute myeloid leukemia. J Exp Med 211: 605-612 (2014).

[73] Jia J, Zhang L, Zhang Q, Tong C, Wang B, Hou F, Amanai K, Jiang J. Phosphorylation by double-time/CKIepsilon and CKIalpha targets cubitus

interruptus for Slimb/beta-TRCP-mediated proteolytic processing. Dev Cell 9: 819-830 (2005).

[74] Jia J, Tong C, Wang B, Luo L, Jiang J. Hedgehog signalling activity of Smoothened requires phosphorylation by protein kinase A and casein kinase I. Nature 432: 1045--1050 (2004).

[75] Jiang J, Hui CC. Hedgehog signaling in development and cancer. Dev Cell 15: 801–812 (2008).

[76] Jiang J. CK1 in Developmental Signaling: Hedgehog and Wnt. Curr Top Dev Biol 123: 303-329 (2017).

[77] Jiang K, Liu Y, Fan J, Epperly G, Gao T, Jiang J, Jia J. Hedgehog-regulated atypical PKC promotes phosphorylation and activation of Smoothened and Cubitus interruptus in Drosophila. Proc Natl Acad Sci U S A 111: 4842-4850 (2014).

[78] Kalousi A, Mylonis I, Politou AS, Chachami G, Paraskeva E, Simos G. Casein kinase 1 regulates human hypoxia-inducible factor HIF-1. J Cell Sci 123: 2976-2986 (2010).

[79] Kategaya LS, Hilliard A, Zhang L, Asara JM, Ptacek LJ, Fu YH. Casein kinase 1 proteomics reveal prohibitin 2 function in molecular clock. PLoS One 7: e31987 (2012).

[80] Kelleher FC, Rao A,Maguire A. Circadian molecular clocks and cancer. Cancer Lett 342: 9–18 (2014).

[81] Kennaway DJ, Varcoe TJ, Voultsios A, Salkeld MD, Rattanatray L, Boden MJ. Acute inhibition of casein kinase 1delta/epsilon rapidly delays peripheral clock gene rhythms. Mol Cell Biochem 398: 195-206 (2015).

[82] Knippschild U, Gocht A, Wolff S, Huber N, Lohler J, Stoter M. The casein kinase 1 family: participation in multiple cellular processes in eukaryotes. Cell Signal 17: 675-689 (2005).

[83] Knippschild U, Kruger M, Richter J, Xu P, Garcia-Reyes B, Peifer C, Halekotte J, Bakulev V, Bischof J. The CK1 Family: Contribution to Cellular Stress Response and Its Role in Carcinogenesis. Front Onco l 4: 96 (2014).

[84] Knippschild U, Milne D, Campbell L, Meek D. p53 N-terminus-targeted protein kinase activity is stimulated in response towild type p53 andDNAdamage. Oncogene 13: 1387–1393 (1996).

[85] Knippschild U, Milne DM, Campbell LE, DeMaggio AJ, Christenson E, Hoekstra MF, Meek DW. p53 is phosphorylated in vitro and in vivo by the delta and epsilon isoforms of casein kinase 1 and enhances the level of casein kinase 1 delta in response to topoisomerase-directed drugs. Oncogene 15: 1727-1736 (1997).

[86] Knippschild U, Wolff S, Giamas G, Brockschmidt C, Wittau M, Wurl PU, Eismann T, Stoter M. The role of the casein kinase 1 (CK1) family in different signaling pathways linked to cancer development. Onkologie 28: 508-514 (2005).

[87] Kosten J, Binolfi A, Stuiver M, Verzini S, Theillet FX, Bekei B, van Rossum M, Selenko P. Efficient modification of alpha-synuclein serine 129 by protein kinase CK1 requires phosphorylation of tyrosine 125 as a priming event. ACS Chem Neurosci 5: 1203-1208 (2014).

[88] Kostich M, English J, Madison V, Gheyas F, Wang L, Qiu P, Greene J, Laz TM. Human members of the eukaryotic protein kinase family. Genome Biol 3: RESEARCH0043 (2002).

[89] Krönke J, Fink EC, Hollenbach PW, MacBeth KJ, Hurst SN, Udeshi ND, Chamberlain PP, Mani DR, Man HW, Gandhi AK, Svinkina T, Schneider RK, McConkey M, Järås M, Griffiths E, Wetzler M, Bullinger L, Cathers BE, Carr SA, Chopra R, Ebert BL. Lenalidomide induces ubiquitination and degradation of CK1α in del(5q) MDS. Nature 523: 183-188 (2015).

[90] Kulikov R, Winter M, Blattner C. Binding of p53 to the central domain of Mdm2 is regulated by phosphorylation. J Biol Chem 281: 28575-28583 (2006).

[91] Kumar A, Rajendran V, Sethumadhavan R, Purohit R. Relationship between a point mutation S97C in CK1delta protein and its effect on ATP-binding affinity. J Biomol Struct Dyn 32: 394-405 (2014).

[92] Lai S, Safaei J, Pelech S. Evolutionary Ancestry of Eukaryotic Protein Kinases and Choline Kinases. J Biol Chem 291:5199–5205 (2016).

[93] Li G, Yin H, Kuret J. Casein kinase 1 delta phosphorylates tau and disrupts its binding to microtubules. J Biol Chem 279: 15938-15945 (2004).

[94] Lin SH, Lin YM, Yeh CM, Chen CJ, Chen MW, Hung HF, Yeh KT, Yang SF. Casein kinase 1 epsilon expression predicts poorer prognosis in low T-stage oral cancer patients. Int J Mol Sci. 15: 2876-2891 (2014).

[95] Lindemann RK. Stroma-initiated hedgehog signaling takes center stage in B-cell lymphoma. Cancer Res 68: 961-964 (2008).

[96] Liu C, Witt L, Ianes C, Bischof J, Bammert M, Henne-Bruns D, Xu P, Kornmann M, Peifer C, Knippschild U. Newly developed CK1-specific inhibitors show specifically stronger effects on CK1 mutants and colon cancer cell lines. Int. J. Mol. Sci. 2019, 20, 6184.

[97] Logan CY, Nusse R. The Wnt signaling pathway in development and disease. Annu Rev Cell Dev Biol 20: 781-810 (2004).

[98] Löhler J, Hirner H, Schmidt B, Kramer K, Fischer D, Thal DR, Leithäuser F, Knippschild U. Immunohistochemical characterisation of cell-type specific expression of CK1delta in various tissues of young adult BALB/c mice. PLoS One 4: e4174 (2009).

[99] Lolli ML, Giorgis M, Tosco P, Foti A, Fruttero R, Gasco A. New inhibitors of dihydroorotate dehydrogenase (DHODH) based on the 4-hydroxy-1,2,5-oxadiazol-3-yl (hydroxyfurazanyl) scaffold. Eur J Med Chem 49: 102-109 (2012).

[100] Longenecker KL, Roach PJ, Hurley TD. Three-dimensional structure of mammalian casein kinase I: molecular basis for phosphate recognition. J Mol Biol 257: 618-631 (1996).

[101] Longenecker KL, Roach PJ, Hurley TD. Crystallographic studies of casein kinase I delta toward a structural understanding of auto-inhibition. Acta Crystallogr D Biol Crystallogr 54: 473-475 (1998).

[102] MacDonald BT, Tamai K, He X. Wnt/beta-catenin signaling: components, mechanisms, and diseases. Dev Cell 17: 9–26 (2009).

[103] MacLaine NJ, Oster B, Bundgaard B, Fraser JA, Buckner C, Lazo PA, Meek DW, Höllsberg P, Hupp TR. A central role for CK1 in catalyzing phosphorylation of the p53 transactivation domain at serine 20 after HHV-6B viral infection. J Biol Chem 283: 28563-28573 (2008).

[104] Mangelsdorf DJ, Evans RM. The RXR heterodimers and orphan receptors. Cell 83: 841–850 (1995).

[105] Mashhoon N, DeMaggio AJ, Tereshko V, Bergmeier SC, Egli M, Hoekstra MF, Kuret J. Crystal structure of a conformation-selective casein kinase-1 inhibitor. J Biol Chem 275: 20052-20060 (2000).

[106] Meng Z, Capalbo L, Glover DM, Dunphy WG. Role for casein kinase 1 in the phosphorylation of Claspin on critical residues necessary for the activation of Chk1. Mol Biol Cell 22: 2834–2847 (2011).

[107] Meng Z, Moroishi T, Guan KL. Mechanisms of Hippo pathway regulation. Genes Dev 30: 1–17 (2016).

[108] Meng QJ1, Maywood ES, Bechtold DA, Lu WQ, Li J, Gibbs JE, Dupré SM, Chesham JE, Rajamohan F, Knafels J, Sneed B, Zawadzke LE, Ohren JF, Walton KM, Wager TT, Hastings MH, Loudon AS. Entrainment of disrupted circadian behavior through inhibition of casein kinase 1 (CK1) enzymes. Proc Natl Acad Sci U S A 107: 15240-15245 (2010).

[109] Meng Z, Bischof J, Ianes C, Henne-Bruns D, Xu P, Knippschild U. CK1delta kinase activity is modulated by protein kinase C alpha (PKCalpha)-mediated site-specific phosphorylation. Amino Acids 48: 1185-1197 (2016).

[110] Milne DM, Looby P, Meek DW. Catalytic activity of protein kinase CK1 delta (casein kinase 1delta) is essential for its normal subcellular localization. Exp Cell Res 263: 43-54 (2001).

[111] Momand J, Zambetti GP, Olson DC, George D, Levine AJ. The mdm-2 oncogene product forms a complex with the p53 protein and inhibits p53-mediated transactivation. Cell 69(7): 1237-1245 (1992).

[112] Monastyrskyi A, Nilchan N, Quereda V, Noguchi Y, Ruiz C, Grant W, Cameron M, Duckett D, Roush W. Development of dual casein kinase 1δ/1ε (CK1δ/ε) inhibitors for treatment of breast cancer. Bioorg Med Chem 26: 590-602 (2018).

[113] Nusse R, Clevers H. Wnt/beta-Catenin Signaling, Disease, and Emerging Therapeutic Modalities. Cell 169: 985-999 (2017).

[114] Okamura A, Iwata N, Tamekane A, Yakushijin K, Nishikawa S, Hamaguchi M, Fukui C, Yamamoto K, Matsui T. Casein kinase I epsilon down-regulates phospho-Akt via PTEN, following genotoxic stress-induced apoptosis in hematopoietic cells. Life Sci 78: 1624-1629 (2006).

[115] Oumata N, Bettayeb K, Ferandin Y, Demange L, Lopez-Giral A, Goddard ML, Myrianthopoulos V, Mikros E, Flajolet M, Greengard P, Meijer L, Galons H. Roscovitine-derived, dual-specificity inhibitors of cyclin-dependent kinases and casein kinases 1. JMedChem 51: 5229–5242 (2008).

[116] Pangou E, Befani C, Mylonis I, Samiotaki M, Panayotou G, Simos G, Liakos P. HIF-2alpha phosphorylation by CK1delta promotes erythropoietin secretion in liver cancer cells under hypoxia. J Cell Sci 129: 4213-4226 (2016).

[117] Partch CL, Shields KF, Thompson CL, Selby CP, Sancar A. Posttranslational regulation of the mammalian circadian clock by cryptochrome and protein phosphatase 5. Proc Natl Acad Sci U S A 103: 10467-10472 (2006).

[118] Peifer C, Abadleh M, Bischof J, Hauser D, Schattel V, Hirner H, Knippschild U, Laufer S. 3,4-Diaryl-isoxazoles and -imidazoles as Potent Dual Inhibitors of p38α Mitogen Activated Protein Kinase and Casein Kinase 1δ. Journal of Medicinal Chemistry 52: 7618–7630 (2009).

[119] Penas L, Ramachandran V, Simanski S. Casein kinase 1-dependent wee1 protein degradation. J Biol Chem 289(27):18893-18903 (2014).

[120] Perez DI, Gil C, Martinez A. Protein kinases CK1 and CK2 as new targets for neurodegenerative diseases. Med Res Rev 31: 924-954 (2011).

[121] Piao S, Lee SJ, Xu Y, Gwak J, Oh S, Park BJ, Ha NC. CK1epsilon targets Cdc25A for ubiquitin-mediated proteolysis under normal conditions and in response to checkpoint activation. Cell Cycle 10: 531-537 (2011).

[122] Pinacho R, Villalmanzo N, Meana JJ, Ferrer I, Berengueras A, Haro JM, Villén J, Ramos B. Altered CSNK1E, FABP4 and NEFH protein levels in the dorsolateral prefrontal cortex in schizophrenia. Schizophr Res 177: 88-97 (2016).

[123] Price MA, and Kalderon D. Proteolysis of the Hedgehog signaling effector Cubitus interruptus requires phosphorylation by Glycogen Synthase Kinase 3 and Casein Kinase 1. Cell 108: 823-835 (2002).

[124] Rena G, Bain J, Elliott M, Cohen P. D4476, a cell-permeant inhibitor of CK1, suppresses the site-specific phosphorylation and nuclear exclusion of FOXO1a. EMBO Rep 5: 60-65 (2004).

[125] Richter J, Bischof J, Zaja M, Kohlhof H, Othersen O, Vitt D, Alscher V, Pospiech I, García-Reyes B, Berg S, Leban J, Knippschild U. Difluoro-dioxolo-benzoimidazol-benzamides as potent inhibitors of CK1delta and epsilon with nanomolar inhibitory activity on cancer cell proliferation. J Med Chem 57: 7933-7946 (2014).

[126] Richter J, Ullah K, Xu P, Alscher V, Blatz A, Peifer C, Halekotte J, Leban J, Vitt D, Holzmann K, Bakulev V, Pinna LA, Henne-Bruns D, Hillenbrand A, Kornmann M, Leithäuser F, Bischof J, Knippschild U. Effects of altered expression and activity levels of CK1delta and varepsilon on tumor growth and survival of colorectal cancer patients. Int J Cancer 136: 2799-2810 (2015).

[127] Robinson DR, Wu YM, Lin SF. The protein tyrosine kinase family of the human genome. Oncogene 19: 5548-5557 (2000).

[128] Rodriguez N, Yang J, Hasselblatt K, Liu S, Zhou Y, Rauh-Hain JA, Ng SK, Choi PW, Fong WP, Agar NY, Welch WR, Berkowitz RS, Ng SW. Casein kinase I epsilon interacts with mitochondrial proteins for the growth and survival of human ovarian cancer cells. EMBO Mol Med 4: 952–963 (2012).

[129] Rosenberg LH, Lafitte M, Quereda V, Grant W, Chen W, Bibian M, Noguchi Y, Fallahi M, Yang C, Chang JC, Roush WR, Cleveland JL, Duckett DR. Therapeutic targeting of casein kinase 1δ in breast cancer. Sci Transl Med 7: 318ra202 (2015).

[130] Roskoski R. Classification of small molecule protein kinase inhibitors based upon the structures of their drug-enzyme complexes. Pharmacol Res 103: 26-48 (2016).

[131] Rowles J, Slaughter C, Moomaw C, Hsu J, Cobb MH. Purification of casein kinase I and isolation of cDNAs encoding multiple casein kinase I-like enzymes. Proc Natl Acad Sci U S A 88: 9548-9552 (1991).

[132] Sakaguchi K, Saito S, Higashimoto Y, Roy S, Anderson CW, Appella E. Damage-mediated phosphorylation of human p53 threonine 18 through a cascade mediated by a casein 1-like kinase. Effect on Mdm2 binding. J Biol Chem 275: 9278-9283 (2000).

[133] Salado IG, Redondo M, Bello ML, Perez C, Liachko NF, Kraemer BC, Miguel L, Lecourtois M, Gil C, Martinez A, Perez DI. Protein kinase CK-1 inhibitors as new potential drugs for amyotrophic lateral sclerosis. J Med Chem 57: 2755-2772 (2014).

[134] Santos JA, Logarinho E, Tapia C, Allende CC, Allende JE, Sunkel CE. The casein kinase 1 alpha gene of Drosophila melanogaster is developmentally regulated and the kinase activity of the protein induced by DNA damage. J Cell Sci 109: 1847-1856 (1996).

[135] Schittek B, Sinnberg T. Biological functions of casein kinase 1 isoforms and putative roles in tumorigenesis. Mol Cancer 13: 231 (2014).

[136] Schwab C, Demaggio AJ, Ghoshal N, Binder LI, Kuret J, McGeer PL. Casein kinase 1 delta is associated with pathological accumulation of tau in several neurodegenerative diseases. Neurobiol Aging 21: 503-510 (2000).

[137] Shi Q, Li S, Li S, Jiang A, Chen Y, Jiang J. Hedgehog-induced phosphorylation by CK1 sustains the activity of Ci/Gli activator. Proc Natl Acad Sci U S A 111: 5651-5660 (2014).

[138] Shin DH, Choi YJ, Park JW. SIRT1 and AMPK mediate hypoxia-induced resistance of non-small cell lung cancers to cisplatin and doxorubicin. Cancer Res 74: 298-308 (2014).

[139] Sillibourne JE, Milne DM, Takahashi M, Ono Y, Meek DW. Centrosomal anchoring of the protein kinase CK1delta mediated by attachment to the large, coiled-coil scaffolding protein CG-NAP/AKAP450. J Mol Biol 322: 85-97 (2002).

[140] Singh TJ, Grundke-Iqbal I, Iqbal K. Phosphorylation of tau protein by casein kinase-1 converts it to an abnormal Alzheimer-like state. J Neurochem 64: 1420-1423 (1995).

[141] Sinnberg T, Menzel M, Kaesler S, Biedermann T, Sauer B, Nahnsen S, Schwarz M, Garbe C, Schittek B. Suppression of casein kinase 1 alpha in melanoma cells induces a switch in beta- catenin signaling to promote metastasis. CancerRes 70: 6999–7009 (2010).

[142] Swiatek W, Kang H, Garcia BA, Shabanowitz J, Coombs GS, Hunt DF, Virshup DM. Negative regulation of LRP6 function by casein kinase I epsilon phosphorylation. J Biol Chem 281: 12233–12241 (2006).

[143] Taipale J, Cooper MK, Maiti T, Beachy PA. Patched acts catalytically to suppress the activity of Smoothened. Nature 418: 892–897 (2002).

[144] Tarapore P, Fukasawa K. Loss of p53 and centrosome hyperamplification. Oncogene 21: 6234-6240 (2002).

[145] Toh KL, Jones CR, He Y, Eide EJ, Hinz WA, Virshup DM, Ptácek LJ, Fu YH. An hPer2 phosphorylation site mutation in familial advanced sleep phase syndrome. Science 291: 1040-1043 (2001).

[146] Toyoshima M, Howie HL, Imakura M, Walsh RM, Annis JE, Chang AN, Frazier J, Chau BN, Loboda A, Linsley PS, Cleary MA, Park JR, Grandori C. Functional genomics identifies therapeutic targets for MYC-driven cancer. Proc Natl Acad Sci U S A 109: 9545-9550 (2012).

[147] Tsai IC, Woolf M, Neklason DW, Branford WW, Yost HJ, Burt RW, Virshup DM. Disease-associated casein kinase I delta mutation may promote adenomatous polyps formation via a Wnt/beta-catenin independent mechanism. Int J Cancer 120 1005-1012 (2007).

[148] Umar S,WangY,MorrisAP, Sellin JH. Dual alterations in casein kinase I-epsilon and GSK-3beta modulate beta-catenin stability in hyperproliferating colonic epithelia. Am J Physiol Gastrointest Liver Physiol 292: 599–607 (2007).

[149] Ursu A, Illich DJ, Takemoto Y, Porfetye AT, Zhang M, Brockmeyer A, Janning P, Watanabe N, Osada H, Vetter IR, Ziegler S, Schöler HR, Waldmann H. Epiblastin A Induces Reprogramming of Epiblast Stem Cells Into Embryonic Stem Cells by Inhibition of Casein Kinase 1. Cell Chem Biol 23: 494-507 (2016).

[150] Vancura A, Sessler A, Leichus B, Kuret J. A prenylation motif is required for plasma membrane localization and biochemical function of casein kinase I in budding yeast. J Biol Chem 269: 19271-19278 (1994).

[151] Varelas X, Miller BW, Sopko R, Song S, Gregorieff A, Fellouse FA, Sakuma R, Pawson T, Hunziker W, McNeill H, Wrana JL, Attisano L. The Hippo pathway regulates Wnt/beta-catenin signaling. Dev Cell 18: 579-591 (2010).

[152] Varjosalo M, Taipale J. Hedgehog: functions and mechanisms. Genes Dev 22: 2454-2472 (2008).

[153] Vasta JD, Corona CR, Wilkinson J, Zimprich CA, Hartnett JR, Ingold MR, Zimmerman K, Machleidt T, Kirkland TA, Huwiler KG, Ohana RF, Slater M, Otto P, Cong M, Wells CI, Berger BT, Hanke T, Glas C, Ding K, Drewry DH, Huber KVM, Willson TM, Knapp S, Müller S, Meisenheimer PL, Fan F, Wood KV, Robers MB. Quantitative, Wide-Spectrum Kinase Profiling in Live Cells for Assessing the Effect of Cellular ATP on Target Engagement. Cell Chem Biol 25: 206-214 (2018).

[154] Venerando A, Marin O, Cozza G, Bustos VH, Sarno S, Pinna LA. Isoform specific phosphorylation of p53 by protein kinase CK1. Cell Mol Life Sci 67: 1105-1118 (2010).

[155] Wade M, Li YC, Wahl GM. MDM2, MDMX and p53 in oncogenesis and cancer therapy. Nat Rev Cancer 13: 83-96 (2013).

[156] Walton KM, Fisher K, Rubitski D, Marconi M, Meng QJ, Sládek M, Adams J, Bass M, Chandrasekaran R, Butler T, Griffor M, Rajamohan F, Serpa M, Chen Y, Claffey M, Hastings M, Loudon A, Maywood E, Ohren J, Doran A, Wager TT. Selective inhibition of casein kinase 1 epsilon minimally alters circadian clock period. J Pharmacol Exp Ther 330: 430-439 (2009).

[157] Wang PC, Vancura A, Mitcheson TG, Kuret J. Two genes in Saccharomyces cerevisiae encode a membrane-bound form of casein kinase-1. Mol Biol Cell 3: 275-286 (1992).

[158] Wang Z, Inuzuka H, Zhong J, Fukushima H, Wan L, Liu P, Wei W. DNA damage-induced activation of ATM promotes beta-TRCP-mediated Mdm2 ubiquitination and destruction. Oncotarget 3: 1026-1035 (2012).

[159] Wicking C, Smyth I, Bale A. The hedgehog signalling pathway in tumour genesis and development. Oncogene 18: 7844-7851 (1999).

[160] Winter M, Milne D, Dias S, Kulikov R, Knippschild U, Blattner C, Meek D. Protein kinase CK1delta phosphorylates key sites in the acidic domain of murine double-minute clone 2 protein (MDM2) that regulate p53 turnover. Biochemistry 43: 16356-16364 (2004).

[161] Wolff S, Xiao Z, Wittau M, Sussner N, Stoter M, Knippschild U. Interaction of casein kinase 1 delta (CK1 delta) with the light chain LC2 of microtubule associated protein 1A (MAP1A). Biochim Biophys Acta 1745:196-206 (2005).

[162] Wu F, Zhang Y, Sun B, McMahon AP, Wang Y. Hedgehog Signaling: From Basic Biology to Cancer Therapy. Cell Chem Biol 24: 252-280 (2017).

[163] Wu P, Clausen MH, Nielsen TE. Allosteric small-molecule kinase inhibitors. Pharmacol Ther 156: 59-68 (2015).

[164] Xu P, Ianes C, Gärtner F, Liu C, Burster T, Bakulev V, Rachidi N, Knippschild U, Bischof J. Structure, regulation, and (patho-)physiological functions of the stress-induced protein kinase CK1 delta (CSNK1D). Gene 715: 144005 (2019).

[165] Xu RM, Carmel G, Sweet RM, Kuret J, Cheng X. Crystal structure of casein kinase-1, a phosphate-directed protein kinase. EMBO J 14:1015–1023 (1995).

[166] Xu F, Wang YL, Chang JJ, Du SC, Diao L, Jiang N, Wang HJ, Ma D, Zhang J. Mammalian sterile 20-like kinase 1/2 inhibits the Wnt/beta-catenin signalling pathway by directly binding casein kinase 1epsilon. Biochem J 458: 159-169 (2014).

[167] Xu RM, Carmel G, Kuret J, Cheng X. Structural basis for selectivity of the isoquinoline sulfonamide family of protein kinase inhibitors. Proc Natl Acad Sci U S A. 93: 6308-6313 (1996).

[168] Yin H, Laguna KA, Li G, Kuret J. Dysbindin structural homologue CK1BP is an isoform-selective binding partner of human casein kinase-1. Biochemistry 45: 5297-5308 (2006).

[169] Yang LL, Li GB, Yan HX, Sun QZ, Ma S, Ji P, Wang ZR, Feng S, Zou J, Yang SY. Discovery of N6-phenyl-1H-pyrazolo[3,4-d]pyrimidine-3,6-diamine derivatives as novel CK1 inhibitors using common-feature pharmacophore model based virtual screening and hit-to-lead optimization. Eur J Med Chem 56:30-38 (2012).

[170] Yang WS, Stockwell BR. Inhibition of casein kinase 1-epsilon induces cancer-cell-selective, PERIOD2-dependent growth arrest. Genome Biol 9: R92 (2008).

[171] Yasojima K, Kuret J, DeMaggio AJ, McGeer E, McGeer PL. Casein kinase 1 delta mRNA is upregulated in Alzheimer disease brain. Brain Res 865: 116-120 (2000).

[172] Zeringo NA, Murphy L, McCloskey EA, Rohal L, Bellizzi JJ 3rd. A monoclinic crystal form of casein kinase 1 δ. Acta crystallographica. Section F, Structural biology and crystallization commun 69: 1077-1083 (2013).

[173] Zhao Y, Qin S, Atangan LI, Molina Y, Okawa Y, Arpawong HT, Ghosn C, Xiao JH, Vuligonda V, Brown G, Chandraratna RA. Casein Kinase 1a Interacts with Retinoid X Receptor and Interferes with Agonist- induced Apoptosis. J Biol Chem 279: 30844–30849 (2004).

[174] Zhao B, Li L, Tumaneng K, Wang CY, Guan KL. A coordinated phosphorylation by Lats and CK1 regulates YAP stability through SCF (beta-TRCP). Genes Dev 24: 72-85 (2010).

[175] Zuccotto F, Ardini E, Casale E, Angiolini M., Through the "gatekeeper door": exploiting the active kinase conformation. J Med Chem 53: 2681-2694 (2010).

Acknowledgement

The Acknowledgement is removed for reasons of data protection

The Acknowledgement is removed for reasons of data protection

Curriculum Vitae

The Curriculum vitae is removed for reasons of data protection

Statutory declaration

I hereby declare that I composed the present dissertation with the topic

“Effects of CK1 specific inhibitors on wild type and mutant CK1δ in vitro and their ability to inhibit growth of tumor cell lines”

independently and that I have used no other sources that those cited. I have identified the passages in each individual case, which are taken word for word or meanings by stating the source from other works.

I also declare that I have completed my academic work according to the principles of good scientific in accordance with the valid “Ulm University Statutes for Safeguarding Good Scientific Practice”.

Place, Date **Signature**